Designing of Dual Axis Timer Based Sun Tracker System to Improve Efficiency of Solar Receptor

A thesis submitted in partial fulfillment of the requirement for the Master of Science in Mechanical Design

By

Getaw Ayay

Advisors: ***Dr. Daniel Tilahun***

August 15, 2013

Acknowledgement

A special thank is given to my advisors Dr. Daniel Tilahun and Dr-Ing. Zewdu Abdi. Your continuous advice, comments, guidance and corrections make my job much easier, and yours dedicated advising are greatly appreciated. I am grateful for your help. In addition, I would like to thank my friends Abreham E., Samuel T. and Mebratu Y. for your friendly cooperativeness. The last but not the least I would like to say thank you to all of my friends and families who always encourage me morally to accomplish this thesis.

Contents

List of figures

List of Tables

Used Symbols

A-----area

B-----distance across flat

AST----apparent solar time

C-------spring index, end condition of cylinder

d-------diameter

D------diameter

DS-----daylight saving

E------modulus of elasticity, east

ET-----equation of time

E-W---east west

F------force

G-----Modulus of rigidity

g------gravity

H-----head thickness

h ----hour angle, height

I-----moment of inertia

k_a ------ Load factor

k_{sur} ----surface finish factor

k_{sz} ----Size factor

L ----local latitude, length, height, stroke length

LL------local longitude

LST----local standard time

K----kilo, radius of gyration

m------mass, meter

M-----mega

Min----minutes

N------day numbers, north, number of teeth, Newton, number of coils

N-S---north south

n------stroke number, factor of safety

P-----pressure, pitch

Pa----Pascal

Q-----discharge rate

r------radius

R ----sun - earth distance, radius

S-------south

SL------standard longitude

t------time, thickness

TL----thread length

V------volume

v------velocity

W----weight, west

w-----unit weight, width

x-----variable

y-----variable

z ----- azimuth angle

α ----mean sun - earth distance, solar altitude angle

β ----- surface tilt angle

δ ----declination, deflection of spring

Φ ----solar zenith angle

θ ----- solar incidence angle

υ ----- poison's ratio

ρ ----- density

σ ----- stress

τ ------ stress

ω ----rotational speed

Abstract

The dual axis sun tracker is important to improve the efficiency of the solar system that will be applicable in different sectors by aligning sun-receptor position in a perpendicular position. Improvement of the efficiency is achieved by following always the sun by the receptor using sun tracker mechanism. Hence, the aim of the thesis is to design a system that always tracks the sun.

Designing of an effective solar tracker is achieved by applying the standard methods of designing mechanical systems. These methods are literature review, selecting a best mechanism among different alternatives, mathematical modeling, technical analysis, manufacturing process and cost analysis.

An efficient mechanism is designed based on crank slider mechanism that operates using hydraulic media. In the system, there are two pumps, two hydraulic powerhouses, one motor, one timer and two-limit switch. One of the pump and powerhouse is used to rotate the receptor in the azimuth direction on the other hand one pump and powerhouse is used to rotate the receptor in the zenith direction. The azimuth rotation is operated automatically by a motor while the zenith rotation is operated manually.

The overall dimension of the tracker is 2000mmx1768mmx979mm and a weight of 40 kg and it costs 3007.76 birr. Since the sun tracker is dual axis, it can track the sun accurately. The system rotates the panel 170^o from which it starts at 5^o and stops at 175^o in azimuth. This is due to the geometry limitation of the system. However, the panel rotates perfectly 47^o angle along zenith. The number of strokes to rotate in the azimuth angle is 88200 during extending and 8200 during retracting per day to cover 170^o and On the other hand, 360 strokes to lower and 990 strokes to lift the panel are required in the zenith direction to cover 23.5^o. A maximum of 0.017923 m^3 (17.923 Littre) fluid is required to extend both the azimuth and zenith rotation.

Chapter 1 Introduction

1.1. Background

In recent years, the growing global interest in the conservation of environment has provided a fresh impetus for research in the area of solar energy utilization. Solar energy is one of the best environment friendly forms of energy. Hence converting it into useful form of energy is unquestionable from different perspective in this century. Already, installation of solar energy extraction devices such as solar panels, solar water heaters, solar cookers etc. is becoming popular in urban buildings. To extract a maximum solar energy the solar receptor should always facing towards the sun ray.

The diurnal and seasonal movement of earth affects the radiation intensity on the solar systems. The first movement is due to rotation of earth about its rotation axis but the second movement is due to rotation of earth around the sun. The diurnal movement of earth has a great effect on the intensity of the solar energy since earth rotates one revolution per day in its axis. Hence, Sun trackers move the solar receptor systems to compensate for these motions, keeping the best orientation relative to the sun position. This device always tries to make the angle between the sun and the receptor perpendicular. If this position is achieved, a considerable amount of energy can be saved.

In solar tracking systems, solar panels are mounted on a structure, which moves to track the movement of the sun throughout the day. There are three methods of tracking: active, passive and chronological tracking (Nader Barsoum, 2011). These methods can then be configured either as single-axis or dual-axis solar trackers. In active tracking, the position of the sun in the sky during the day is continuously determined by sensors. The sensors will trigger the motor or actuator to move the mounting system so that the solar panels will always face the sun throughout the day. This method of sun tracking is reasonably accurate except on very cloudy days when it is hard for the sensor to determine the position of the sun in the sky thus making it hard to reorient the structure.

Passive Tracking unlike active tracking which determines the position of the sun in the sky, a passive tracker moves in response to an imbalance in pressure between two points at both ends of the tracker. The imbalance is caused by solar heat creating gas pressure on a “low boiling point compressed gas fluid that is driven to one side or the other” which then moves the structure. However, this method of sun tracking is not accurate.

A chronological tracker is a timer-based tracking system whereby the structure is moved at a fixed rate throughout the day. The theory behind this is that the sun moves across the sky at a fixed rate. Thus, the motor or actuator is programmed to rotate continuously at a “slow average rate of one revolution per day (15 degrees per hour)”. This method of sun tracking is very accurate (Nader Barsoum, 2011). However, the continuous rotation of the motor or actuator means more power consumption and tracking the sun on a very cloudy day is unnecessary. Since the system works based on timer, it rotates the panel between sunrise and sunset continuously. The continuous rotation of the motor means more power consumption. This more consumption of power is compensated since the timer based sun tracker is more accurate than other types of sun trackers.

1.2. Statement of the Problem

Nowadays, use of solar energy is common in hotels, large buildings, satellites, rural areas, military sites and in individual homes for different purposes like electrifying, cooking and heating using solar panel, solar cooker and solar heater respectively. The efficiency of these devices depends on the relative position between the sun and the receptor. There should be a mechanism (sun tracker) that always makes the receptor perpendicular to the sun ray.

The sun-receptor position is affected by two relative conditions. The first one is due to east-west rotation of the earth that leads to 24 hours different intensity of solar energy onto the receptor. The second reason, that affects the relative position, is the 23.5^0 North-South inclination of the sun from equator annually. Although the problem arises due to the above reasons, the east-west rotation of the earth has a more significant adverse effect on the intensity of the solar energy.

The thesis aimed to increase the efficiency of the solar system by tracking the sun by using two axes rotation. These are;

- East-west rotation of the solar receptor about north-south axis
- North-south rotation about the east-west axis

1.3. Significance of the Study

The result of the study is important to improve the efficiency of the solar system that will be applicable in different sectors by aligning sun-receptor position in a perpendicular position. The different applicable sectors are like rural area electrification, hotels water heaters, individual home cooking purposes and satellite electrifying. Improvement of the efficiency is achieved by following always the sun by the receptor using sun tracker mechanism.

1.4. Objectives

General Objectives

The general objective of the thesis is to design a mechanism that rotates and makes the receptor of a solar system automatically towards the sun solar intensity. The mechanism could rotate the receptor about two axes these axes are east west (180^{o}) and north south (23.5^{o}).

Specific Objectives

The study will focus on;

- Brain storming and finding a best mechanism of receptor rotators
- Appropriate material selection for the different components of the sun tracker mechanism
- Designing and stress analysis by considering different loads
- Making a clear guidance of manufacturing process of each parts
- Listing the assembly and disassembly procedures as well as the maintenance guide if there is
- Finally cost analysis based on the current market conditions

1.5. Research Methodology

Designing of an effective solar tracker is achieved by following the standard methods of designing mechanical systems. The research methodology of this thesis is as follows.

1. Literature Review: in this stage, previously filed works related to solar tracker, earth-sun position and length of days are studied and reviewed. The main focus of the review will be in previously designed solar trackers of their mechanism, operation principles, efficiency and limitations.
2. Selecting a best mechanism among different alternatives: This is achieved;
    a. firstly by formal need analysis of the problem
    b. Secondly, by bringing a system analysis of the different parts that compose the mechanism
    c. Thirdly, by interconnecting the function of the different parts for one purpose
    d. Finally selecting the best mechanism using prioritizing criteria
3. Technical Analysis: the different parts and components of the selected mechanism are designed in detail by considering different internal and external effects on the mechanism.
4. Manufacturing Process: The steps and process of manufacturing of the different parts are studied under this stage. In addition assembly process, disassembly process and maintenance procedures will be studied.
5. Cost analysis: Finally, the total cost of the solar tracker is calculated that will be expended for all aspects of manufacturing the mechanism.

1.6. Scope of the Thesis

This study will deeply focus on finding a best mechanism that is suitable to follow the path of the sun. After that, it will concentrate on designing the mechanism by considering different factors. The thesis will not cover the designing of timer, motor, limit switches, hydraulic hoses and fittings. It directly utilizes them from standard. It only studies the mechanism that tracks the sun.

Chapter 2 Literature Review

2.1. Environmental Characteristics

The sun is a sphere of intensely hot gaseous matter with a diameter of 1.39×10^9 m (see Appendix P 2.45). The sun is about 1.5×10^8 km away from earth, so, because thermal radiation travels with the speed of light in a vacuum (300,000 km/s), after leaving the sun solar energy reaches our planet in 8 min and 20 s. As observed from the earth, the sun disk forms an angle of 32 min of a degree. This is important in many applications, especially in concentrator optics, where the sun cannot be considered as a point source and even this small angle is significant in the analysis of the optical behavior of the collector (Soteris Kalogirou , 2009).

The sun has an effective blackbody temperature of 5760 K. The temperature in the central region is much higher. In effect, the sun is a continuous fusion reactor in which hydrogen is turned into helium. The sun's total energy output is 3.8×10^{20} MW, which is equal to 63 MW/m2 of the sun's surface. This energy radiates outward in all directions. The earth receives only a tiny fraction of the total radiation emitted, equal to 1.7×10^{14} kW; however, even with this small fraction, it is estimated that 84 min of solar radiation falling on earth is equal to the world energy demand for one year (about 900 EJ) (Soteris Kalogirou , 2009).

As observed from earth, the path of the sun across the sky varies throughout the year. The shape described by the sun's position, considered at the same time each day for a complete year, is called the analemma. The most obvious variation in the sun's apparent position through the year is a north-south swing over 47° of angle (because of the 23.5° tilt of the earth axis with respect to the sun), called declination. The north-south swing in apparent angle is the main cause for the existence of seasons on earth.

Knowledge of the sun's path through the sky is necessary to calculate the solar radiation falling on a surface, the solar heat gain, the proper orientation of solar collectors, the placement of collectors to avoid shading, and many more factors.

Reckoning of Time

In solar energy calculations, apparent solar time (AST) must be used to express the time of day. Apparent solar time is based on the apparent angular motion of the sun across the sky. The time when the sun crosses the meridian of the observer is the local solar noon. It usually does not coincide with the 12:00 o'clock time of a locality. To convert the local standard time (LST) to apparent solar time, two corrections are applied; the equation of time and longitude correction. These are analyzed next.

Equation of Time

Due to factors associated with the earth's orbit around the sun, the earth's orbital velocity varies throughout the year, so the apparent solar time varies slightly from the mean time kept by a clock running at a uniform rate. The variation is called the equation of time (ET). The equation of time arises because the length of a day, that is, the time required by the earth to complete one revolution about its own axis with respect to the sun, is not uniform throughout the year. Over the year, the average length of a day is 24 h; however, the length of a day varies due to the eccentricity of the earth's orbit and the tilt of the earth's axis from the normal plane of its orbit. Due to the ellipticity of the orbit, the earth is closer to the sun on January 3 and furthest from the sun on July 4. Therefore the earth's orbiting speed is faster than its average speed for half the year (from about October through March) and slower than its average speed for the remaining half of the year (from about April through September) (Soteris Kalogirou , 2009).

The values of the equation of time as a function of the day of the year (N) can be obtained approximately from the following equations:

$$ET = 9.87\sin(2B) - 7.53\cos(B) - 1.5\sin(B)\,[\text{min}]$$

$$B = (N - 81)\frac{360}{364}\,[\text{Appendix N } 2.46] \quad \text{……………………………………...……………….}\mathbf{2\text{-}1}$$

Longitude Correction

The standard clock time is reckoned from a selected meridian near the center of a time zone or from the standard meridian, the Greenwich, which is at longitude of 0°. Since the sun takes 4 min to transverse 1° of longitude, a longitude correction term of 4x(Standard longitude-Local longitude) should be either added or subtracted to the standard clock time of the locality. This correction is constant for a particular longitude, and the following rule must be followed with respect to sign convention. If the location is east of the standard meridian, the correction is added to the clock time. If the location is west, it is subtracted.

The general equation for calculating the apparent solar time (AST) is,

$$AST = LST + ET \pm 4(SL - LL) - DS \text{ ………………………………………………………………...}\mathbf{2\text{-}2}$$

where LST = local standard time, ET = equation of time, SL = standard longitude, LL = local longitude and DS = daylight saving (it is either 0 or 60 min)

If a location is east of Greenwich, the sign of AST is minus (-), and if it is west, the sign is plus (+). If a daylight saving time is used, this must be subtracted from the local standard time. The term DS depends on whether daylight saving time is in operation (usually from end of March to end of October) or not. This term is usually ignored from this equation and considered only if the estimation is within the DS period.

Solar Angles

The earth makes one rotation about its axis every 24 h and completes a revolution about the sun in a period of approximately 365.25 days. This revolution is not circular but follows an ellipse with the sun at one of the foci, as shown in Appendix P 2.47. The eccentricity, e, of the earth's orbit is very small, equal to 0.01673. Therefore, the orbit of the earth round the sun is almost circular. The sun-earth distance, R, at perihelion (shortest distance, at January 3) and aphelion (longest distance, at July 4) is given by Garg (1982):

$$\mathrm{R} = \alpha(1 \pm \mathrm{e}) \ \text{ where } \alpha = \text{mean sun - earth distance} = 149.5985\mathrm{x}10^{6}\,km \quad \textbf{2-3}$$

The plus sign in the above equation is for the sun-earth distance when the earth is at the aphelion position and the minus sign for the perihelion position. The solution of the above equation gives values for the longest distance equal to 152.1x10^6 km and for the shortest distance equal to 147.1x10^6 km, as shown in Appendix P 2.47. The difference between the two distances is only 3.3%. The mean sun-earth distance, a, is defined as half the sum of the perihelion and aphelion distances.

The sun's position in the sky changes from day to day and from hour to hour. It is common knowledge that the sun is higher in the sky in the summer than in winter. The relative motions of the sun and earth are not simple, but they are systematic and thus predictable. Once a year, the earth moves around the sun in an orbit that is elliptical in shape. As the earth makes its yearly revolution around the sun, it rotates every 24 h about its axis, which is tilted at an angle of 23° 27.14 min (23.45°) to the plane of the elliptic, which contains the earth's orbital plane and the sun's equator, as shown in Appendix P 2.48.

The most obvious apparent motion of the sun is that it moves daily in an arc across the sky, reaching its highest point at midday. As winter is replaced by spring and then summer, the sunrise and sunset points move gradually northward along the horizon. In the Northern Hemisphere, the days get longer as the sun rises earlier and sets later each day and the sun's path gets higher in the sky. On June 21, the sun is at its most northerly position with respect to the earth. This is called the summer solstice and during this day, the daytime is at a maximum. Six months later, on December 21, the winter solstice, the reverse is true and the sun is at its most southerly position (Appendix P 2.48). In the middle of the six-month range, on March 21 and September 21, the length of the day is equal to the length of the night. These are called spring and fall equinoxes, respectively. The summer and winter solstices are the opposite in the Southern Hemisphere; that is, summer solstice is on December 21 and winter solstice is on June 21. It should be noted that all these dates are approximate and that there are small variations (difference of a few days) from year to year (Kalogirou , 2009).

For the purposes of this thesis, the Ptolemaic view of the sun's motion is used in the analysis that follows, for simplicity; that is, since all motion is relative, it is convenient to consider the earth fixed and to describe the sun's virtual motion in a coordinate system fixed to the earth with its origin at the site of interest.

For most solar energy applications, one needs reasonably accurate predictions of where the sun will be in the sky at a given time of day and year. In the Ptolemaic sense, the sun is constrained to move with 2 degrees of freedom on the celestial sphere; therefore, its position with respect to an observer on earth can be fully described by means of two astronomical angles, the solar altitude (α) and the solar azimuth (z). The following is a description of each angle, together with the associated formulation. An approximate method for calculating these angles is by means of sun-path diagrams.

Declination, δ

The earth axis of rotation (the polar axis) is always inclined at an angle of 23.45° from the ecliptic axis, which is normal to the ecliptic plane. The ecliptic plane is the plane of orbit of the earth around the sun. As the earth rotates around the sun, it is as if the polar axis is moving with respect to the sun. The solar declination is the angular distance of the sun's rays north (or south) of the equator, north declination designated as positive. It is the angle between the sun-earth centerline and the projection of this line on the equatorial plane. Declinations north of the equator (summer in the Northern Hemisphere) are positive, and those south are negative. Appendix P 2.49 shows the declination during the equinoxes and the solstices. As can be seen, the declination ranges from 0° at the spring equinox to +23.45° at the summer solstice, 0° at the fall equinox, and -23.45° at the winter solstice (Soteris Kalogirou , 2009).

The variation of the solar declination throughout the year is shown in Appendix P 2.50. The declination, δ , in degrees for any day of the year (N) can be calculated approximately by the equation (ASHRAE, 2007)

$$\delta = 23.45 \sin\left[\frac{360}{365}(284+N)\right] \qquad \text{2-4}$$

As shown in Appendix P 2.50, the Tropics of Cancer (23.45°N) and Capricorn (23.45°S) are the latitudes where the sun is overhead during summer and winter solstice, respectively. Another two latitudes of interest are the Arctic (66.5°N) and Antarctic (66.5°S) Circles. As shown in Appendix P 2.50, at winter solstice all points north of the Arctic Circle are in complete darkness, whereas all points south of the Antarctic Circle receive continuous sunlight. The opposite is true for the summer solstice. During spring and fall equinoxes, the North and South Poles are equidistant from the sun and daytime is equal to nighttime, both of which equal 12 h (Soteris Kalogirou , 2009).

Hour Angle, h

The hour angle, h, of a point on the earth's surface is defined as the angle through which the earth would turn to bring the meridian of the point directly under the sun. Appendix P 2.49 shows the hour angle of point P as the angle measured on the earth's equatorial plane between the projection of OP and the projection of the sun-earth center-to-center line. The hour angle at local solar noon is zero, with each 360/24 or 15° of longitude equivalent to 1 h, afternoon hours being designated as positive. Expressed symbolically, h, the hour angle in degrees is,

h = ±0.25(Number of minutes from local solar noon where the plus sign applies to afternoon hours and the minus sign to morning hours.

The hour angle can also be obtained from the apparent time (AST); i.e., the corrected local solar time is

$h = (AST - 12)15$ **2-5**

At local solar noon, AST=12 and h=0^o. Therefore the local standard time (the time shown by our clocks at local solar noon) is $LST = 12 - ET \mp 4(SL - LL)$ (Soteris Kalogirou , 2009).

Solar Altitude Angle, α

The solar altitude angle is the angle between the sun's rays and a horizontal plane, as shown in Appendix P 2.52. It is related to the solar zenith angle, Φ, which is the angle between the sun's rays and the vertical. Therefore, $\Phi + \alpha = \pi / 2 = 90^o$

The mathematical expression for the solar altitude angle is

$\sin(\alpha) = \cos(\Phi) = \sin(L)\sin(\delta) + \cos(L)\cos(\delta)\cos(h)$ **2-6**

where L= local latitude, defined as the angle between a line from the centre of the earth to the site of interest and the equatorial plane. Values north of the equator are positive and those south are negative.

Solar Azimuth Angle, z

The solar azimuth angle, z, is the angle of the sun's rays measured in the horizontal plane from due south (true south) for the Northern Hemisphere or due north for the Southern Hemisphere; westward is designated as positive. The mathematical expression for the solar azimuth angle is

$\sin(z) = \dfrac{\cos(\delta)\sin(h)}{\cos(\alpha)}$ **2-7**

This equation is correct, provided that (ASHRAE, 1975) $\cos(h) > \tan(\delta)/\tan(L)$. If not, it means that the sun is behind the E-W line, as shown in Figure 2.52, and the azimuth angle for the morning hours is $-\pi + |z|$ and for the afternoon hours is $\pi - z$.

At solar noon, by definition, the sun is exactly on the meridian, which contains the north-south line, and consequently, the solar azimuth is 0°. Therefore the noon altitude α_n is; $\alpha_n = 90^o - L + \delta$

Sun Rise and Sun Set times and Day Length

The sun is said to rise and set when the solar altitude angle is zero. So, the hour angle at sunset, h_{ss}, can be found by solving $\sin\alpha = \cos\Phi = \sin(L)\sin(\delta) + \cos(L)\cos(\delta)\cos(h)$ for h when $\alpha = 0^o$:

$$\sin(\alpha i = \sin(0) = \sin(L)\sin(\delta) + \cos(L)\cos(\delta)\cos(h) \rightarrow \cos(h_{ss}) = -\frac{\sin(L)\sin(\delta)}{\cos(L)\cos(\delta)} \quad \text{...............}\mathbf{2\text{-}8}$$

which reduces to $\cos(h_{ss}) = -\tan(L)\tan(\delta)$ where h_{ss} is taken as positive at sunset.

Since the hour angle at local solar noon is 0°, with each 15° of longitude equivalent to 1 h, the sunrise and sunset time in hours from local solar noon is then

$$h_{ss} = -h_{sr} = \frac{1}{15}\cos^{-1}[-\tan(L)\tan(\delta)] \text{...}\mathbf{2\text{-}9}$$

The day length is twice the sunset hour, since the solar noon is at the middle of the sunrise and sunset hours. Therefore, the length of the day in hours is

$$\text{Day length} = \frac{2}{15}\cos^{-1}[-\tan(L)\tan(\delta)] \text{ ....}\mathbf{2\text{-}10}$$

Incidence Angle, θ

The solar incidence angle, θ**,** is the angle between the sun's rays and the normal on a surface. For a horizontal plane, the incidence angle, θ, and the zenith angle, Φ, are the same. The angles shown in Appendix P 2.53 are related to the basic angles, shown in Appendix P 2.49, with the following general expression for the angle of incidence (Kreith and Kreider, 1978; Duffie and Beckman, 1991):

$$\text{Cos } (\theta) = \{ \sin(L)\sin(\delta)\cos(\beta) - \cos(L)\sin(\delta)\sin(\beta)\cos(Z_s) + \cos(L)\cos(\delta)\cos(h)\cos(\beta)$$
$$+\sin(L)\cos(\delta)\cos(h)\sin(\beta)\cos(Z_s) + \cos(\delta)\sin(h)\sin(\beta)\sin(Z_s) \} \text{.......................................}\mathbf{2\text{-}11}$$

where β = surface tilt angle from the horizontal and Z_s = surface azimuth angle, the angle between the normal to the surface true south, westward is designated as positive

The Incidence Angle for Moving Surfaces

For the case of solar-concentrating collectors, some form of tracking mechanism is usually employed to enable the collector to follow the sun. This is done with varying degrees of accuracy and modes of tracking, as indicated in Appendix P 2.53.

Full Tracking

For a two-axis tracking mechanism, keeping the surface in question continuously oriented to face the sun (Appendix P 2.53 a) at all times has an angle of incidence, θ, equal to $\cos(\theta) = 1$ or $\theta = 0^o$. This, of course, depends on the accuracy of the mechanism. The full tracking collects the maximum possible sunshine. The perfromance of this mode of tracking with respect to the amount of radiation collected during one day under standard condition is shown in Appendix N 2.54. The slope of this surface (β) is equal to solar zenith angle (Φ), and the surface azimuth angle (Z_s) is equal to the solar azimuth angle (z).

Tilted N-S Axis with Tilt Adjusted Daily

For a plane moved about a north-south axis with a single daily adjustment so that its surface normal coincides with the solar beam at noon each day, (θ) is equal to (Meinel and Meinel, 1976; Duffie and Beckman, 1991);

$$\cos(\theta) = \sin^2(\delta) + \cos^2(\delta)\cos(h) \qquad \textbf{2-12}$$

For this mode of tracking, we can accept that, when the sun is at noon, the angle of the sun's rays and the normal to the collector can be up to a 4° declination, since for small angles cos(4°)=0.998~1. Appendix P 2.55 shows the number of consecutive days that the sun remains within this 4° "declination window" at noon. As can be seen in Appendix P 2.55, most of the time the sun remains close to either the summer solstice or the winter solstice, moving rapidly between the two extremes. For nearly 70 consecutive days, the sun is within 4° of an extreme position, spending only nine days in the 4° window, at the equinox. This means that a seasonally tilted collector needs to be adjusted only occasionally.

The problem encountered with this and all tilted collectors, when more than one collector is used, is that the front collectors cast shadows on adjacent ones. This means that, in terms of land utilization, these collectors lose some of their benefits when the cost of land is taken into account. The performance of this mode of tracking (Appendix P 2.56) shows the peaked curves typical for this assembly.

Polar N-S Axis with E-W Tracking

For a plane rotated about a north-south axis parallel to the earth's axis, with continuous adjustment, (θ) is equal to $\cos(\theta) = \cos(\delta)$

This configuration is shown in Appendix P 2.53b. As can be seen, the collector axis is tilted at the polar axis, which is equal to the local latitude. For this arrangement, the sun is normal to the collector at equinoxes (δ = 0°) and the cosine effect is maximum at the solstices. The same comments about the tilting of the collector and shadowing effects apply here as in the previous configuration. The performance of this mount is shown in Appendix P 2.56.

The equinox and summer solstice performance, in terms of solar radiation collected, are essentially equal; i.e., the smaller air mass for summer solstice offsets the small cosine projection effect. The winter noon value, however, is reduced because these two effects combine. If it is desired to increase the winter performance, an inclination higher than the local latitude would be required; but the physical height of such configuration would be a potential penalty to be traded off in cost effectiveness with the structure of the polar mount. Another side effect of increased inclination is shadowing by the adjacent collectors, for multi-row installations.

The slope of the surface varies continuously and is given by $\tan(\beta) = \frac{\tan(\mathrm{L})}{\cos(\mathrm{Z_s})}$

The surface azimuth angle is given by $\mathrm{Z_s} = \tan^{-1}\frac{\sin(\Phi)\sin(\mathrm{z})}{\cos(\theta')\sin(\mathrm{L})} + 180C_1C_2$ **…………………2-13**

where $\cos(\theta') = \cos(\Phi)\cos(\mathrm{L}) + \sin(\Phi)\sin(\mathrm{L})\cos(\mathrm{z})$

$$\mathrm{C_1} = \begin{cases} 0 \text{ if } \left(\tan^{-1}\dfrac{\sin(\Phi)\sin(z)}{\cos(\theta')\sin(L)}\right) z \ge 0 \\ 1 \text{ otherwise} \end{cases} \quad \text{and} \quad \mathrm{C_2} = \begin{cases} 1 & \text{if } \mathrm{z} \ge 0^{\mathrm{o}} \\ -1 & \text{if } \mathrm{z} < 0^{\mathrm{o}} \end{cases}$$

Horizontal E-w Axis with N-S Tracking

For a plane rotated about a horizontal east-west axis with continuous adjustment to minimize the angle of incidence, θ can be obtained from (Kreith and Kreider, 1978; Duffie and Beckman, 1991),

$\cos(\theta) = \sqrt{1-\cos^2(\delta)\sin^2(h)}$ **……………………………………………………………………2-14**

or from this equation (Meinel and Meinel, 1976): $\cos(\theta) = \sqrt{\sin^2(\delta)+\cos^2(\delta)\cos^2(h)}$

The basic geometry of this configuration is shown in Appendix P 2.53c. The shadowing effects of this arrangement are minimal. The principal shadowing is caused when the collector is tipped to a maximum degree south (δ =23.5°) at winter solstice. In this case, the sun casts a shadow toward the collector at the north. This assembly has an advantage in that it approximates the full tracking collector in summer (Appendix P 2.58), but the cosine effect in winter greatly reduces its effectiveness. This mount yields a rather "square" profile of solar radiation, ideal for leveling the variation during the day. The winter performance, however, is seriously depressed relative to the summer one.

The slope of this surface is given by $\tan(\beta) + \tan(\Phi)\,|\cos(\mathrm{z})|$

The surface orientation for this mode of tracking changes between 0° and 180°, if the solar azimuth angle passes through $\pm 90°$. For either hemisphere,

If $|\mathrm{z}| < 90^o, Z_s = 0^o$ and If $|\mathrm{z}| > 90^o, Z_s = 180^o$

Horizontal N-S Axis with E-W Tracking

For a plane rotated about a horizontal north-south axis with continuous adjustment to minimize the angle of incidence, θ can be obtained from (Kreith and Kreider, 1978; Duffie and Beckman, 1991)

$$\cos(\theta) = \sqrt{\sin^2(\alpha) + \cos^2(\delta)\sin^2(h)} \quad \text{.......... 2-15}$$

Or from this equation (Meinel and Meinel, 1976); $\cos(\theta) = \cos(\Phi)\cos(h) + \cos(\delta)\sin^2(h)$

The basic geometry of this configuration is shown in Appendix P 2.53d. The greatest advantage of this arrangement is that very small shadowing effects are encountered when more than one collector is used. These are present only at the first and last hours of the day. In this case, the curve of the solar energy collected during the day is closer to a cosine curve function (Appendix P 2.59).

The slope of this surface is given by $\tan(\beta) = \tan(\Phi)\,|\cos(Z_s - z)|$

The surface azimuth angle (Zs) is 90° or -90°, depending on the solar azimuth Angle:

If $z > 0^o, Z_s = 90^o$ and If $z < 0^o, Z_s = -90^o$

Comparison

The performance of the various modes of tracking is compared to the full tracking, which collects the maximum amount of solar energy, shown as 100% in Table2.5. From this table it is obvious that the polar and the N-S horizontal modes are the most suitable for one-axis tracking, since their performance is very close to the full tracking, provided that the low winter performance of the latter is not a problem (Soteris Kalogirou , 2009).

Sun path diagrams

For practical purposes, instead of using the preceding equations, it is convenient to have the sun's path plotted on a horizontal plane, called a sun path diagram, and to use the diagram to find the position of the sun in the sky at any time of the year. The solar altitude angle, α, and the solar azimuth angle, z, are functions of latitude, L, hour angle, h, and declination, δ. In a two dimensional plot, only two independent parameters can be used to correlate the other parameters; therefore, it is usual to plot different sun path diagrams for different latitudes. Such diagrams show the complete variations of hour angle and declination for a full year. Appendix P 2.60 shows the sun path diagram for 35°N latitude. Lines of constant declination are labeled by the value of the angles. Points of constant hour angles are clearly indicated. It should be noted that Appendix P 2.60 applies for the Northern Hemisphere. For the Southern Hemisphere, the sign of the declination should be reversed.

2.2. Tracking Mechanisms

A tracking mechanism must be reliable and able to follow the sun with a certain degree of accuracy, return the collector to its original position at the end of the day or during the night, and track during periods of intermittent cloud cover. Additionally, tracking mechanisms are used for the protection of collectors, i.e., they turn the collector out of focus to protect it from hazardous environmental and working conditions, such as wind gusts, overheating, and failure of the thermal fluid flow mechanism. The required accuracy of the tracking mechanism depends on the collector acceptance angle.

Various forms of tracking mechanisms, varying from complex to very simple, have been proposed. They can be divided into two broad categories: mechanical and electrical-electronic systems. The electronic systems generally exhibit improved reliability and tracking accuracy. These can be further subdivided into:

1. Mechanisms employing motors controlled electronically through sensors, which detect the magnitude of the solar illumination (Kalogirou, 1996)
2. Mechanisms using computer-controlled motors, with feedback control provided from sensors measuring the solar flux on the receiver (Briggs, 1980; Boultinghouse, 1982)

A tracking mechanism developed by Kalogirou (1996) uses three light-dependent resistors, which detect the focus, sun-cloud, and day night conditions and give instruction to a DC motor through a control system to focus the collector, follow approximately the sun path when cloudy conditions exist, and return the collector to the east during night.

The system, which was designed to operate with the required tracking accuracy, consists of a small direct current motor that rotates the collector via a speed reduction gearbox. The system employs three sensors. These are focus sensor, cloud sensor and daylight sensor, of which the focus sensor is installed on the east side of the collector shaded by the frame, whereas the other two are installed on the collector frame. The “focus” sensor, i.e., it receives direct sunlight only when the collector is focused. As the sun moves, it becomes shaded and the motor turns “on.” The “cloud” sensor, and cloud cover is assumed when illumination falls below a certain level. The condition when all three sensors receive sunlight is translated by the control system as daytime with no cloud passing over the sun and the collector in a focused position.

The sensors used are light-dependent resistors (LDRs).The main disadvantage of LDRs is that they cannot distinguish between direct and diffuse sunlight. However, this can be overcome by adding an adjustable resistor to the system, which can be set for direct sunlight (i.e., a threshold value). This is achieved by setting the adjustable resistor so that for direct sunlight, the appropriate input logic level (i.e., 0) is set.

As mentioned previously, the motor of the system is switched on when any of the three LDRs is shaded. Which sensor is activated depends on the amount of shading determined by the value set on the adjustable resistor, i.e., threshold value of radiation required to trigger the relays. Sensor A is always partially shaded. As the shading increases due to the movement of the sun, a value is reached that triggers the forward relay, which switches the motor on to turn the collector and therefore re-exposes sensor A.

The system also accommodates cloud cover, i.e., when sensor B is not receiving direct sunlight, determined by the value of another adjustable resistor, a timer is automatically connected to the system and this powers the motor every 2 min for about 7 s. As a result, the collector follows approximately the sun's path and when the sun reappears, the collector is re-focused by the function of sensor A.

The system also incorporates two limit switches, the function of which is to stop the motor from going beyond the rotational limits. These are installed on two stops, which restrict the overall rotation of the collector in both directions east and west. The collector tracks to the west as long as it is daytime. When the sun goes down and sensor C determines that it is night, power is connected to a reverse relay, which changes the motor's polarity and rotates the collector until its motion is restricted by the east limit switch. If there is no sun during the following morning, the timer is used to follow the sun's path as under normal cloudy conditions. The tracking system just described, comprising an electric motor and a gearbox, is for small collectors. For large collectors, powerful hydraulic units are required.

According to Solar Tracker (http://Wikipedia.org/wiki/solar tracker), sunlight has two components, the "direct beam" that carries about 90% of the solar energy, and the "diffuse sunlight" that carries the remainder - the diffuse portion is the blue sky on a clear day and increases proportionately on cloudy days. As the majority of the energy is in the direct beam, maximizing collection requires the sun to be visible to the panels as long as possible.

The energy contributed by the direct beam drops off with the cosine of the angle between the incoming light and the panel. In addition, the reflectance (averaged across all polarizations) is approximately constant for angles of incidence up to around 50°, beyond which reflectance degrades rapidly.

Table 2.1 Direct power lost (%) due to misalignment (angle i)

i	Lost=1-cos(i)		i	hours	Lost
0.0^0	0.00%		15^0	1	3.4%
1.0^0	0.015%		30^0	2	13.4%
3.0^0	0.14%		45^0	3	30.0%
8.0^0	1.00%		60^0	4	>50.0%
23.4^0	8.30%		75^0	5	>75.0%

For example, trackers that have accuracies of ± 5° can deliver greater than 99.6% of the energy delivered by the direct beam plus 100% of the diffuse light. As a result, high accuracy tracking is not typically used in non-concentrating PV applications.

The sun travels through 360 degrees east to west per day, but from the perspective of any fixed location the visible portion is 180 degrees during an average 1/2 day period (more in spring and summer; less, in fall and winter). Local horizon effects reduce this somewhat, making the effective motion about 150 degrees. A solar panel in a fixed orientation between the dawn and sunset extremes will see a motion of 75 degrees to either side, and thus, according to the table above, will lose 75% of the energy in the morning and evening. Rotating the panels to the east and west can help recapture those losses. A tracker rotating in the east-west direction is known as a single-axis tracker.

The sun also moves through 46 degrees north and south during a year. The same set of panels set at the midpoint between the two local extremes will thus see the sun move 23 degrees on either side, causing losses of 8.3%. A tracker that accounts for both the daily and seasonal motions is known as a dual-axis tracker. Generally speaking, the losses due to seasonal angle changes are complicated by changes in the length of the day, increasing collection in the summer in northern or southern latitudes. This biases collection toward the summer, so if the panels are tilted closer to the average summer angles, the total yearly losses are reduced compared to a system tilted at the spring/fall solstice angle (which is the same as the site's latitude).

An attempt has been made to develop a simple yet efficient sun tracking mechanism (SSTM) using smart Shape Memory Alloy (SMA) (Jeya Ganesh N, et al). The SMA element incorporated in the SSTM device performs the dual functions of sensing and actuating in such a way as to position the solar receptor tilted appropriately to face the sun directly at all times during the day. The mechanism has been designed such that the thermal stimulus needed to activate the SMA element is provided by the concentration and direct focusing of the incident sun rays on to the SMA element.

In all the above, the sun tracking mechanisms there is a requirement for a certain amount of electrical energy input for the controlling units(PLC, micro-controller, electronic circuit), for the actuators (electrical motor),and, for the sensors (Photo Detector, Light Dependent Resistors). Since electrical energy is needed as an external source to energize the motor, the employability of such mechanisms is restricted only to areas where electrical energy is easily and continuously available or when the unit itself is an electricity generator.

However, the need for an electrical energy source could be dispensed with, if one could replace the electric motor by a tilting device that can be activated directly by solar heating.

Some tracking mechanisms for solar collectors were proposed in the early 1980s, which required no electric power supply and no electronic control devices for simplifying their mechanisms. These devices included heat responsive elements that could exert a thrust when they were heated by the radiant energy from the sun and become limp in its absence. But, the tracking mechanisms based on these could change their position to only two or three positions of the movement of the sun over the entire day.

It is well known that Shape Memory Alloy (SMA) based actuators can respond to a thermal stimulus in such a way as to induce a movement by exerting a significant force on a movable element. It is being used in a variety of applications such as military, medical, safety, and robotic applications. Nitinol (a SMA material) couplers are in use in F-14 fighter planes since the late 1960s. Thus, it appears possible to design a SMA based device that can be energized by solar heating to achieve the appropriate tilting of the solar receptor. A patent for a tracking mechanism using shape memory alloys (SMAs) as heat responsive elements had been taken initially by Hashizume. The system outlined in the patent requires a number of parabolic trough reflectors or compound parabolic concentrators SMA springs, and pulleys depending on the number of positions of the movement sought. The returning of the solar receptor after completing one day is not addressed. The SMA functional degradation and cyclic behavior of the SMA are not considered in the design, and therefore, may be difficult to achieve controlled, repeatable movement in the system.

An electromechanical system to follow the position of the sun was designed and built at the Solar Evaluation Laboratory of the Technical University Federico Santa Maria (UTFSM) in Valparaiso by P. Roth, A. Georgiev, H. Boudinov (2003). It allows the automatic measurement of direct solar radiation with a pyrheliometer. It operates automatically, guided by a closed loop servo system. A four-quadrant photo detector senses the position of the sun and two small DC motors move the instrument platform keeping the sun's image at the center of the four-quadrant photo detectors. Under cloudy conditions, when the sun is not visible, a computing program calculates the position of the sun and takes control of the movement, until the detector can sense the sun again. The constructed system was tested in the climatic conditions of the city of Valparaiso, Chile. The presented tracker proves the effective work of a simple and cheap mechanism, which can be adapted also to work with larger following installations like solar cell panels, concentrators, etc. The efficiency of sun-tracking solar cell panels can be increased more than two times.

An opportunity payload was proposed by N.Viswanatha, et al, in India on GSAT-2, an experimental geo-stationary communication satellite. The payload required Sun pointing within ±10, when the communication satellite is pointing to earth. This requirement necessitated two drives, i.e., one for continuous tracking in pitch axis at one rotation per orbit and another to correct sun declination in roll axis. These rotations about two orthogonal axes generally call for two orthogonal mounted motor drives. However, after detailed study, a novel concept was proposed to achieve these two motions using only one motor drive, also a separate launch hold down was not required in the configuration proposed. In addition to mass saving, with the achieved compact size, it became feasible to accommodate the payload within the envelope allowed on the spacecraft.

Sun was visible for approximate half orbit only (N.Viswanatha, et al), so the mechanism was to track the sun for 11 hrs and 20 minutes in a 24 hours orbit. This required about 170 degrees rotation about satellite pitch axis. Pitch axis sun tracking was accomplished by harmonic geared stepper motor drive. For the other perpendicular axis declination correction, the pitch axis drive was designed to move/Over-drive about10 degrees beyond 170degrees of tracking angle on both ends. A special “declination drive” mechanism, gets activated in the over-drive zone and drives the payload package about declination axis proportional to over-drive angle.

The zone in which the “over-drive” (East end or west end) is done will decide the direction of tilt. Every day at the end of the days sun tracking, the required declination angle for the next day is set by over-driving the mechanism before fly back, at west end or after fly back at east end(depending on the direction of correction). Then the mechanism is positioned and kept ready for next day’s sun tracking in clock mode.

Chapter 3 Selection of Suitable hydraulic Media

The hydraulic media is used to rotate the solar receptor both in the azimuth and zenith directions. When the fluid is pumped, a power is transmitted from either from motor or hand to the powerhouse. The piston of the power is extended or retracted. Hence, the solar receptor is rotated by the piston rod.

Working Conditions

Temperature and Pressure: The operating conditions of the sun tracker are under atmospheric temperature and pressure although these have different values at different places. Therefore, the fluid does not need additives to fit for extreme working condition.

Load: The force applied on the fluid is very small. It is only required 1500N force to rotate the solar receptor.

Materials Compatibility: The materials, which compose the powerhouse, are steels and seal. Hence, the fluid should compatible with these construction materials.

Synthetic oils display superior performance, compared to mineral oil-based fluids, in one or more of the following respects:

- thermal stability,
- oxidation stability,
- viscosity: temperature properties (VI),
- low temperature fluidity,
- operational temperature limits,
- resistance to nuclear radiation,
- fire resistance

According to their chemical composition, the individual synthetic media nevertheless possess greatly differing properties, and mineral oil-based fluids may be advantageous regarding:

- hydrolytic stability,
- corrosion protection,
- toxicity,
- compatibility with elastomers and constructional materials,
- solubility of additives,
- frictional characteristics,
- cost and availability

Therefore, mineral oil based is selected. Paraffinic mineral oil (HVI) is selected due to its advantageous properties of viscosity index, vapour pressure (volatility), elastomeric compatibility. Its physical properties are a density of 870 kg/m^3 at 15^o, viscosity of 8.3 mm^2/s at 40 ^oC, kinematic viscosity index of 49, pour point 143 ^oC and initial boiling point of 278 ^oC.

There is an additive into the paraffinic mineral oil. This is corrosive inhibitor because the components are susceptible to corrosion.

Chapter 4 Preliminary Design of Sun Tracker

Step 1: Formal Need Statement: A mechanism, which rotates the solar receptor to increase the amount of energy collected by receptor that is applicable in solar panel, solar heater and cooker

Step 2: The Mechanism depends on: Electrical energy, Human force and Weight of the solar receptor and the supports

Step 3: The technical object is Dual Axis Sun tracker

Step 4: It is expected to accomplish to rotate the solar receptor 180^0 east-west or vice versa and 47^0 north-south or vice versa

4.1. System Analysis

It is possible to represent schematically the components or environments on the Tracker as shown below.

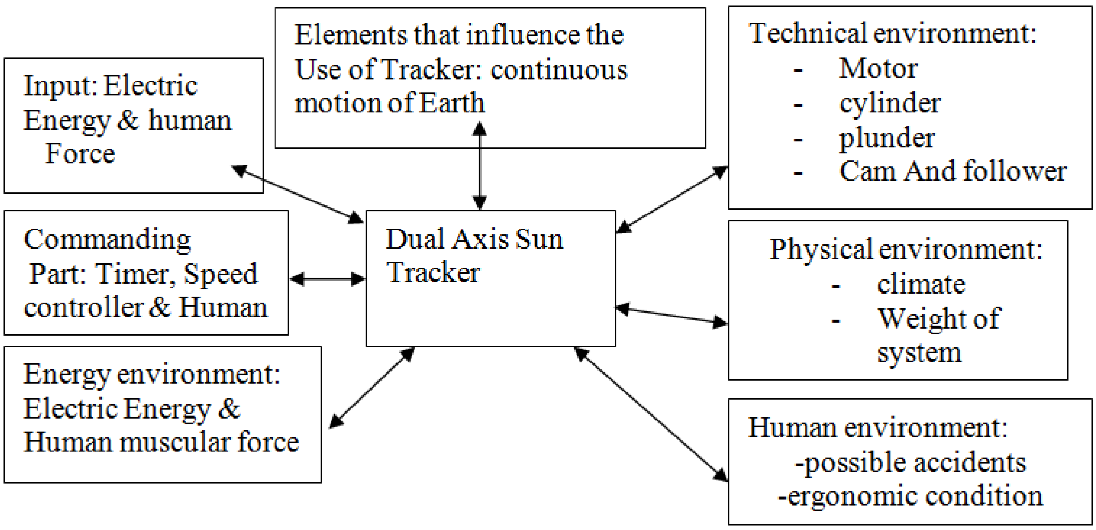

Figure 4-4-1 System Analysis

4.2. Development of Alternative Basic Structure

The following three means of rotations are considered

- Automatic Azimuth rotation and Manual Zenith rotation
- Automatic rotation of both Azimuth and Zenith
- Manual rotation of both Azimuth and zenith

These ways of operations are compared for the following criterion; ease of operation, accuracy, cost, energy usage and complexity.

The above criterion has values between one and five. One has a minimum weight and five has a maximum weight. Thus, let us make a table.

Table 4.2 Prioritizing of the means of operation of the sun tracker

Operation of rotation	Ease of operation	Accuracy	Cost	Energy usage	Complexity	Average
Azimuth-Automatic & Zenith-Manual	4	4	4	3	3	3
Azimuth-Automatic & Zenith-Automatic	5	5	1	2	2	2.5
Azimuth-Manual & Zenith-Manual	1	1	5	4	4	2.5

Based on the above prioritizing the selected operation of the sun tracker is automatic azimuth and manual zenith rotations.

4.3. Basic Structure

(Automatic Azimuth and Manual Zenith Rotation of the Sun Tracker)

There are two axis rotations. These are Azimuth and Zenith. Hence, the Azimuth rotation can be attained by the following mechanisms.

1. A motor is used to rotate the receptor along the Azimuth and the speed of the motor is reduced by gearbox.
2. A motor is used to rotate along the Azimuth and the speed of the motor is reduced by using a combination of pumps.
3. A motor is used to rotate along the Azimuth and the speed of the motor is reduced by combining the above two mechanisms, i.e., using a small gearbox and a combination of smaller pumps

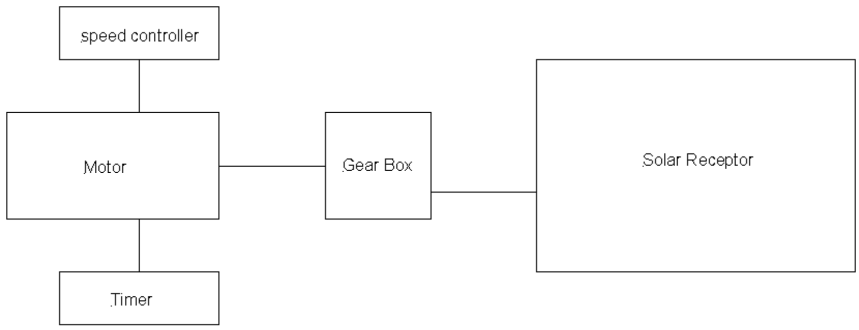

Figure 4.4-2 Schematic diagram of speed reducer using gearbox

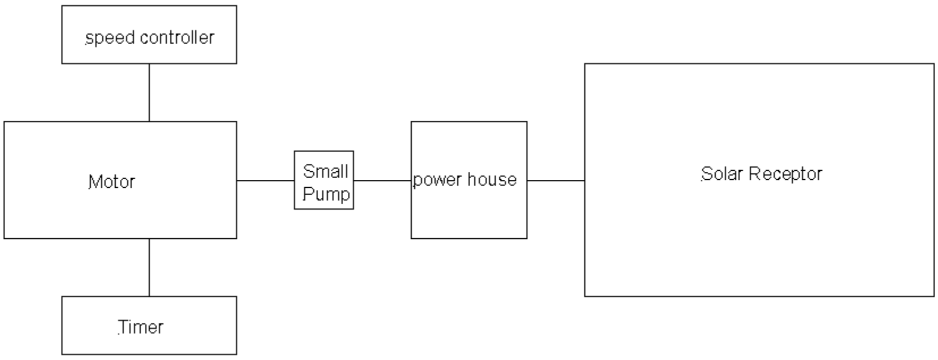

Figure 4.4-3 Schematic diagram of speed reducer using pump

The receptor is expected to rotate 180^0 per maximum of 24 hours, i.e., the speed of the receptor is 180^0/24hr (0.002083 deg/s), which is very slow. To attain this very slow speed, let us use gearbox. By using a gearbox, it is possible to reduce the speed of the motor with a speed relation as follows;

$$N_2 = N_1 \frac{\omega_1}{\omega_2} \qquad \textbf{4-1}$$

Where N_1 and N_2 are the number of teeth of the input and output shaft, ω_1 and ω_2 are the speed of the input and output shaft.

Let us assume that a minimum speed of the input shaft is 360 deg/s and the number of teeth is 24. Since the speed of the output shaft is 0.002083 deg/s, the number of teeth can be calculated for the output shaft as follows:

$$N_2 = N_1 \frac{\omega_1}{\omega_2} = 24 \times \frac{360}{1/480} = 4{,}147{,}200$$

This implies that the gearbox should be very huge which has a capacity of 24:4147200 (1:172800) gear train ratios. The gearbox is very large and expensive. Therefore, speed reduction using gearbox is not feasible.

Let us consider the second option that is the speed reducer-using pump. Here a small pump that pumps a very small amount of fluid (a droplet of fluid per stroke) and relatively small piston-cylinder are used. The pump continuously delivers a droplet of fluid into the piston-cylinder that in turn rotates the receptor. The feasibility of this system can analyze as follows by assuming the dimensions of the pump diameter and piston-cylinder.

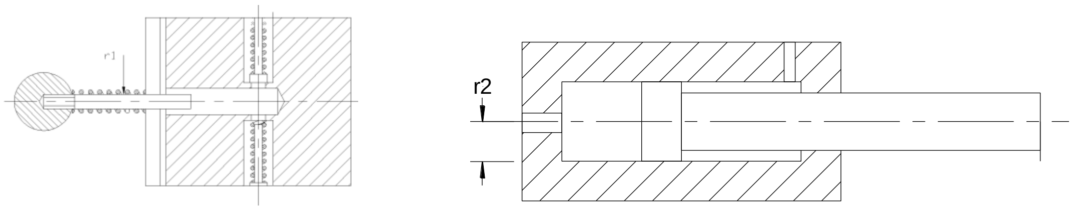

Figure 4.4-4 Sketch of Pump (left) and powerhouse (Right)

The piston of the powerhouse is extended only once per a maximum of 24 hours. This is filled by continuous delivery of the pump with many strokes. The volume of the powerhouse and pump are calculated as follows:

$$V_2 = \pi\left(\frac{D_2}{2}\right)^2 \Delta L = \pi r_2^{\,2} \Delta L \ \text{ and } \ V_1 = \pi\left(\frac{D_1}{2}\right)^2 L = \pi r_1^{\,2} L \qquad \textbf{4-2}$$

The numbers of stroke of the pump can be calculate by dividing the V_2 by V_1

$$n = \frac{V_2}{V_1} = \frac{\pi r_2^{\,2} \Delta L}{\pi r_1^{\,2} L} = \frac{r_2^{\,2} \Delta L}{r_1^{\,2} L} \qquad \textbf{4-3}$$

Let us assume the dimension r2=100 mm, r1=10mm, L=100mm and ΔL=500mm

$$n = \frac{V_2}{V_1} = \frac{\pi r_2^{\,2} \Delta L}{\pi r_1^{\,2} L} = \frac{r_2^{\,2} \Delta L}{r_1^{\,2} L} = \frac{100^2 \times 500}{10^2 \times 10} = 5000 \cdots \text{stroke}$$

The time required to complete one stroke is calculated:

$$= \frac{n}{t} = \frac{5000}{24\text{hr}} = \frac{5000}{24 \times 60\text{min}} = \frac{5000}{24 \times 60 \times 60\text{s}} = \frac{25\text{stroke}}{432\text{s}} = \frac{1\text{stroke}}{17.28\text{s}}$$

Based on the assumption, one stroke is completed within 17.28 seconds. Even if we cannot apply this directly, pump and piston-cylinder is feasible to reduce speed of the motor by incorporating a small gearbox. Therefore, the schematic diagram of the mechanism is sketched below.

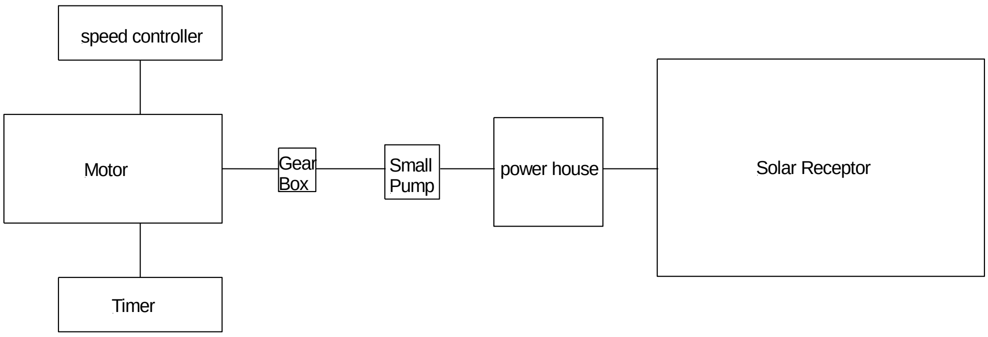

Figure 4.4-5 Schematic diagrams of Pump and piston-cylinder with gearbox sun tracker

4.4. Functional analysis

Global Function: the main function of the tracker is to rotate the receptor both in east-west and north-south directions

The function or means tree of the sun tracker is as follows:

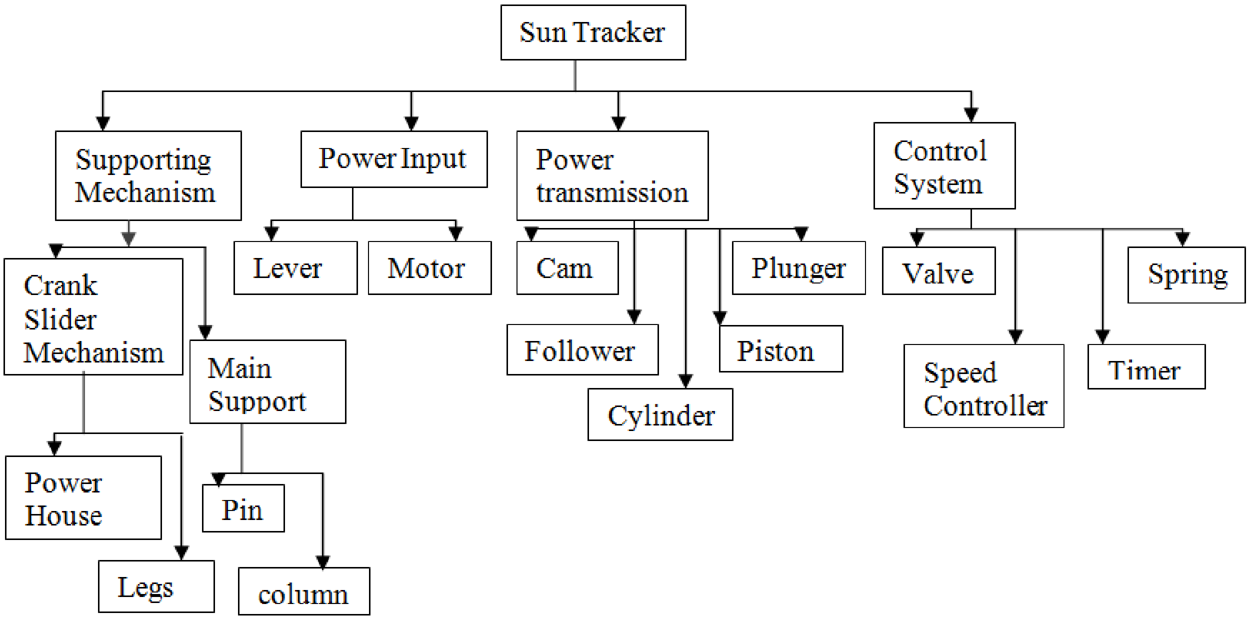

Figure 4.4-6 Functions or Means Tree

Chapter 5 Detail Design of Sun Tracker

5.1. Mathematical Equation and Simulation along Azimuth Rotation

The solar receptor is affected by two factors. The first factor is the 360^0 rotation of the earth about its orbit, which is called azimuth, within 24 hours. Within a day the earth is under two conditions that is, it can be either day or night, the length of which is depends on the season of the year. The receptor should be rotated by the tracker for 180^0 from west to east or vise versa to capture the complete available energy of the sun. The second factor is the rotation of the earth around the sun that leads inclination between ±23.5 degrees to north or south hemisphere, which is called zenith. The azimuth rotation has a great adverse effect than the zenith rotation because the azimuth rotation covers 360^0 per day where as the zenith rotation covers around 23.5^0 within three months. Hence the receptor shall rotate 180^0 per day (1^0 per 8 minutes) east west (vise versa) and 23.5 degree per three month (1^0 per 3.83 days) north south (vise versa).

Simple estimation

East-West Rotation (Azimuth): 180^0 rotation takes a maximum of 24 hours

$$\rightarrow 180^0 = 24hr = 24\times 60\min = 1440\min \qquad \rightarrow x = \frac{1^0 \times 1440\min}{180^0} = 8\min$$

$$1^0 = x?$$

This indicates that to rotate one degree, it takes 8 minutes.

North-South Rotation (Zenith): three months are required to cover 23.5^0

$$\rightarrow 23.5^0 = 3\times 30 days = 3\times 30\times 24hr = 129600\min$$

$$1^0 = x? \qquad \rightarrow x = \frac{1^0 \times 90 days}{23.5^0} = 3.83 days$$

This indicates that 3.83 days are required to rotate one degree along north south.

The sun tracker is dual axis i.e., it rotates both east-west and north-south axis. Based on the above results it is advisable to make the azimuth rotation automatic and north-south rotation manual operated. This is due to simplifying the mechanism, to reduce cost and to save the amount of energy used to drive the system.

Based on the prioritized mechanism, it was selected the crank slider mechanism. The preferred dimensions of the links can be iterated and selected from the following estimation. There are two piston cylinder systems. The first one is a plunger pump, which pumps a very small amount of fluid per stroke. The second piston cylinder system is the powerhouse, which receives fluid from Plunger pump and changes the length of the link, which in turn rotates the receptor east-west direction.

The receptor should rotate 180^0 per a maximum of 24 hours. Hence, the powerhouse should rotate the receptor 180^0 per a maximum of 24 hours based on the location of the site. Hence, the amount of fluid pumped by the Plunger pump has only a capacity of extending or retracting the powerhouse once per day. So that, a great care should be taken when the iteration is done.

Let us designate the dimensions for the pump, powerhouse and the crank slider mechanism.

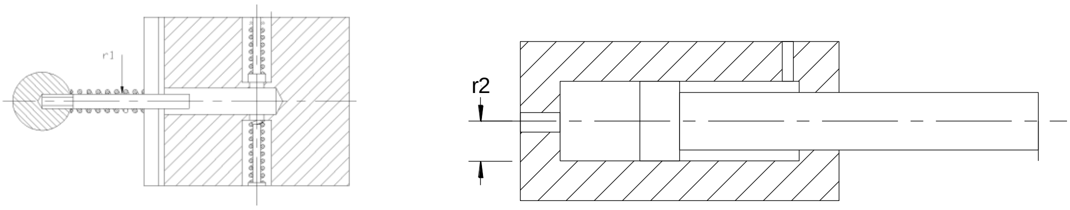

Figure 5.5-1 Simple Representations of Plunger pump and Powerhouse

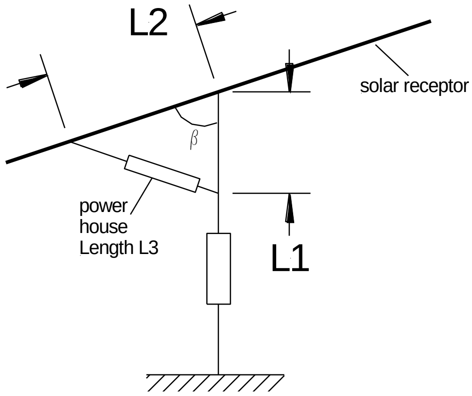

Figure 5.5-2 Free body diagram of crank slider mechanisms

The length of the link along the powerhouse in the crank slider mechanism has maximum of L_2+L_1 and a minimum of L_2-L_1. Hence, the total change in length of this link is equal to:

$$\Delta L = L_{max} - L_{min} = (L_2 + L_1) - (L_2 - L_1) = 2L_1 \quad \textbf{5-1}$$

When the powerhouse is assembled to the system, there should be a space on both ends, which can be approximated as small as possible to minimize size and reduce cost. Therefore, this can be estimated 100 mm on one end and another 100 mm on the other end. Hence, the maximum length of the powerhouse becomes:

$$L_{max} = 2\times\Delta L + 100 + 100 = (4L_1 + 200)\text{mm},\ L_{min} = L_{max} - 2L_1 \text{ and } L_2 = L_{max} - L_1 \quad \textbf{5-2}$$

The lengths $L_1, \Delta L, L_{max}, L_{min}$ and L_2 are unkonws, hence, these dimensions are estimated and optimized by iteration. Using the above relationship between these dimensions it is possible to iterate and optimized by using EXCEL [Appendix B].

ΔL is the length of the stroke of the powerhouse , L is the stroke of the plunger pump and t is the time required for one stroke of the plunger pump. The volume of the powerhouse (V_2) and the plunger pump (V_1) are calculated as follows:

$$V_2 = \pi r_2^{\,2}\Delta L \text{ and } V_1 = \pi r_1^{\,2} L \quad \textbf{5-3}$$

V_2 is filled within a maximum of 24 hours, i.e., the flow rate is equal to:

$$Q_2 = \frac{V_2}{t} = \frac{V_2}{24\text{hr}} = \frac{V_2}{24 \times 60\text{min}} = \frac{V_2}{24 \times 60 \times 60\text{s}} \quad \textbf{5-4}$$

V_1 is the volume of the plunger pump per stroke. The volume of the powerhouse is equal to

$V_2 = nV_1 = n\pi \times r_1^2 L$ Where n is the numbers of stroke of the plunger pump per a maximum of 24 hours. Hence;

$$n = \frac{V_2}{V_1} = \frac{\pi r_2^2 \Delta L}{\pi r_1^2 L} = \frac{r_2^2 \Delta L}{r_1^2 L} \quad \textbf{5-5}$$

Therefore the speed of the plunger pump is; $v = \frac{n}{24\text{hr}} = \frac{n}{24 \times 60\text{min}} = \frac{n}{24 \times 60 \times 60\text{s}}$

The internal diameters of both the powerhouse and the plunger pump, the stroke length of the plunger pump are unknown. To iterate these dimensions the length of stroke of the power should be known. The standard available size of the solar panel is between $285 \times 385 \times 45$ mm and $1650 \times 992 \times 45mm$. Since solar receptor is feasible for medium and large solar panels, the dimensions should be intermediate between medium and large. Hence, the side of the crank slider (solar panel supporter) is chosen to be 950 mm. The corresponding dimensions are Appendix B;

$\Delta L = 500\text{mm}$, $L1 = 250$ mm, $L2 = 950$ mm, $L\max = 1200$ mm and $L\min = 700$ mm.

These chosen dimensions are the core of the work of these designs. Based on these data it is possible to get D_1, D_2 and L. Based on [Appendix C], the iterations and seamless tube tables, it is advisable to choose the dimensions of:

$D_2=2r_2=210$ mm, $D_1=2r_1=5$ mm, $L_1=250$ mm, $L_2=950$ mm, $L_{max}=1200$ mm, $L_{min}=700$ mm, L=10 mm and n=88200 during extending and 8200 during retracting.

Where L_{max} is the maximum length of the powerhouse and L_{min} is the minimum length of the powerhouse. D_1 and D_2 are the internal diameters of the Plunger pump and the cylinder of the powerhouse respectively. L is the stroke of the plunger pump. L_1 and L_2 are the length of the crank slider.

The relationship between the powerhouse 1 length and the angle β can found by the following mathematical formula. Using the cosine law see figure 5.26;

$$L_3 = \sqrt{\left(L_1^2 + L_2^2 - 2 \times L_1 \times L_2 \times \cos\beta\right)} \quad \textbf{5-6}$$

The lengths L_1 and L_2 are 250 mm and 950 mm respectively. The length of the powerhouse 1 and the angle β are directly proportional to each other. The maximum length L_3 is 1200 mm at ($\beta = 180^o$) and minimum is 700 mm at ($\beta = 0^o$). The value of the length L_3 for the angle between $\beta\left[0^o, 180^o\right]$ is iterated at Appendix M.

It is shown in graph 5.1 that the length L_3 and the azimuth has a relationship that when the angle is increasing the length L3 is also increasing. The power house length is simplified by substituting L_1 and L_2 to

$$L_3 = \sqrt{(0.965 - 0.475\cos\beta)}\ \text{m}$$

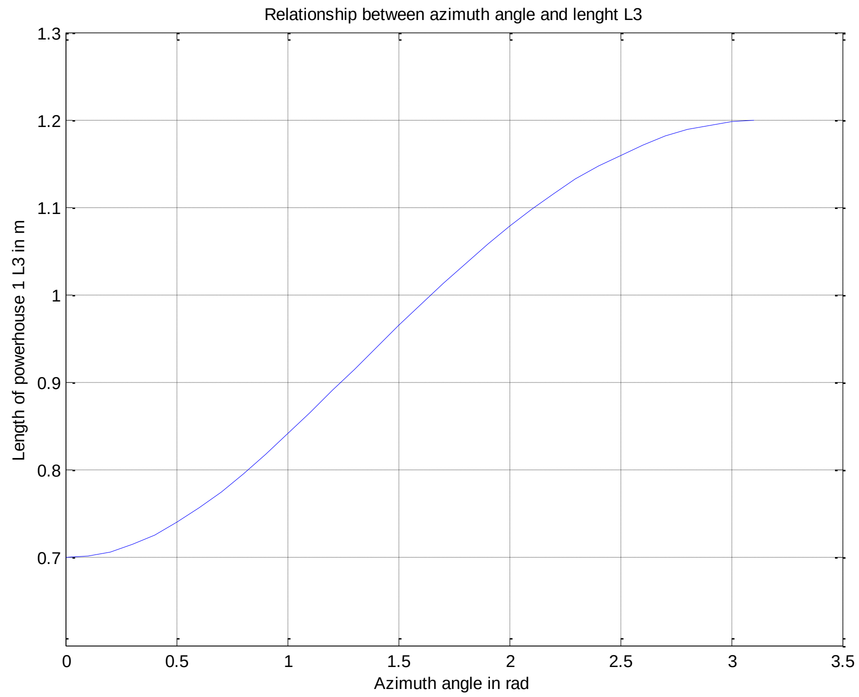

Graph 5.1. Azimuth angle vs length of power house 1

The stroke length of powerhouse 1 ΔL is equals to the difference between L_3 and minimum length of L_3.

$$\Delta L = L_3 - 700 = \sqrt{(0.965 - 0.475\cos\beta)} - 0.7\ \text{m} \quad \textbf{5-7}$$

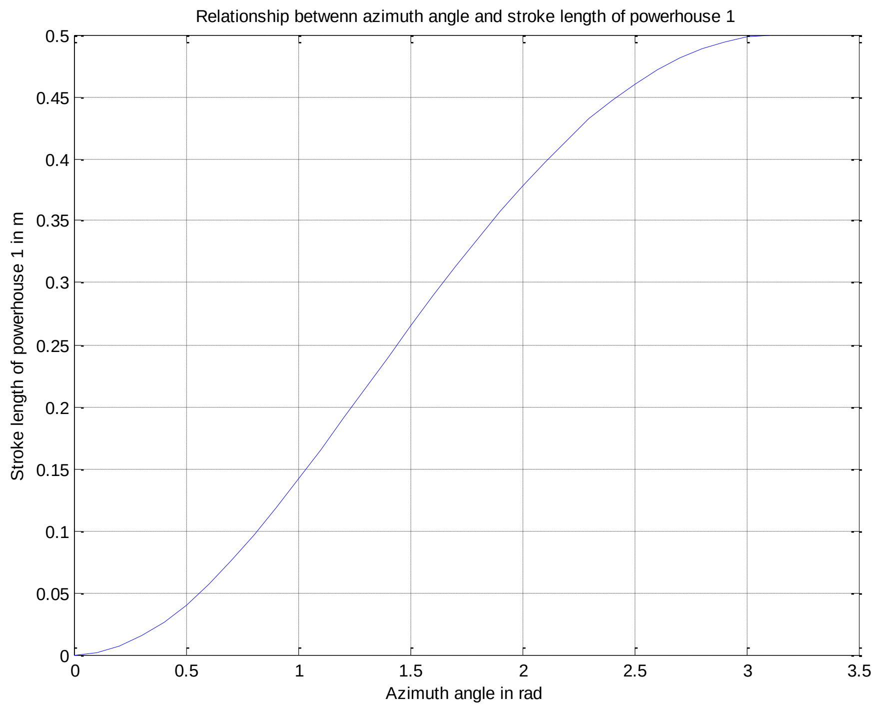

Graph 5.2 Azimuth angle vs stroke length of powerhouse 1

The rate of change of the stroke in (m/s) is simply calculated by derivating equation 5.2;

$$\Delta L' = (L_3 - 700)' = (\sqrt{(0.965 - 0.475\cos\beta)} - 0.7\text{ m})' = \frac{0.2375\beta'\sin\beta}{\sqrt{(0.965 - 0.475\cos\beta)}} \text{.....................} \mathbf{5\text{-}8}$$

β' is the angular speed of the solar receptor which is constant per day and it is between

$$\beta' = \omega = [\frac{\pi\text{rad}}{24\text{hr}}, \frac{\pi\text{rad}}{0\text{hr}}]$$

Graph 5.3 Azimuth angle vs. rate of change of stroke of powerhouse 1

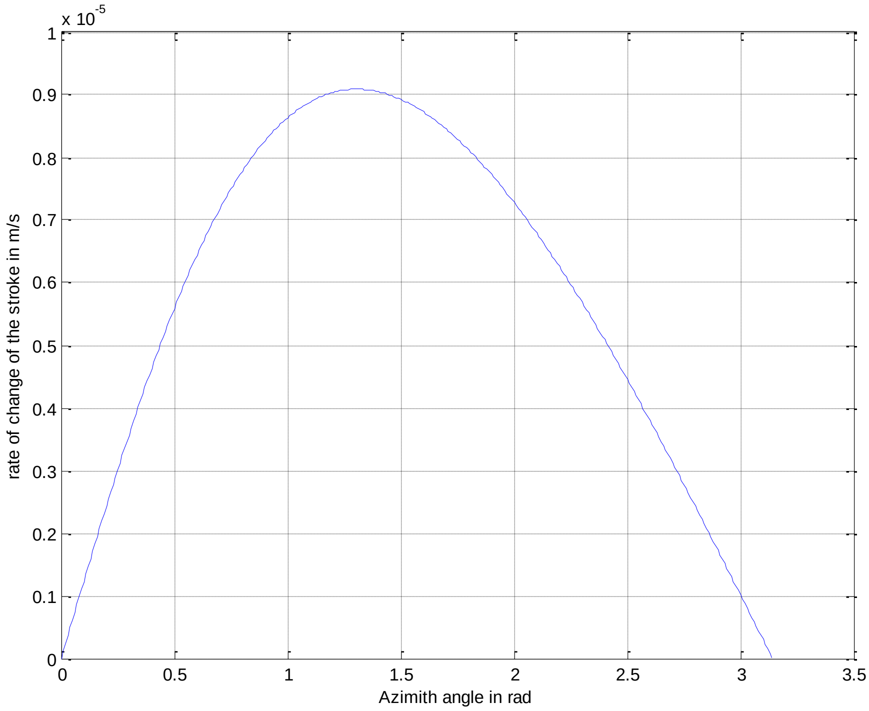

The relationship between azimuth angle and rate of change of stroke is plotted as shown in graph 5.3 using MATLAB for 12 hours length of day.

The piston has zero velocity at the two extreme points and a maximum velocity ($0.909\text{x}10^{-5}$m/s) at the azimuth angle of 1.31 rad.

General Gathered Information

The designing of the powerhouse and the plunger pump requires the amount of load applied on them. To get this applied force let us start from the standard weight of the solar panel and the weight of the supporting mechanism. The minimum and maximum weights of the solar panel are 1.5 kg and 50 kg respectively [5]. However, the weights of the supporting elements are unknown exactly. Therefore, it is possible to take an engineering approximation. The maximum dimension of the solar panel is 2000mm by 1000mm [5].

If the support elements have 5 mm thickness and 7000km/m^3 density, its weight becomes:

$$\text{mass(m)} = \text{volume} \times \text{density} = \text{v} \times \rho = [4(1 \times 0.05 \times 0.005) + 3(2 \times 0.05 \times 0.005)] \times 7000 = 17.5\text{kg}$$

By considering the mounting mechanisms, electric cable, valves and the like, the total mass of the support becomes around 25 kg. Hence, the weight is calculated as

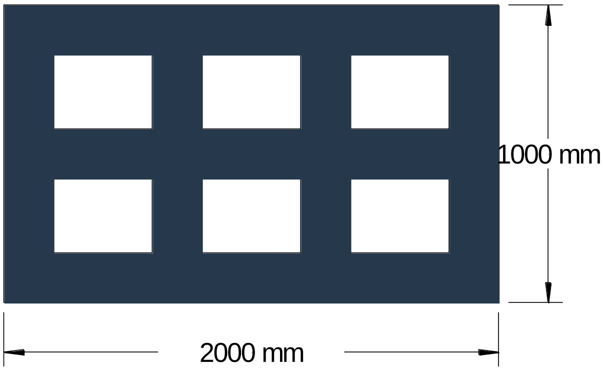

Figure 5.5-3 Solar Panel horizontal support

$$W = mg = 25 \times 9.81 = 245.25N$$

So that the total weight is equals to the sum of the weight of the solar panel and the support.

$$W = \text{weight of panel} + \text{weight of support} = 50 \times 9.81 + 245.25 = 735.75N$$

This amount of force is applied on the powerhouse of the crank slider, which comes from a single solar panel. However, the solar panel may be two, which are symmetrical about the support. The powerhouse should exert a force, which is more than twice the total weight (1471.5N force) of the system. 1471.5N amount of force should be exerted by the pressure that is created inside the powerhouse to rotate the solar receptor. Mathematically, we can relate the force and the pressure during extending the linkage as follows:

$$\text{Force(F)} = \text{Pressure(P)} \times \text{Area}(A_2)$$

Where A_2 is the inside area of the cylinder of the powerhouse which has an inside diameter of 210 mm. hence the area becomes;

$$A_2 = \pi {r_2}^2 = \pi \times 0.105^2 = 0.03464m^2$$

The pressure inside the powerhouse is equal to;

$$P = \frac{F}{A} = \frac{1500}{0.03464} = 43307.468\frac{N}{m^2} = 43.308KPa$$

Therefore, 43.308 KPa pressure should be created to rotate the receptor. This pressure is equal to pressure inside the Plunger pump but there is pressure loss in the fittings and pipelines. Even if the amount of pressure lose is not known exactly let us take 5% loss that means the pressure inside the plunger pump is equal to 1.05 times of the pressure inside the powerhouse (1.05x43.308=45.473Kpa). Hence, the amount of force that is exerted on plunger is equal to:

$$\text{Force(F)} = \text{Pressure(P)} \times \text{Area}(A_1)$$

Where A_1 is the area of the plunger of the Plunger pump, which has a diameter of 5 mm, hence the area becomes; $A_1 = \pi r_1^2 = \pi \times 0.0025^2 = 19.635 \times 10^{-6} m^2$

$F = PA_1 = 45.473 KPa \times 19.635 m_2 = 0.893 N$

Based on the above result 0.893N force should be applied on the plunger. But there are springs and frictional forces in addition to the pressure force.

5.2. Design of Pump 1

This pump 1 is used to supply hydraulic fluid to the powerhouse 1. This pump is similar to pump 2, hence its shape and dimension is taken from pump2.

Design of Pump Cover

Step 1: The Pump cover is a cylindrical shape used to make a boundary between the fluid and the environment. The maximum pressure applied on pump cover is 45.473KPa. It should have a capacity to resist wear and corrosion.

Step 2: Gathered information: The maximum pressure applied on the pump cover is P=45.473kPa

Since the plunger has outside diameter of 5 mm, the diameter of the pump cover that is subjected to pressure force should be greater than the outside diameter of the plunger. D>5mm

Step 3: Problem statement: Designing of a pump cover, which is capable of resisting 45.473KPa force that is applied intermittently.

Step 4: Determining the shape of a pump cover that is compatible with the plunger, plunger head, pump and the spring.

Among the alternative shapes of Appendix N 5.23, type A is selected because its shape can be manufactured easily. There is only one critical region in the pump cover, which is due to shearing.

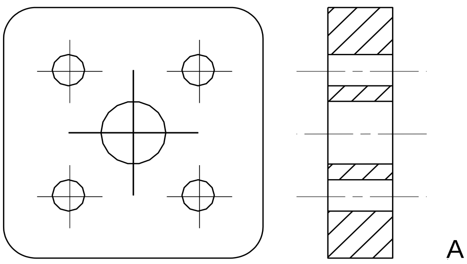

Figure 5.5-4 Selected pump cover

The cover is subjected to shearing stress. Therefore, the pump cover is designed based on the above-induced stress.

Step 5: Material selection and working stress: The material should have resistance to corrosion and wear, has low coefficient of friction and relatively low cost and weight. Aluminium alloy is the best material for corrosion resistance but it is highly affected by wear. Since the pump cover is always in contact with the plunger it should be manufactured from the wear resistant material. The plain carbon steel, Alloy steel and carbon steel have excellent resistance to wear and moderate resistance to corrosion. Therefore, carbon steel is selected since it is the cheapest of all and suitable for machining [Appendix D]. To make the system compact in size and light in weight, the factor of safety should be minimum which is 2.

Working stress= the yield stress ╱ factor of safety $\rightarrow \sigma_w = \dfrac{\sigma_y}{n}$ **5-9**

But the pump cover is subjected to reverse pressure force. We know that for reversed axial loading correction factor ka=0.8. The endurance limit for reversed axial load;

$\sigma_{ea} = \sigma_e \times k_a \times k_{sur} \times k_{sz}$ **5-10**

k_{sur} = surface finish factor=0.89 for machined with ultimate strength of 435Mpa

k_{sz} = Size factor=0.85 since nominal diameter is between 7.65 mm and 50mm

σ_e =0.8σ_y for carbon steel=0.8×217=173.6Mpa

σ_{ea} =173.6×0.8×0.89×0.85=105.063Mpa

$$\text{Working stress} = \frac{\text{Endurance limit stress}}{\text{Factor of safety}},\ \sigma_w = \frac{\sigma_{ea}}{n} \rightarrow \sigma_w = \frac{\sigma_{ea}}{n} = \frac{105.531}{2} = 52.531\text{MPa}$$

Step 6: Detailed stress analysis: The pump cover is under shearing due to a pressure of 45.473kPa force. The magnitude of the force that is applied on the cover is equal to the product of pressure inside the pump and the area of the cover in contact with the pressurized fluid.

$F = PA$ Where p is the pressure in the cylinder (45.473 KPa) and A is the net area of the cover

$A = \dfrac{\pi}{4}(D^2 - D_1^{\,2})$ Where D (10.757mm) is the inside diameter of the cylinder and D_1 $(5\,\text{mm})$ is diameter of the plunger

$$A = \frac{\pi}{4}(10.757^2 - 5^2) = 71.246\text{mm}^2 = 71.246 \times 10^{-6}\,\text{m}^2$$

The force becomes, $F = 45.473\text{KPa} \times 71.246 \times 10^{-6}\,\text{m}^2 = 3.235\text{N}$

The shear stress due to the pressure force $\sigma = \dfrac{F}{A}$**,** but $A = \pi(D - D_1)t$

$$A = \frac{F}{\sigma} = \frac{3.235\text{N}}{52.531 \times 10^6\,\text{N/m}^2} = 6.159 \times 10^{-8}\,\text{m}^2 = 0.0616\text{mm}^2$$

$$t = \frac{A}{\pi(D - D_1)} = \frac{0.0616mm^2}{\pi(10.757 - 5)} = 0.00341mm$$

Since the thickness becomes very small, we have to maximize it to a higher value, the thickness is maximized to 5 mm. The outside diameter of the pump cover should be equal to the outside diameter of the pump that is equal to 58 mm.

Design of Spring 1 and 2

Step 1: The spring 1 and 2 are compressive type of springs that is used to open or close the suction or discharge valves of the plunger pump respectively after it pumps the fluid. The force that pushes this spring is the internal pressure (45.473KPa) created inside the cylinder. Hence, the spring has a capacity to return the valve to its closed position.

Step 2: Gathered information: The maximum pressure applied on the valve is P=45.473kPa. In addition, the maximum possible diameter of the valve and spring should less than the internal diameter (10.757mm) of the cylinder because the valve seat is placed inside the cylinder.

The deformed length should also be smaller to minimize the back flow of the fluid because the amount of fluid pumped per stroke is very small (196.25 mm^3).

Step 3: Problem statement: Designing of a spring which is capable of compressed by 45.473KPa pressure force

Step 4: Determining the shape of a spring that is compatible with the valve, valve seat and valve cover. The type of spring is ground closed end because it is stable and suitable for the valve.

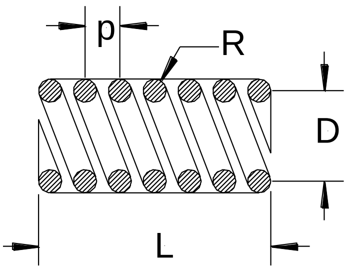

Figure 5.5-5 Spring 1

Since the spring is axially loaded, it is subjected to shearing and twisting its total effect is shearing.

Step 5: Material selection and working stress: The material should have resistance to corrosion and wear, good elastic nature, low coefficient of friction and relatively low cost and weight.

Common spring wires with the highest strengths are ASTMA228 (music wire) and ASTMA401 (oil-tempered chrome silicon). Wires having slightly lower tensile strength and with surface equality suitable for static applications are ASTMA313 type 302 (stainless steel), ASTMA230 (oil-tempered carbon valve-spring-quality steel), and ASTMA232 (oil-tempered chrome vanadium). For most fatigue applications ASTMA227 (hard-drawn carbon steel) and ASTMA229 (oil-tempered carbon steel) are available at lower strength levels [3]. Hence ASTMA230 (oil-tempered carbon valve-spring-quality steel) is selected [Appendix E]. The allowable shear stress of the ASTMA230 (oil-tempered carbon valve-spring-quality steel) is 525MPa for light service.

The spring is under fatigue load so that the endurance limit should be calculated as follows;

$$\tau_{ea} = \tau_e \times k_a \times k_{sur} \times k_{sz}$$

k_a =0.8 load factor for reverse axial loading

k_{sur}= surface finish factor =0.75 for machined with ultimate strength of 1120Mpa

k_{sz} =Size factor=1 since nominal diameter is less than7.65 mm

$\tau_e = 0.8\tau_{all}$ for carbon steel=0.8×525=420Mpa

$\tau_{ea} = 420 \times 0.8 \times 0.75 \times 1 = 252\text{MPa}$

$$\text{Working stress} = \frac{\text{Endurance limit stress}}{\text{Factor of safety}} \quad \tau_w = \frac{\tau_{ea}}{n} = \frac{252}{2} = 126MPa$$

Step 6: Detailed stress analysis: The spring is pushed by a pressure of 45.473kPa force. The magnitude of the force applied on the spring is equal to the product of pressure and inside diameter of the cylinder for the strength purpose.

$F = PA$ Where p is the pressure in the cylinder (45.473KPa) and A is the net area of the cover

$$A = \frac{\pi}{4}(D_i^{\ 2})$$

Where D_i is the inside diameter of the cylinder and $D_i = 10.757\text{mm}$

$$A = \frac{\pi}{4}(10.757^2) = 90.881\text{mm}^2 = 90.881 \times 10^{-6}\text{m}^2$$

The force becomes, $F = 45.473\text{KPa} \times 90.881 \times 10^{-6}\text{m}^2 = 4.133\text{N}$

The maximum shear stress in the spring is found by using, $\tau_{max} = \frac{8FD}{\pi d^3} + \frac{4F}{\pi d^2}$

Where D and d are mean and wire diameters of the compression spring. Substituting the working shear stress and the force in the above equation;

$$126 \times 10^6 = \frac{8 \times 4.133D}{\pi d^3} + \frac{4 \times 4.133}{\pi d^2} = \frac{10.525D}{d^3} + \frac{5.262}{d^2}$$

The minimum and maximum standard wire diameter of the oil-tempered carbon valve-spring is between 1.3mm and 6.35 mm [3]. The optimized size of the spring is found by iterating for the wire diameter between 1.3 and 6.35 mm using the above formula.

According to the [appendix F], the mean diameter is between 5.98 mm and 769.79 mm. The space available for the outer diameter is less than 10.575 mm. Therefore, the mead diameter of the spring should as small as possible is preferred. Hence, the smallest values are selected to meet the space requirement.

D=5.98mm and d=1.3mm

The outside diameter of the spring becomes; D_o=D+d=5.98+1.3=7.28mm

The spring index is becomes, $C = \frac{D}{d} = \frac{5.98}{1.3} = 4.6$

The maximum induced shear stress in the spring is equal to,

$$\tau_{max} = \frac{8FD}{\pi d^3} + \frac{4F}{\pi d^2} = \frac{8 \times 4.133N \times 5.98 \times 10^{-3} m}{\pi \times (1.3 \times 10^{-3} m)^3} + \frac{4 \times 4.133N}{\pi \times (1.3 \times 10^{-3} m)^2} = 28646835 + 18620.443 = 28.665MPa$$

The maximum induced stress is less than the endurance limit of the spring; this implies that the design is safe.

Now let us check the stability of the spring. The spring is fabricated from steel, so that the following criteria should be fulfilled for steel [4].

$$L < 2.63 \frac{D}{\alpha}$$

Where α is the end condition constant, since the spring end condition is spring supported between flat parallel surfaces (fixed ends) is 0.5. Therefore, the free length becomes,

$$L < 2.63 \times \frac{5.98mm}{0.5} = 31.455mm$$

A very small amount of length is preferred to make compact and strong to prevent buckling of the spring. But there should be enough space free length of the spring to have free movement of fluid. Hence, its preferred free length is 20 mm.

L=20 mm

The free length for closed end and ground spring is found by using the following formula;

$$L = P \times N + 2d \rightarrow 20mm = P \times N + 2 \times 1.3mm$$

Where p is the pitch and N is the number of active coils. Since none of these two (P or N) parameters are unknown they can be analyzed by iteration.

Table 5.3 iteration of spring N and p

N	1	2	3	4	5	6	7	8	9	10	11	12	13	14	15	16	17	18
P(mm)	17.400	8.700	5.800	4.350	3.480	2.900	2.486	2.175	1.933	1.740	1.582	1.450	1.338	1.243	1.160	1.088	1.024	0.967

The pitch should greater than the wire diameter of the spring (1.3mm). The pitch is advisable to make 2.486 mm and the corresponding numbers of active coils are 7. The total number of coils is found by using the following equation.

$$N_t = \frac{L - 2d}{P} + 2 = \frac{20mm - 2 \times 1.3mm}{2.486mm} + 2 = 9$$

Solid length of the spring is calculated as follows, $L_s = N_t \times d = 5 \times 1.3mm = 11.7mm$

The maximum deflection of the spring should be advisable as small as possible to prevent the back flow of the fluid, which in turn disturbs the timing of the tracker. So that the maximum deflection of the spring is equals to the difference between the free length and solid length of the spring.

$$\delta = L - L_s = 20 - 11.7 = 8.3mm$$

Design of Valve

Step 1: The valve is used to prevent the back flow of the fluid. It should withstand a pressure force of 45.473KPa and be wear resistant.

Step 2: Gathered information: The maximum pressure applied on the valve is P=45.473KPa and its outer diameter should be less than the inside diameter of the valve seat.

Step 3: Problem statement: Designing of a valve that is capable of resisting 45.473KPa pressure force, which is applied intermittently

Step 4: Determining the shape of the valve, which is compatible with the valve seat and spring.

Among the alternative forms in Appendix N 5.24, A is chosen because its manufacturing simplicity, compact in size and compatible to the valve seat and the spring.

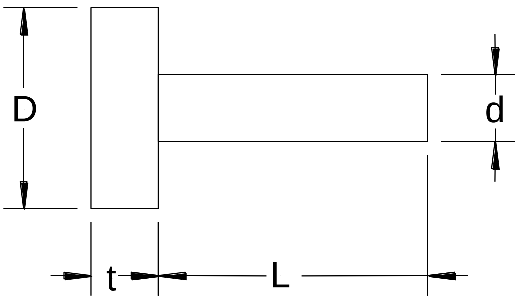

Figure 5.5-6 Valve

The diameter (d) of valve is equal to the inside diameter of the spring. The length of the valve is less than the length of the spring. In addition, the diameter (D) of the valve is approximately equals to the outer diameter of the spring.

$$d = \text{mean diameter - wire diameter} = 5.98 - 1.3 = 4.68mm$$

$$L = \text{length of the spring - clearance} = 20 - 5 = 15mm \text{ and}$$

$$D = \text{mean diameter of the spring} = 5.98mm \cong 6mm$$

The head of the valve is under shearing stress.

Step 5: Material selection and working stress: The material should have resistance to corrosion and wear, has low coefficient of friction and relatively low cost and weight. Aluminium alloy is the best material for corrosion resistance but it is highly affected by wear. Since the valve is always in sliding motion it should be manufactured from the wear resistant material. The plain carbon steel, Alloy steel and carbon steel have excellent resistance to wear and moderate resistance to corrosion. Therefore, carbon steel is selected since it is the cheapest of all and suitable for machining [Appendix D]. To make the system compact in size and light in weight, the factor of safety should be minimum which is 2.

Working stress= the yield stress ∕ factor of safety

However, the valve is subjected to reverse axial loading. We know that for reversed axial loading correction factor ka=0.8. The endurance limit for reversed axial load;

$$\tau_{ea} = \tau_e \times k_a \times k_{sur} \times k_{sz}$$

k_{sur}= surface finish factor =0.89 for machined with ultimate strength of 435Mpa

k_{sz} =Size factor=1 since nominal diameter is less than 7.65mm

τ_e=0.8 τ_y for carbon steel=0.8×217=173.6Mpa

τ_{ea}=173.6×0.8×0.89×1=123.603Mpa

$$\text{Working stress} = \frac{\text{Endurance limit stress}}{\text{Factor of safety}} \quad \tau_w = \frac{\tau_{ea}}{n} = \frac{123.603}{2} = 61.802MPa$$

Step 6: Detailed stress analysis: The valve head is under shearing due to a pressure of 45.473kPa force. The magnitude of the force that is applied on the cover is equal to the product of pressure inside the cylinder and the area of the valve head in contact with the pressurized fluid. The maximum force applied on the valve for strength purpose is 4.133N force:

$$\tau = \frac{F}{A}, \text{ but } A = \pi(d)t, \ \mathrm{A} = \frac{\mathrm{F}}{\tau} = \frac{4.133\mathrm{N}}{61.802\times10^{6}\,\mathrm{N/m^2}} = 6.687\times10^{-8}\mathrm{m}^2 = 0.0669\mathrm{mm}^2$$

$$\mathrm{t} = \frac{\mathrm{A}}{\pi \mathrm{d}} = \frac{0.0669\mathrm{mm}^2}{\pi\times4.68\mathrm{mm}} = 0.00455\mathrm{mm}$$

The thickness of the valve head is very small so that it is advisable to maximize its thickness to prevent bending and deflecting from normal shape to 3 mm.

Design of Spring 3

Step 1: The spring 3 is a compressive type of spring, which is used to return the plunger to its normal position, to prepare it for the next stroke. There is an opposing force created inside the cylinder due to vacuum creation. Therefore, the force of spring 3 must be greater than the pressure force inside the cylinder.

Step 2: Gathered information: The plunger pump is totally isolated from the atmospheric air.

Thus, the external pressure applied on the cylinder is only due to the fluid pressure. The density of the fluid is 870 Kg/m^3. When the plunger pump is opened the external fluid oppose its motion. This opposing force is $F = PA = \rho ghA$

Where ρ is density of the fluid g is gravity, h is height of the fluid with a maximum of 1 m and A is area of the plunger cover (17.165 mm diameter)

$$F = PA = \rho ghA = 870\frac{Kg}{m^3}\times 9.81\frac{m}{s^2}\times 1m\times\frac{\pi\times(17.165\times 10^{-3}m)^2}{4} = 1.975N$$

More than 1.975 N force is required the plunger pump cylinder cover. This means the spring 3 should have a capacity to apply more than 1.975 N after compression. By considering other frictional and drag force it is possible to maximized this force to spring 2 force (F=4.782 N). The deflection of the spring 3 should greater than the stroke of length (10mm) of the plunger. It is possible to use the same type of spring for both spring 2 and spring 3. Hence, the spring 3 has the following parameters

$d = 1.5\,mm,\ D = 6.5\,mm,\ D_o = 8mm,\ N = 7,$ and $P = 3.143\,mm$

$$N_t = \frac{L-2d}{P} + 2 = \frac{25mm - 2\times 1.5mm}{3.143mm} + 2 = 9$$

Solid length of the spring is calculated as follows, $L_s = N_t \times d = 9\times 1.5mm = 13.5mm$

The maximum deflection of the spring is equals to the difference between the free length and solid length of the spring.

$\delta = L - L_s = 25 - 13.5 = 11.5mm$

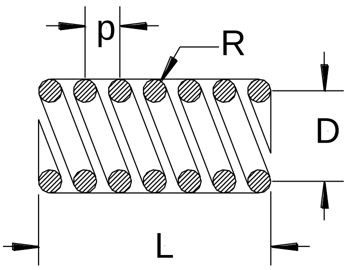

Figure 5.5-7 Spring 3

Design of Plunger

Step 1: The Plunger is a cylindrical shape used to displace the fluid in the cylinder by using a force comes from the cam. This plunger should withstand a maximum force of 4.782 N. Since the plunger has a contact with climate, it should be capable to resist corrosion.

Step 2: Gathered information: The maximum force applied on the plunger is F=4.782 N and the diameter of the plunger is, D=5mm

Step 3: Problem statement: Designing of a plunger, which is capable of resisting 4.782 N forces that is applied intermittently.

Step 4: Determining the shape of a plunger, which is compatible with the cylinder, springs, casing, and the two ends.

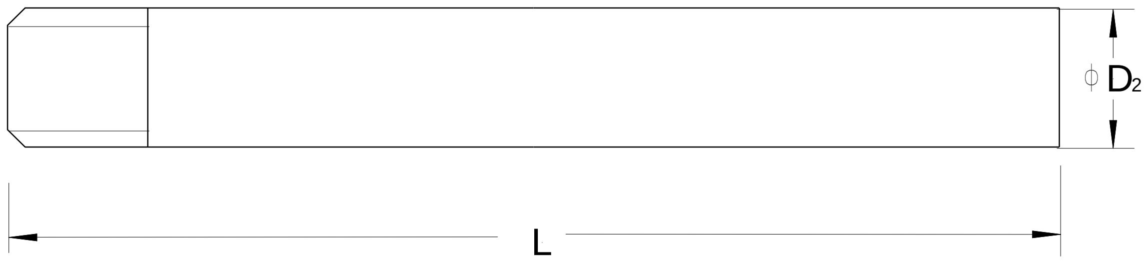

Figure 5.5-8 Plunger

There is two critical regions in the plunger, which are the threaded part and d (spring hold). The spring hold diameter is simply taken from the outside diameter of the spring. The diameter of the plunger is subjected to repeated stress (both compressive and tensile) and the length of the plunger is subjected to buckling.

Step 5: Material selection and working stress: The material should have resistance to corrosion and wear, has low coefficient of friction and relatively low cost and weight. Aluminium alloy is the best material for corrosion resistance but it is highly affected by wear. Since the plunger is always in sliding motion it should be manufactured from the wear resistant material. The plain carbon steel, Alloy steel and carbon steel have excellent resistance to wear and moderate resistance to corrosion. Therefore, carbon steel is selected since it is the cheapest of all and suitable for machining [Appendix D]. To make the system compact in size and light in weight, the factor of safety should be minimum which is 2.

Working stress= the yield stress ╱ factor of safety $\rightarrow \sigma_w = \frac{\sigma_y}{n}$

But the plunger is subjected to reverse axial loading. We know that for reversed axial loading correction factor ka=0.8. The endurance limit for reversed axial load;

$\sigma_{ea} = \sigma_e \times k_a \times k_{sur} \times k_{sz}$

k_{sur}= surface finish factor =0.89 for machined with ultimate strength of 435Mpa

k_{sz} =Size factor=1 since nominal diameter is less than 7.65 mm

σ_e =0.8σ_y for carbon steel=0.8×217=173.6Mpa

σ_{ea} =173.6×0.8×0.89×1=123.603Mpa

$$\text{Working stress} = \frac{\text{Endurance limit stress}}{\text{Factor of safety}} \rightarrow \sigma_w = \frac{\sigma_{ea}}{n} \frac{123.603}{2} = 61.802\text{MPa}$$

Step 6: Detailed stress analysis

1. Checking for diameter: of the diameter of the plunger is strong enough to withstand

the 4.782 N force:

$$\sigma=\frac{F}{A},\text{but } A=\pi\left(\frac{d^2}{4}\right)=\frac{F}{\sigma}=\frac{4.782\text{ N}}{61.802\times10^6\,\text{N/m}^2}=0.077\text{mm}^2\rightarrow d=\sqrt{\left(\frac{4\times A}{\pi}\right)}=0.3134\text{mm}$$

But, the actual diameter is 5 mm which shows the plunger is safe.

2. Calculating the length of the plunger; the length of the plunger is calculated by applying buckling principle.

The critical force that can be applied on a given length L of column is;

$F_{crit}=\frac{n^2\pi^2EI}{L^2}$ Where n is the type of buckling, which has a value of one with a form of Appendix N 5.41;

E=201 G Pa for carbon steel and $I=\frac{\pi r^2}{4}=\frac{\pi\times(2.5\times10^{-3})^2}{4}=4.909\times10^{-6}\text{m}^4$

$$4.782\text{ N}=\frac{1^2\times\pi^2\times201\times10^9\times4.909\text{Pa}\times10^{-6}\text{m}^4}{L^2}=\frac{9.738\times10^6\,\text{Pa}\times\text{m}^4}{L^2}$$

$$L^2=\frac{9.738\times10^6\,\text{Pa}\times\text{m}^4}{4.782\text{ N}}=2.036\times10^6\text{m}^2\rightarrow L=1427.032\text{m}$$

This implies that the plunger can withstand 1427.032 m length without buckling but the actual length is very much smaller this we will decide the exact length after calculating the length of the springs and the thickness of the casing (52 mm).

5.3. Detail Design of Powerhouse 1

The powerhouse is one link of the Crank Slider mechanism in which its function is to rotate the solar receptor by either extending or retracting this link. This piston-cylinder assembly is

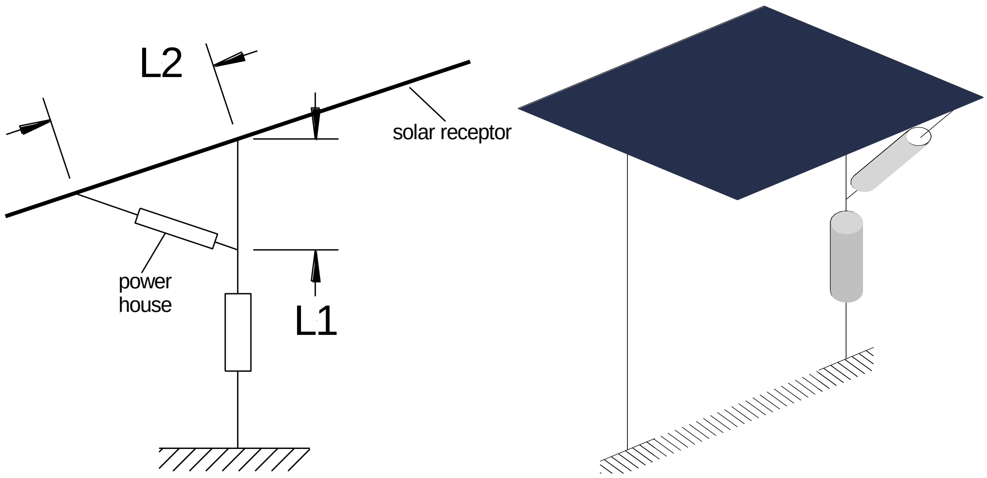

Figure 5.5-9 simple sketch of the Crank Slider mechanism

operated by the fluid that comes from the Plunger pump. The simple sketch of the crank slider is drawn in figure 5.15.

The powerhouse has alternative forms in Appendix N 5.27. Among them, we can prioritize

the best shape.
Shape A and B are somewhat similar and both have thread joint with the cover. Type A is shorter in length and wider than type B. On the other hand, type B is thinner, longer, and susceptible to leak via the thread joint. In both cases, manufacturing time is longer and more difficult than type C. In contrary type C is easy to manufacture, assemble and disassemble due to the bolt and nut connection. And also it has negligible leakage. Therefore, it is preferable to select type C.
The selected form has the alternatives shown in Appendix N 5.27. Between these two alternatives form C-A is better than C-B because the length of the cylinder is reduced. In addition, the dimension of the crank slider can be reduced. Due to these reasons the cost, weight and size are reduced considerably.
The detail drawing is sketch as shown below.

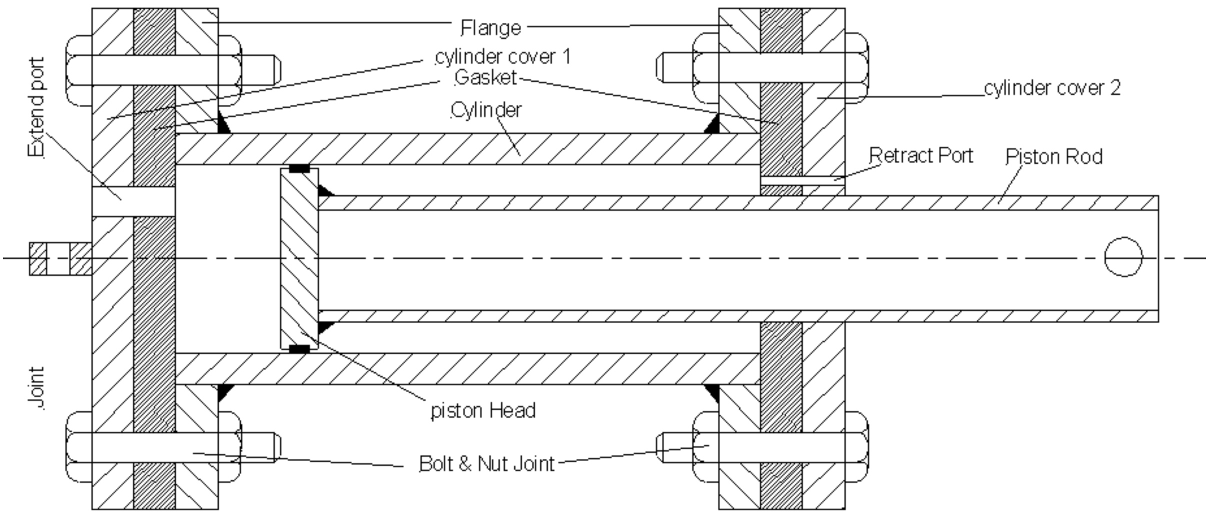

Figure 5.5-10 Detail Representation of the powerhouse

When the fluid is entered into the cylinder via extending port the piston is pushed forward and the receptor is forced to rotate from its initial position (morning) towards final position (night). At night the fluid is entered via retract port which retracts the link of the powerhouse. This in turn brings the receptor towards its initial position. Since the volume in the retract side is very small it takes few time to retract while the volume in extend port is large hence it take more times to extend with a maximum of 24 hours. Thus, energy can be saved during retraction of the piston.

Design of the Cylinder

Step1: The cylinder is a hollow cylindrical shaped material, which is used to receive the fluid from the plunger pump and transmits power to the piston rod. The cylinder should have strength to resist the stress caused by the internal pressure. The parameters that make the cylinder strong enough are the material of the cylinder and the thickness of the cylinder, since the cylinder is always in contact with fluid and climate, it should be fabricated from corrosion resistant materials.

Step2: Gathered information: The internal pressure induced in the cylinder is $P_i = 43.308 Kpa = 43.308 \frac{N}{m^2}$, the internal diameter of the cylinder is 210 mm and its stroke length is 500 mm.

Step3: Problem statement: Designing a pressure cylinder, which has capable of resisting 43.30KPa, internal diameter of 210 mm and the stroke of the piston is 500 mm.

Step4: Determine the shape of the cylinder, which is compatible with the piston, cylinder cover and joints. The critical stress region in the cylinder is in its thickness. On the thickness of the cylinder, it should be checked for hope stress and longitudinal stress.

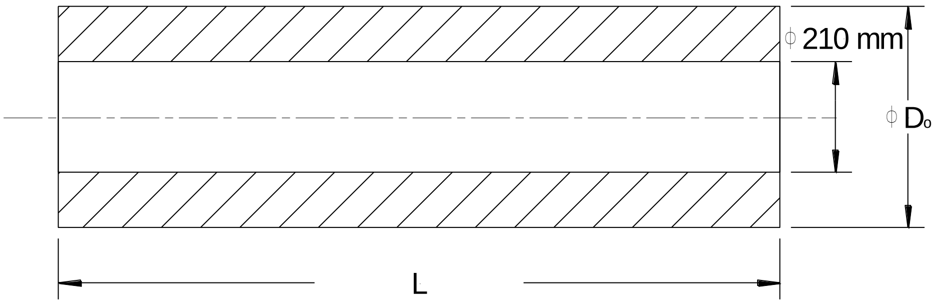

Figure 5.5-11 Cylinder

Step5: Material selection and working stress: Since welding is used for fabricating this cylinder only weldable material with less than 0.3% carbon should be considered. Plain carbon steel is unsuitable for welding. Alloy-steel is weldable but it is very expensive. Al-alloy has excellent casting characteristics, pressure tightness, good wed ability and very good corrosion resistance, but it is the most expensive. Galvanized carbon steel is weldable material. In addition, it is the cheapest of all. Therefore, the material for cylinder is galvanized carbon steel [Appendix D]. The factor of safety shall be two to make a compact size, reduced weight and cost cylinder.

$$\text{working stress} = \frac{\text{yield stress}}{\text{factor of safety}} = \frac{\text{yield stress}}{n} \rightarrow \sigma_w = \frac{\sigma_y}{n} = \frac{217 MPa}{2} = 108.5 MPa$$

Step6: detailed stress analysis;

1. Calculation of the minimal thickness of the cylinder:

The cylinder should be classified either thin or thick. If the ratio of the wall thickness and the internal diameter of the cylinder is less than 0.1 it is thin cylinder. On the other hand if it is greater than 0.1 the cylinder is thick [2]. Using the seamless tube standard data the possible minimum and maximum thickness of the cylinder is 3.967 mm and 4.781 mm respectively

[1]. Dividing these (3.967 mm and 4.781 mm) to the internal diameter of the cylinder (210 mm) results a ratios of 0.019 and 0.023 respectively. Since the ratio is less than 0.1, the cylinder is thin.

In thin cylinder, the longitudinal stress is half of the circumferential or hoop stress. Therefore, the design of a pressure vessel must be based on the maximum stress i.e. hoop stress [1]. The thickness is calculated by the formula,

$$t = \frac{P \times d}{2\sigma_w} \text{ where P is internal fluid pressure} = 43.308\text{KPa and d is internal cylinder diameter} = 210\text{ mm}$$

$$t = \frac{43.308\text{KPa} \times 0.21\text{m}}{2 \times 108.5\text{MPa}} = 41.911 \times 10^{-6}\text{m} = 0.0419\text{mm}$$

The thickness of the cylinder that can withstand the 43.308KPa internal pressure becomes very small. Hence, the minimum available standard thickness should be selected [2]. The minimum standard thickness is, $t = 3.967\text{mm}$

The corresponding outside diameter of the cylinder becomes,

$$D_o = D_i + 2t = 210 + 2 \times 3.967 = 217.934\text{mm}$$

The length of the cylinder is equal to the sum of the stroke of the piston and clearance between the cylinder and the cylinder cover. The stroke of the piston is 500 mm.

Design of Piston

Step1: The piston is a cylindrical shaped material, which is used to receive the fluid power and transfers to the solar receptor to rotate it. The end of the piton rod should be closed to prevent accumulation of water and other entries.

Step2: Gathered information: The internal pressure induced in the cylinder is $P_i = 43.308\text{Kpa} = 43.308\frac{\text{N}}{\text{m}^2}$, the internal diameter of the cylinder is 210 mm and its stroke length is 500 mm.

Step3: Problem statement: Designing a piston, which has capable of resisting 43.30KPa, internal diameter of less than 210 mm and the stroke of the piston is 500 mm.

Step4: Determine the shape of the piston, which is compatible with the cylinder, cylinder cover and joints.

Among the alternatives in Appendix N 5.28, B is selected because its weight is considerably reduced. The diameter of the piston rod should be as large as possible to make it as a quick return mechanism, i.e., it takes long time to follow up the sun but short time to return to in its initial position. The two parts that is the piston head and the piston rod are joined by welding. The critical stress regions in the piston are in the diameter and thickness of piston head, in the diameter, thickness and length of piston rod, and at the welding permanent joint.

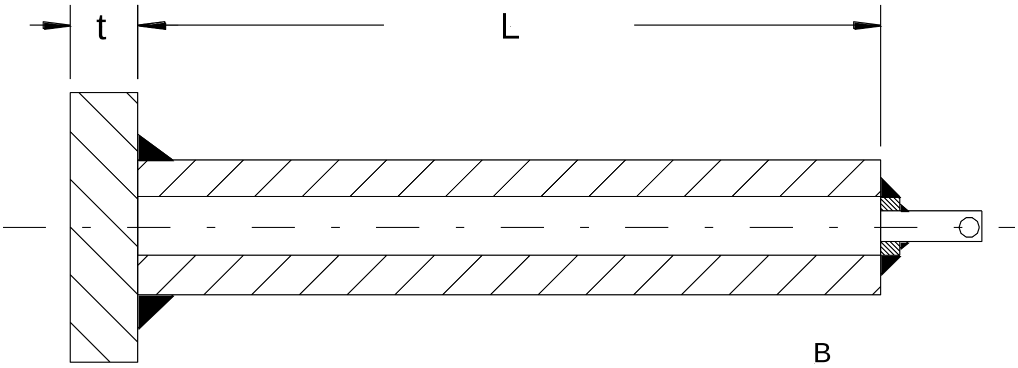

Figure 5.5-12 Selected Piston

Step5: Material selection and working stress: Since welding is used for fabricating this piston only weldable material with less than 0.3% carbon should be considered. Plain carbon steel is unsuitable for welding. Alloy-steel is weldable but it is very expensive. Al-alloy has excellent casting characteristics, pressure tightness, good wed ability and very good corrosion resistance, but it is the most expensive. Galvanized carbon steel is weldable material. In addition, it is the cheapest of all. Therefore, the material for piston is galvanized carbon steel [Appendix D]. The factor of safety shall be two to make a compact size, reduced weight and cost piston.

$$\text{working stress} = \frac{\text{yield stress}}{\text{factor of safety}} = \frac{\text{yield stress}}{n} \rightarrow \sigma_w = \frac{\sigma_y}{n} = \frac{217\text{MPa}}{2} = 108.5\text{MPa}$$

Step6: detailed stress analysis

1. Finding the thickness of the piston head; the diameter of the piston head is known which is equal to the internal diameter of the cylinder (210 mm). The shearing force is equals to the product of fluid pressure and piston head area,

$$\text{F} = \text{PA where A} = \pi\frac{d^2}{4} = \pi\frac{0.21^2}{4} = 0.03464\text{m}^2 \rightarrow \text{F} = 43.308\text{KPa}\times 0.03464\text{m}^2 = 1500.018N$$

The piston head will fail due to shear stress. Hence the stress developed in the head is,

$$\tau = \frac{F}{A} \text{ where A} = \pi D_p t \text{ and F} = \text{PA} \rightarrow \text{A} = \frac{F}{\tau} = \frac{1500.018\text{N}}{108.5\text{MPa}} = 13.825\text{mm}^2 \rightarrow t = \frac{A}{\pi D_p} = \frac{13.825\text{mm}^2}{\pi\times 210\text{mm}} = 0.021\text{mm}$$

The thickness of the piston head is becomes very small so we have to maximize it because there is a welding between the piston head and the piston rod. Hence, the thickness becomes 5 mm.

2. Finding the diameter and length of the piston rod: The piston rod is selected from standard seamless tube where its outer diameter is less than the internal diameter of the cylinder (210 mm). The standard diameter of the seamless tube less than 210 mm is 200 mm and the thickness is equal to 3.048 mm [1]. The piston rod should be

checked for tensile stress and buckling:

The stress induced in the piston rod is,

$$\sigma = \frac{F}{A} A = \frac{\pi}{4}(D_o{}^2 - D_i{}^2) = \frac{\pi}{4}(0.2^2 - 0.194^2) = 1.857\times10^{-3}m^2 \rightarrow \sigma = \frac{1500N}{1.857\times10^{-3}m^2} = 807893.112Pa$$

Since the induced stress is much less the working stress of the design is safe.

According to Euler's theory the buckling load F under various end conditions is represented by a general equation [4],

$$F = \frac{C\pi^2 EAk^2}{L^2} = \frac{C\pi^2 EI}{L^2}$$

Where E= modulus of elasticity for the material of the column, A=area of cross-section

$k =$ least radius of gyration of the cross-section $= \frac{I}{A}$, $I =$ mmoment of inertia, $L =$ length of the column,

and $C =$ constant, representing the end conditions of the column or end fixity coefficient

E=207GPa, $A = 1.857\times10^{-3}m^2$, $I = \frac{\pi}{64}(D_o{}^4 - D_i{}^4) = \frac{\pi}{64}(0.2^4 - 0.194^4) = 9.009\times10^{-6}m^4$ and C=4 for end condition of both ends fixed

$$F = \frac{4\times\pi^2\times207GPa\times9.009\times10^{-6}}{L^2}\ L^2 = \frac{4\times\pi^2\times207GPa\times9.009\times10^{-6}m^4}{1500N} = 49081.227m^2 \rightarrow L = 221.543m$$

The length of the piston rod will not buckle because its actual length is much less than the expected length. Hence, the design is safe for buckling.

Design of the End Hook

Step 1: The end hook is used to connect the powerhouse and the solar receptor with a pinned joint. The hook should have a capacity to resist to corrosion and wear.

Step 2: Gathered information: The maximum force applied on the hook is 1500 N either compressive or tensile.

Step 3: Problem statement: Designing of a hook, which is capable of resisting 1500 N force that is compressive or tensile.

Step 4: Determining the shape of the end hook that is compatible with the plunger, plunger cover, solar receptor and the solar receptor joint

Among the alternative shapes in Appendix N 5.29, type B is selected because its shape can be manufactured easily by casting due to its rectangular shape.

The cover is subjected to shearing stress and the hook is under direct stress in its length but shearing stress in its end hook.

Step 5: Material selection and working stress: The material should have resistance to corrosion and wear, has low coefficient of friction and relatively low cost and weight. The end hook and the plunger cover are joined by welding so that the material should have carbon content less than 0.3%. Al-alloy is a good material to resist corrosion but it is the most expensive. Alloy-steel is also expensive. Hence, the galvanized carbon steel is selected due to its lowest cost and relatively good resistance to corrosion and suitable for welding [Appendix D]. To make the system compact in size and light in weight, the factor of safety should be minimum which is 2.

$$\text{Working stress} = \frac{\text{yield stress}}{\text{Factor of safety}} \rightarrow \sigma_w = \frac{\sigma_y}{n} = \frac{217\text{MPa}}{2} = 108.5\text{MPa}$$

Step 6: Detailed stress analysis

1. Finding the thickness of the hook length; The stress developed in the thickness is equals to,

$$\sigma = \frac{F}{A} \Longrightarrow A = \frac{F}{\sigma_w} = \frac{1500\text{N}}{108.5\text{MPa}} = 13.825\times10^{-6}\text{m}^2 \text{ and } A = t^2 = 13.825\times10^{-6}\text{m}^2 \rightarrow t = 3.718\text{mm}$$

The cross section of the hook is square. The above result shows that a small amount of area is enough to withstand the external applied force. To make the hook suitable for welding the dimension should be maximized to an optimum dimension. Therefore, the thickness is selected to make 10 mm by 10 mm.

2. The plunger cover is under shearing due to a force of 1500 N applied on area of 10mm by 10 mm square. The stress on the cover is shearing and it is calculated by,

$$\tau = \frac{F}{A} \rightarrow A = \text{perimeter} \times \text{thickness} = 4 \times \text{thickness of hook} \times \text{thickness of plunger cover} =$$

$$4\times10\text{mm}\times t = 40t\text{mm}^2, A = \frac{F}{\tau} = \frac{1500\text{N}}{108.5\text{MPa}} = 13.825\text{mm}^2 \rightarrow t = \frac{A}{40} = \frac{13.825\text{mm}^2}{40\text{mm}} = 0.346\text{mm}$$

Even if the thickness of the plunger cover is small it should be increased in order to make convenient for welding hence it becomes 5 mm.

Design of the Bolt and Nut

Step 1: The bolt and nut temporary connections are used to joined tightly the flange of the cylinder and the cylinder cover on both side of the cylinder.

Step 2: Gathered information: According to the type of cylinder head, end condition four bolt-nut connections are required in each ends of the cylinder. We can assume the total force (1500.016N) is shared by these bolt-nut joints equally. Therefore, 375.004N force is supported by each bolt-nut.

Step 3: Problem statement: Designing of a bolt and nut that can withstand 375.004n force

Step 4: Determining the shape of a cylinder cover that is compatible with the cylinder, cylinder cover and the flange. Fortunately, the shape of the bolt-nut has standard shape [7] see Appendix N 5.30.

The bolt is subjected to direct stress in its nominal diameter and shearing stress in its thread while the nut is under shearing stress in its thread.

Step 5: Material selection and working stress: The material should have resistance to corrosion and relatively low cost and weight. The galvanized carbon steel is selected from cost, weight and corrosion resistant aspects appendix D].

$$\text{Working stress} = \frac{\text{yield stress}}{\text{Factor of safety}} \rightarrow \sigma_w = \frac{\sigma_y}{n} = \frac{217\text{MPa}}{2} = 108.5\text{MPa}$$

Step 6: Detailed stress analysis: Calculation of the diameter of the bolts, which connects the square, flange joint. Since the numbers of the bolts are four, the load is divided into four equal amounts.

The load resist by each bolt: $F_b = \frac{F_t}{4} = \frac{1500.016}{4} = 375.04\text{N}$. If d_c is the core diameter of the bolts, then; $F_b = \frac{\pi}{4}(d_c)^2\sigma_{tb} \Rightarrow d = \sqrt{\frac{4F_b}{\pi\sigma_{tb}}}$ where: σ_{tb} = allowable tensile stress for the bolt.

The value of σ_{tb} is usually kept low to allow for initial tightening stress in the bolts.

The diameter of the bolt becomes: $d = \sqrt{\frac{375.04\text{N} \times 4}{\pi \times 108.5\text{M}\frac{\text{N}}{\text{m}^2}}} = 0.0021\text{m} = 2.0979 \times 10^{-3}\text{m} = 2.098\text{mm}$

It may be not that bolts of less than 12mm diameter should never be used for hydraulic joint, because very large tightening stress may be induced in smaller bolts. Even if the bolts are used to support the hydraulic system, we cannot decide directly to select 12 mm diameter because the system is classified as a light hydraulic system so it is advisable to choose a lowered diameter, $d = 8\text{mm}$.

Table 5.4 Standard dimension of bolt & nut [1] see Appendix N 5.50

Designation(mm)	P	Major dia. mm	Pitch dia. mm	Minor dia. Of bolt mm	Minor dia. Of nut mm	Depth of thread mm	B mm	H mm	L<125 mm	TL mm	Stress area mm^2
M8×1.25	1.25	8	7.188	6.466	6.647	0.767	13	5.5	20	12	36.6

Design of Cylinder Cover

Step 1: The Cylinder cover is a cylindrical shape used to make a boundary between the environment and fluid. Therefore, pressure is created inside the cylinder. The maximum pressure applied on the cylinder cover is 43.308KPa. It should have a capacity to resist wear and corrosion since it is faced to climate.

Step 2: Gathered information: The maximum pressure applied on the cylinder cover is 43.308KPa distributed on an area of diameter 210 mm.

Step 3: Problem statement: Designing of a cylinder cover that is capable of resisting 43.308KPa force, which is applied intermittently on area of 210 mm diameter

Step 4: Determining the shape of a cylinder cover, which is compatible with the plunger, plunger head, cylinder and the spring. Among the alternative shapes in Appendix N 5.31, type A is selected because its shape can be manufactured easily. The cover is subjected to shearing stress. Therefore, the cylinder cover is designed based on the above induced stress.

Step 5: Material selection and working stress: The material should have resistance to corrosion and wear, has low coefficient of friction and relatively low cost and weight. The cylinder cover needs some machining and it is subjected to the environment, so that the material should satisfy these requirements. Al-alloy is a good material to resist corrosion but it is the most expensive. Alloy-steel is also expensive. Hence, the galvanized carbon steel is selected due to its lowest cost and relatively good resistance to corrosion [Appendix D]. To make the system compact in size and light in weight, the factor of safety should be minimum which is 2.

$$\text{Working stress} = \frac{\text{yield stress}}{\text{Factor of safety}} \rightarrow \sigma_w = \frac{\sigma_y}{n} = \frac{217\text{MPa}}{2} = 108.5\text{MPa}$$

Step 6: Detailed stress analysis: The cylinder cover is under shearing due to a pressure of 43.308kPa-distributed force. The magnitude of the force, which is applied on the cover, is equal to the product of pressure inside the cylinder and the area of the cover in contact with the pressurized fluid.

$F = PA$ Where p is the pressure in the cylinder (43.308KPa), A is the net area of the cover

$A = \frac{\pi}{4}(D^2)$ Where D is the inside diameter of the cylinder equals to 210 mm

$$A = \frac{\pi}{4}(0.21^2) = 0.034636\text{m}^2$$

The force becomes, $F = PA = 43.308\text{KPa} \times 0.034636\text{m}^2 = 1500.016\text{N} = 1.5\text{KN}$

The shear stress due to the pressure force $\sigma = \frac{F}{A}$, but $A = \pi Dt$

$$A = \frac{F}{\sigma_w} = \frac{1500.016\text{N}}{108.5 \times 10^6\,\text{N/m}^2} = 8.310 \times 10^{-6}\text{m}^2 = 8.31\text{mm}^2$$

$$\rightarrow t = \frac{A}{\pi D} = \frac{8.31\text{mm}^2}{\pi \times 210\text{mm}} = 0.0126\text{mm}$$

Since the thickness becomes very small, we have to maximize it to a higher value. There is an attachment on the cover by welding hence its thickness is increased to $t = 5mm$.
The side of the cylinder cover should be greater than to the outside diameter of the cylinder, which is equal to 217.934 mm.
Note: The force applied on the cylinder cover 2 is less than the force applied on cylinder cover 1 even if the pressure is the same. This is because the area that is subjected to the pressure is less at cover 2 than at cover 1. The thickness of the cylinder cover 1 is become 0.0126 mm but we maximized it to 5 mm. According to the force applied and the area of the dimension of the cylinder 2 and the two flanges becomes less than 0.0126 mm. Therefore, the dimension of the cylinder cover 2 and the two flanges are chosen to be the same dimension as the cylinder cover 1.

Dimensions of Cylinder Cover 2

General information: The internal and external diameter of the cylinder is 210 mm and 217.934 mm respectively. The distance across corner of the bolt and is 15.01 mm [2]. The size of the square flange is equal to the sum of the outside diameter of the cylinder, the distance across corner of the bolt-nut joint and a clearance. [Appendix N 5.32]

$L = 217.934 + 2(1 + 15.01) = 249.954mm = 250mm$, R=4mm the same as radius of bolt and D=200 mm the same as external diameter of the piston head,

$t = 5mm$ the same as the thickness of the cylinder cover 1,

$L = 250$ mm the same as the length of the cylinder cover 1 and $d = 117.472mm$

Design of the Flanges

Gathered Information: The shape and length of the flange is the same as the cylinder cover 1 and 2 see Appendix N 5.32.

$L = 217.934 + 2(1 + 15.01) = 249.954mm = 250mm$, R=4mm the same as radius of bolt and D=217.934 mm the same as external diameter of the cylinder,

$t = 5mm$ the same as the thickness of the cylinder cover 1,

$L = 250$ mm the same as the length of the cylinder cover 1 and $d = 117.472mm$

Design of Cylinder Cover Pin Hold (Lower End)

Step 1: The pin hold is a hollow shape part located at the tail end of the cylinder cover, which is used to hold the pin that connects the powerhouse to the vertical main support see Appendix N 5.33.

Step 2: Gathered information: The maximum force applied on the pin hold is the sum of the weight of the powerhouse and 1500 N either compressive or tensile.

The weight of the power is calculated by multiplying the volume by the density of steel since they are manufactured from steel see Appendix O.

$$\text{weight of cylinder(W)} = \text{volume in m}^3 \times \text{unit weight in } \frac{\text{KN}}{\text{m}^3} = \text{V} \times \text{w}, \text{ where } \text{w} = 76.5\frac{\text{KN}}{\text{m}^3} \text{ and}$$

$$\text{volume of cylinder V} = \frac{\pi}{4}(D_o^{\ 2} - \text{D}_\text{i}^{\ 2})\Delta\text{L} = \frac{\pi}{4}(217.934^2 - 210^2)500\text{mm}^3 = 1{,}33{,}303.058mm^3 = 1.333\times10^{-3}m^3$$

$$W = V \times w = 1.333\times10^{-3}m^3 \times 76.5\frac{KN}{m^3} = 101.975N$$

$$\text{total force applied on the pin hold} = 1500 + 256.085 = 1756.085\ \text{N}$$

Step 3: Problem statement: Designing of a pin hold that is capable of resisting 1756.085 N forces, which is compressive or tensile.

Step 4: Determining the shape of the pin hold, which is compatible with the cylinder cover, the pin and the support. Among the alternative shapes in Appendix N 5.34, type B is selected because its shape can be manufactured easily by casting due to its rectangular shape.

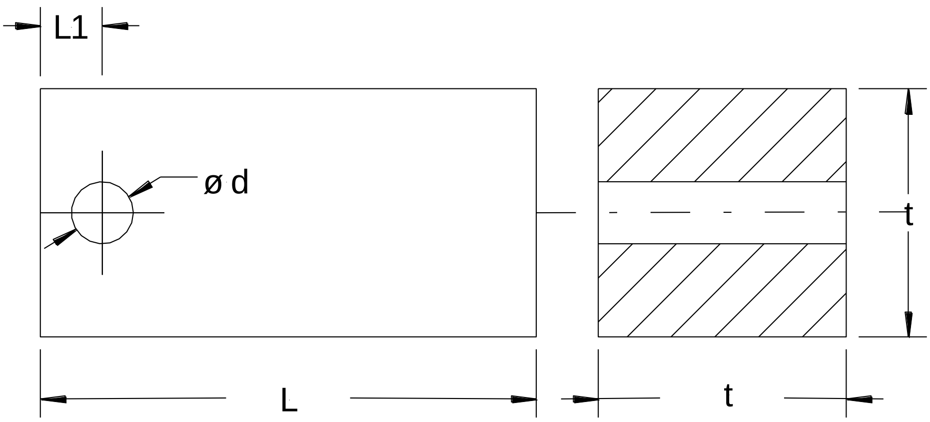

Figure 5.5-13 Selected pin hold

The pin hold is under direct stress in its length but shearing stress in its end hook.

Step 5: Material selection and working stress: The material should have resistance to corrosion and wear, has low coefficient of friction and relatively low cost and weight. The end hook and the plunger cover are joined by welding so that the material should have carbon content less than 0.3%. Al-alloy is a good material to resist corrosion but it is the most expensive. Alloy-steel is also expensive. Hence, the galvanized carbon steel is selected due to its lowest cost and relatively good resistance to corrosion and suitable for welding [Appendix D]. To make the system compact in size and light in weight, the factor of safety should be minimum which is 2.

$$\text{Working stress} = \frac{\text{yield stress}}{\text{Factor of safety}} \rightarrow \sigma_w = \frac{\sigma_y}{n} = \frac{217\text{MPa}}{2} = 108.5\text{MPa}$$

Step 6: Detailed stress analysis

1. Finding the thickness of the hook length; The stress developed in the thickness is equals to,

$$\sigma = \frac{F}{A} \Longrightarrow A = \frac{F}{\sigma_w} = \frac{1500N}{108.5MPa} = 13.825 \times 10^{-6} m^2 \rightarrow A = t^2 = 13.825 \times 10^{-6} m^2 \rightarrow t = 3.718 \times 10^{-3} m = 3.718mm$$

The cross section of the hook is square. The above result shows that a small amount of area is enough to withstand the external applied force. To make the hook suitable for welding the dimension should be maximized to an optimum dimension. Therefore, the thickness is selected to make 10 mm by 10 mm.

Design of Cam and Follower

The type of cam used is a reciprocating curved shoe spring loaded follower with eccentric cam. An eccentric cam is effective in design and a very inexpensive cost can be used even for generating a very complicated functions.

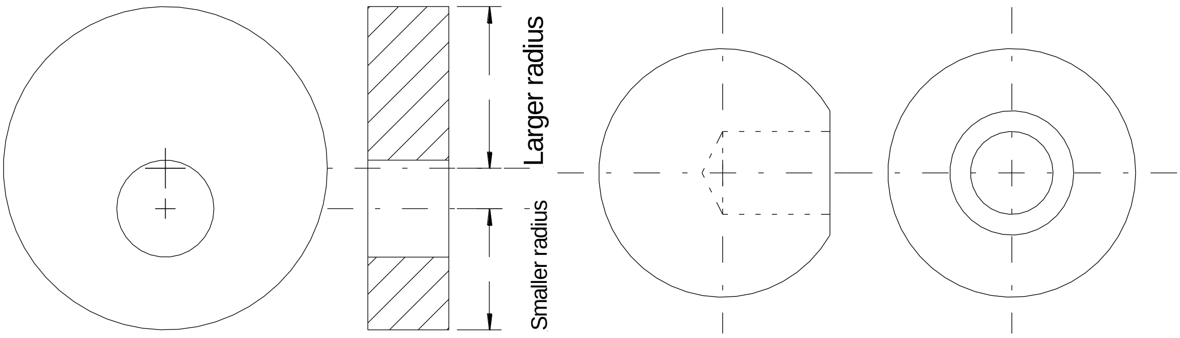

Figure (a) Cam (b) Follower

Stroke length=Larger radius-Smaller radius=10 mm

The cam is used to create a 10 mm stroke of the plunger pump. Hence, the difference between the smaller and the larger radius of the eccentric cam should be 10 mm. the internal diameter of the cam is 60 mm and its outside diameter is 90 mm with a thickness of 10 mm. The follower has spherical shape with a diameter of 20 mm, which is inserted at the end of the plunger.

5.4. Design of the Crank Slider Mechanism

There are two possibilities in the arrangement of position of powerhouse of the azimuth and zenith rotator. These arrangements are;

1. When the azimuth rotator is below the zenith rotator: In this case, the azimuth rotation is disturbed by the zenith rotation. Hence, the accuracy of the east-west rotation cannot be maintained
2. When the azimuth rotator is above the zenith rotator: This arrangement gives accurate rotation of both in the azimuth and zenith axis.

Therefore, the mechanism that suits the requirement is type B see Appendix N 5.35. The maximum dimension of the solar panel is 1650x992x45 (Lxwxt) mm.

5.4.1. Mathematical Equation and Simulation along Zenith Rotation

Three dimensions are continuously changing. These are the length L, the height h_2 and the angle α. The mathematical relationship among the geometrical dimensions can formulated as follows using the figure below.

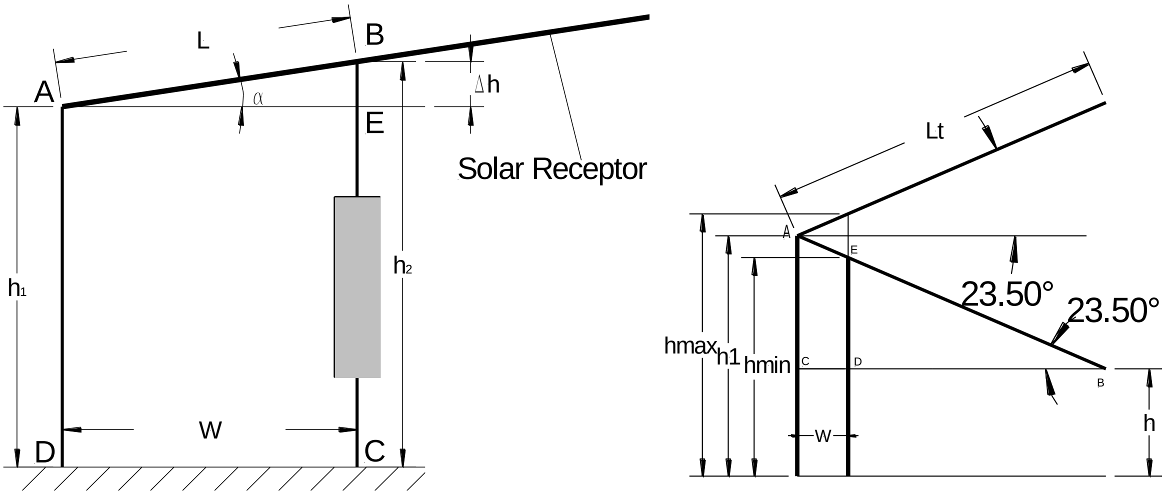

$$\tan\alpha = \frac{\Delta h}{W} = \frac{\Delta h}{W} \rightarrow \Delta h = W\tan\alpha \qquad \text{5-11}$$

The height h_2,

$$h_2 = h_1 + \Delta h \Longrightarrow h_2 = h_1 + W\tan\alpha = h_1 + L\sin\alpha \qquad \text{5-12}$$

$$W = L\cos\alpha \qquad \text{5-13}$$

The values of the height h_1 can be calculated from the following geometry;

The minimum height of h must be 1000 mm, hence $h_1 = h + L_t\sin\alpha = 1657.935\text{mm}$. The height h_2 is minimum and maximum at -23.5^o and 23.5^o respectively.

$$h_2 = h_1 + \Delta h = h + L_t\sin\alpha + W\tan\alpha = 1000 + 1650\sin\alpha + W\tan\alpha = 1657.935 + W\tan\alpha \qquad \text{5-14}$$

The value of W is between 0 and 1513.149 mm. The minimum width should be greater than 218 mm, which is the outer diameter of the powerhouse 1 cylinder. If the width is far from the height h_1, the system will be more stable but the cost will increase due to the increase in size of the support system. Therefore, a 500 mm width is selected and the corresponding minimum height becomes 1440.53 mm. The maximum height h2 is equals to the sum of h1 and $W\tan 23.5$ which is 1875.342 mm.

$$h_1 = 1657.935\,\text{mm},\ W = 500\,\text{mm},\ h_{min} = 1440.53\,\text{mm},\ h_{max} = 1875.342\text{mm and } \alpha[-23.5^o, 23.5^o]$$

The total stroke length of the powerhouse 2 is 434.8124 mm. It is fully extended at 23.5^o and fully retracted at -23.5^o (see graph 5.4).

The height h_2;

$$h_2 = h_1 + \Delta h = h + L_t\sin\alpha + W\tan\alpha = 1000 + 1650\sin\alpha + W\tan\alpha = 1657.935 + W\tan\alpha \text{ mm}$$

The zenith angle and the height h_2 are always directly proportional to each other. The minimum and maximum values of the height is occurred at the two extreme position of the solar receptor, i.e., -23.5^{o} and 23.5^{o} respectively.

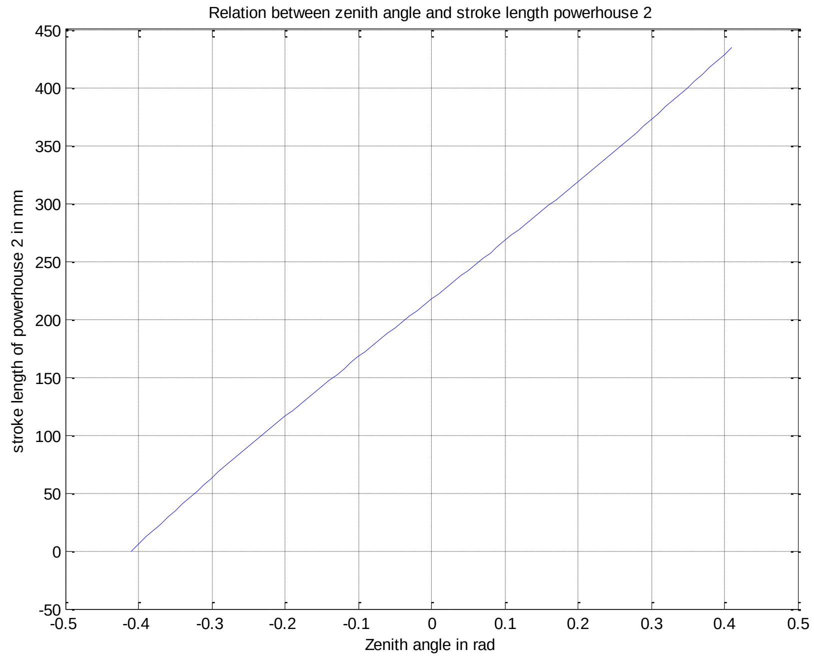

Graph 5.4-zenith angle vs. stroke length of powerhouse 2

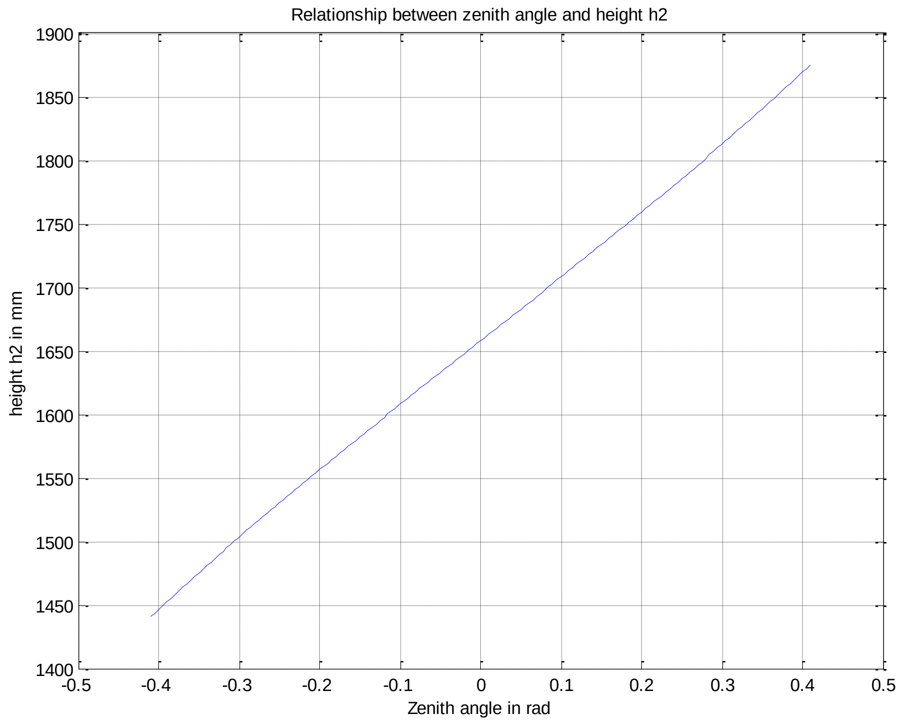

Graph 5.5-zenith angle and height h_2

When the zenith angle changes the length of panel support is changed. When the sun is at the equator, the length and the width are equal (0.5m). However, at any position, the length is greater than the width and finally it has a maximum length of 545.221 mm at zenith angle of

$\pm 23.5^o$.

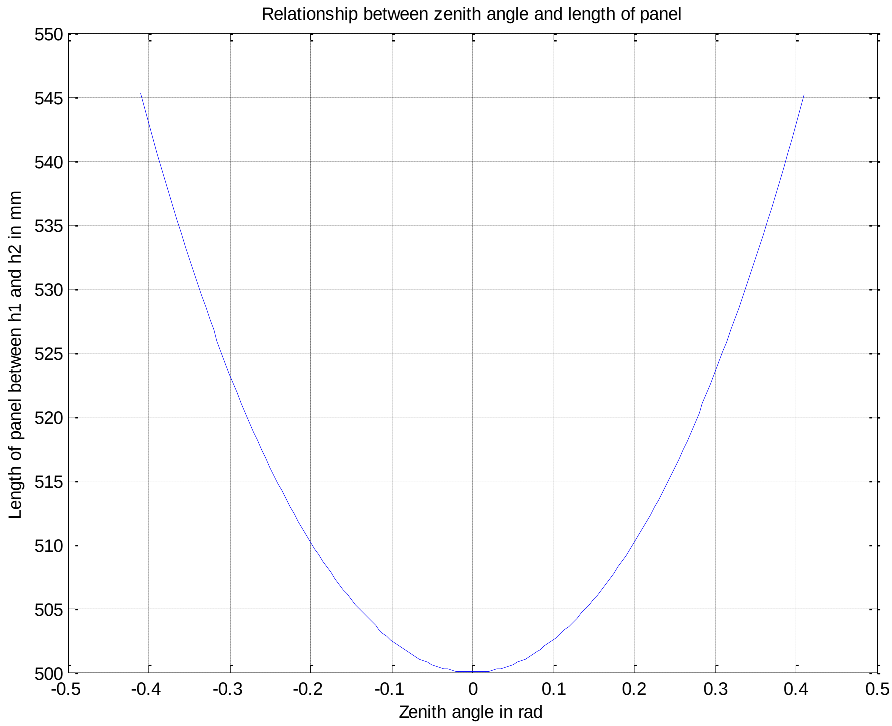

Graph 5.6 zenith angle and length between h_1 and h_2

Design of solar Panel Upper Support

Step 1: This support is one side of the crank slider mechanism, which supports the solar panel vertically upward. Its length is under a constant force even if it can translate vertically up or downward. Thus, it should have strength to support all the components above it.

Step 2: Gathered information: The maximum weight supported by this link is equal to the sum of the weight of the panel, the weight of the panel support and the weight of the powerhouse of the azimuth rotator.

$$F = W = \text{weight of panel} + \text{weight of the panel support} + \text{weight of the power house} = 1500 + 256.085 = 1756.085\text{N}$$

Step 3: Problem statement: Designing of a support which is capable of supporting a weight of 1756.085 N

Step 4: Determining the shape of the support, which is compatible with the panel, powerhouses and the links, see Appendix N 5.36.

The support is under compressive stress so that it should be checked for compressive stress and buckling

Step 5: Material selection and working stress: The material should have resistance to corrosion and wear, has relatively low cost and weight. The support needs some machining and welding and it is subjected to the environment, so that the material should satisfy these requirements. Al-alloy is a good material to resist corrosion but it is the most expensive. Alloy-steel is also expensive. Hence, the galvanized carbon steel is selected due to its lowest cost and relatively good resistance to corrosion [Appendix D]. To make the system compact in size and light in weight, the factor of safety should be minimum which is 2.

$$\text{Working stress} = \frac{\text{yield stress}}{\text{Factor of safety}} \rightarrow \sigma_w = \frac{\sigma_y}{n} = \frac{217\text{MPa}}{2} = 108.5\text{MPa}$$

Step 6: Detailed stress analysis

1. The support is under compressive stress due to the upper side weight of the components,

$$\text{compressive stress} = \frac{\text{upperside weight}}{\text{cross sectional Area of the of support}} \rightarrow \sigma = \frac{W}{A} \text{ where } A = wt = t^2$$

Even if the cross section is rectangle, it is possible to make it square (circular) and then change to a standard size of a rectangle.

$$A = \frac{W}{\sigma} = \frac{1756.085\text{ N}}{108.5\text{ MPa}} = 16.185\text{ mm}^2 \rightarrow t = 4.023\text{ mm}$$

Since the thickness of the cross section becomes very small, it is advisable to make a hollow cross section, which in turn increases the strength and decrease weight. The system is also sometimes subjected to wind energy. The dimension can be maximized using the standard data hollow structural steel tubing [1],

$$D_o = 33.4\text{ mm and } t = 3\text{ mm}$$

The stress induced in the cross section,

$$\sigma = \frac{W}{A} = \frac{W}{\pi(D_o t - t^2)} = \frac{1826.312\text{ N}}{\pi(33.4 \times 3 - 3^2)\text{mm}^2} = 6.374\text{MPA}$$

The induced is less than the allowable stress hence the design is safe.

2. The support should also checked for buckling,

According to Euler's theory the buckling load F under various end conditions is represented by a general equation [4],

$$F = \frac{C\pi^2 EAk^2}{L^2} = \frac{C\pi^2 EI}{L^2} \quad \text{...}\mathbf{5\text{-}15}$$

where E = modulus of elasticity or Young's modulus for the material of the column, A = area of cross section, k = least radius of gyration of the cross-section = $\frac{I}{A}$, I = moment of inertia, L = length of the column, and C = constant, representing the end conditions of the column or end fixity coefficient

=207GPa, $A = \pi(D_o t - t^2) = \pi(33.4 \times 3 - 3^2)\text{mm}^2 = 286.513\text{mm}^2 = 286.513 \times 10^{-6}\text{m}^2$

$$I = \frac{\pi}{64}(D_o{}^4 - (D_o - 2t)^4) = \frac{\pi}{64}((33.4\text{mm})^4 - (33.4\text{mm} - 2 \times 3\text{mm})^4) = 33420.338\text{mm}^4 = 33.420 \times 10^{-9}\text{m}^4$$

C=2 for end condition of one end fixed and other hinged

$$F=\frac{C\pi^2 EI}{L^2}=\frac{2\times\pi^2\times 207GPa\times 33.420\times 10^{-9}m^4}{L^2}\rightarrow L^2=\frac{2\times\pi^2\times 207GPa\times 33.420\times 10^{-9}m^4}{1826.312N}\rightarrow L=4.879m$$

The length of the support, which cannot buckle, is greater than 3 m but the actual length is less than 3 m. Thus, the design is safe for buckling.

5.4.2. Design of Powerhouse 2

The powerhouse 2 is installed below the panel support. This is used to move the solar receptor in the upward or downward direction. A simple schematic representation of the powerhouse is shown below. The mechanism is operated by manual human hand force. It is similar with the hand operated hydraulic bottle jack.

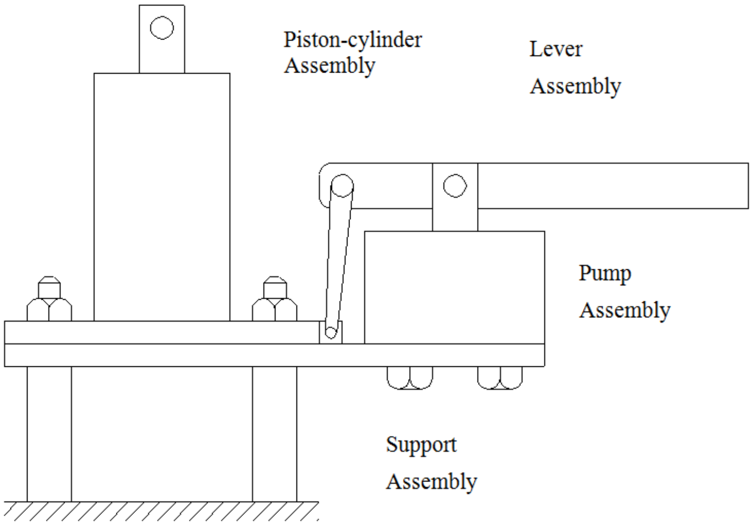

Figure 5.5-14 simple schematic representation of powerhouse 2

The hydraulic fluid is pumped into piston-cylinder assembly. Based on the direction of the valve the fluid is entered into the cylinder, which in turn lifts or lowers the solar receptor. The stroke of the piston is 434.812 mm and the maximum force applied is equal the weight above the piston. This weight has a magnitude of 1826.312 N.

The stroke of the piston is 434.812 mm, which is covered within three months. This amount of stroke is required to rotate the solar receptor 23.5^o in 90 days see Appendix P 2.47. Since 434.812 mm of stroke is needed to cover 23.5^o, one-degree needs

$$434.812mm = 23.5\,^o = 90\text{ days}$$

$$x\,?=1^o=y\,? \qquad \rightarrow x=434.812mm\frac{1^o}{23.5^o}=18.503mm \text{ and } y=90d\text{ days}\frac{1^o}{23.5^o}=3.83days$$

The above result shows that one degree is covered within 3.83 days and it requires 18.503 mm movement of the piston. The daily movement of the piston can be calculated as follows,

$$434.812\text{ mm}=90\text{ days}$$

$$L=1\text{day} \qquad \rightarrow L=434.812\text{ mm}\frac{1\text{ day}}{90\text{ days}}=4.831mm$$

This implies that a length of 4.831 mm movement of the piston is undertaken per a day. So that the pump should be very small to get this small amount of movement of the piston.

Design of Piston Rod

Step 1: This piston rod is used to transmit power from the piston to the panel support. In addition to this, it serves as a supporting mechanism of the weight above it. Thus, it should have strength to support the weight.

Step 2: Gathered information: The maximum weight supported by this rod is equal to the sum of the weight of the panel, the weight of the panel support and the weight of the powerhouse of the azimuth rotator.

$W = 1826.312\ N$

The stroke of the piston is 434.812 mm. Hence, the length of the piston must be greater than the stroke.

Step 3: Problem statement: Designing of a piston rod which is capable of supporting a weight of 1826.312 N

Step 4: Determining the shape of the support, which is compatible with the panel, powerhouses and the links; first let us assume that the cross section of rod is solid circular after that it is possible to change to hollow cross section to increase the strength with the same amount of weight. The rod is under compressive stress so that it should be checked for compressive stress and buckling.

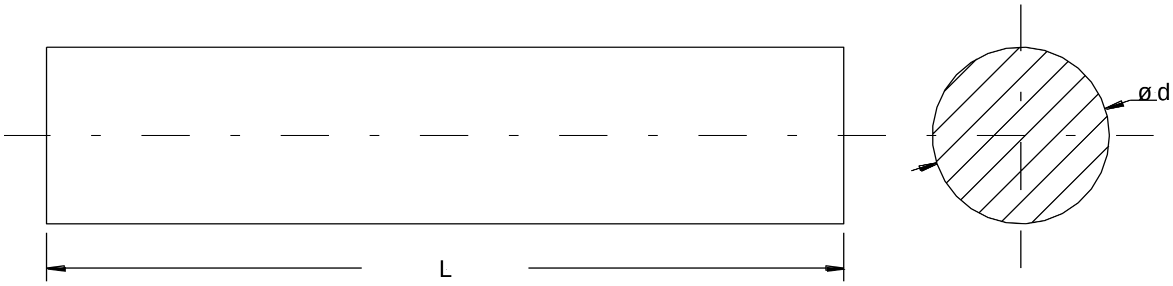

Figure 5.5-15 Piston rod

Step 5: Material selection and working stress: The material should have resistance to corrosion and wear, has relatively low cost and weight. The support needs some machining and welding and it is subjected to the environment, so that the material should satisfy these requirements. Al-alloy is a good material to resist corrosion but it is the most expensive. Alloy-steel is also expensive. Hence, the galvanized carbon steel is selected due to its lowest cost and relatively good resistance to corrosion [Appendix D]. To make the system compact in size and light in weight, the factor of safety should be minimum which is 2.

$$\text{Working stress} = \frac{\text{yield stress}}{\text{Factor of safety}} \rightarrow \sigma_w = \frac{\sigma_y}{n} = \frac{217\text{MPa}}{2} = 108.5\text{MPa}$$

Step 6: Detailed stress analysis

1. The rod is under compressive stress due to the upper side weight of the components,

$$\text{compressive stress} = \frac{\text{upperside weight}}{\text{cross sectional Area of the of support}} \rightarrow \sigma = \frac{W}{A} \text{ where } A = \pi r^2$$

$$A = \frac{W}{\sigma} = \frac{1826.312\text{ N}}{108.5\text{ MPa}} = 16.832\text{ mm}^2 \rightarrow r = 2.315\text{ mm}$$

Since the radius of the cross section becomes very small, it is advisable to make a hollow cross section, which in turn increases the strength with the same weight. The system is also sometimes subjected to wind energy. The dimension can be maximized using the standard data pipe structural steel tubing [1],

$$r = 16.7\text{mm and } t = 3\text{mm}$$

The stress induced in the cross section,

$$\sigma = \frac{W}{A} = \frac{W}{\pi(4rt - 4t^2)} = \frac{1826.312\text{N}}{\pi(4 \times 16.7 \times 3 - 4 \times 3^2)} = 3.536\text{MPA}$$

The induced is less than the allowable stress hence the design is safe.

2. The support should also checked for buckling: According to Euler's theory the buckling load F under various end conditions is represented by a general equation [4],

$$F = \frac{C\pi^2 EAk^2}{L^2} = \frac{C\pi^2 EI}{L^2}$$

where E = modulus of elasticity or Young's modulus for the material of the column, A = area of cross section, k = least radius of gyration of the cross-section $= \frac{I}{A}$, I = moment of inertia, L = length of the column, and C = constant, representing the end conditions of the column or end fixity coefficient

E=207GPa,

$$A = \pi(4rt - 4t^2) = \pi(4 \times 16.7\text{ mm} \times 3\text{mm} + 4(3\text{mm})^2) = 516.478\text{ mm}^2 = 516.478 \times 10^{-6}\text{m}^2$$

$$I = \frac{\pi}{64}(d^4 - (d - 2t)^4) = \frac{\pi}{12}((33.4\text{mm})^4 - (33.4\text{mm} - 2 \times 3\text{mm})^4) = 19163.833\text{mm}^4 = 19.164 \times 10^{-9}\text{m}^4$$

C=4 for end condition of fixed on both ends

$$F = \frac{C\pi^2 EI}{L^2} = \frac{4 \times \pi^2 \times 207\text{GPa} \times 19.164 \times 10^{-9}\text{m}^4}{L^2} L^2 = \frac{4 \times \pi^2 \times 207\text{GPa} \times 19.164 \times 10^{-9}\text{m}^4}{1826.312\text{N}} \rightarrow L = 9.260\text{m}$$

The actual length of the rod is much less than the expected length. Thus, the design is safe for buckling.

Design of the Cylinder

Step 1: This cylinder is installed in the outside of the piston rod that is used to create a pressure to carry the weight of the upper side components

Step 2: Gathered information: The maximum pressure created inside the cylinder is equal to the ratio of the weight and the internal area of the cylinder. Since the internal and external diameter of the cylinder is unknown, it is advisable to select a standard internal diameter, which is greater than the outside diameter of the piston rod. The internal diameter of the piston rod is 33.4 mm. Thus, the nearest highest value of the standard seamless tube is 41.91 mm. The corresponding standard outer diameter is 48.26 mm. The weight supported by the cylinder is1826.312 N and the stroke of the piston is 434.812 mm. Hence, the length of the cylinder must be greater than the stroke.

$D_i = 41.91\text{mm}, D_o = 48.26\text{mm}$ and $t = 3.175\text{mm}$.These dimensions are checked for the applied load.

Step 3: Problem statement: Designing of a cylinder rod, which is capable of supporting a weight of 1826.312N.

Step 4: Determining the shape of the support, which is compatible with the panel, powerhouses and the links see Appendix N 5.39.

The cylinder is under pressure stress so that it should be checked for hoppe stress and longitudinal stress

Step 5: Material selection and working stress: The material should have resistance to corrosion and wear, has relatively low cost and weight. The support needs some machining and welding and it is subjected to the environment, so that the material should satisfy these requirements. Al-alloy is a good material to resist corrosion but it is the most expensive. Alloy-steel is also expensive. Hence, the galvanized carbon steel is selected due to its lowest cost and relatively good resistance to corrosion [Appendix D]. To make the system compact in size and light in weight, the factor of safety should be minimum which is 2.

$$\text{Working stress} = \frac{\text{yield stress}}{\text{Factor of safety}} \rightarrow \sigma_w = \frac{\sigma_y}{n} = \frac{217\text{MPa}}{2} = 108.5\text{MPa}$$

Step 6: Detailed stress analysis: The ratio of the wall thickness and the internal diameter of the cylinder is $r = \frac{t}{D_i} = \frac{3.175\text{mm}}{41.91\text{mm}} = 0.0758$

Since the ratio is less 0.1, it is think cylinder. The dimension of the cylinder is selected from standard so it is necessary to check its strength. In thin cylinder, the longitudinal stress is half of the circumferential or hoop stress. Therefore, the design of a pressure vessel must be based on the maximum stress i.e. hoop stress [1]. The thickness of the cylinder is calculated by the formula,

$$t = \frac{P \times d}{2\sigma_w} = \frac{F \times d}{2\sigma_w \times A} = \frac{4F \times d}{2\sigma_w \times \pi d^2} = \frac{2F}{\sigma_w \times \pi d} = \frac{2 \times 1826.312\text{N}}{108.5\frac{\text{N}}{\text{mm}^2} \times \pi \times 33.4\text{mm}} = 0.321\text{mm}$$

The actual thickness is 3.175 mm; it indicates that the design is safe.

Design of the Cylinder Cup

Step 1: The Cylinder cup is a cylindrical shape used to cover the top end of the cylinder. Pressure is created inside the cylinder.

Step 2: Gathered information: The maximum pressure applied on the cylinder cup is equal to the ratio of the upper side weight of the components and the net area of the cylinder. The upper side weight of the components is 1826.312 N. The internal diameter of the cylinder is 41.91 mm and the outer diameter of the piston rod is 33.4 mm. Hence, the net area and the pressure becomes,

$$A = \frac{\pi}{4}(41.91^2 - 33.4^2) = 672.653\text{mm}^2 \text{ and } P = \frac{F}{A} = \frac{1826.312\text{N}}{672.653\text{mm}^2} = 2.715\text{MPa}$$

A pressure of 2.715 Mpa must be created inside the cylinder to rotate the solar panel in the zenith direction.

Step 3: Problem statement: Designing of a cylinder cup that is capable of resisting 2.715 Mpa forces which is applied on the net area of the cylinder.

Step 4: Determining the shape of a cylinder cup, which is compatible with the piston rod and cylinder head

The cup is subjected to shearing stress see Appendix N 5.40. Therefore, the cylinder cup is designed based on the above induced stress.

Step 5: Material selection and working stress: The material should have resistance to corrosion and wear, has low coefficient of friction and relatively low cost and weight. The cylinder cover needs some machining and it is subjected to the environment, so that the material should satisfy these requirements. Al-alloy is a good material to resist corrosion but it is the most expensive. Alloy-steel is also expensive. Hence, the galvanized carbon steel is selected due to its lowest cost and relatively good resistance to corrosion [Appendix D]. To make the system compact in size and light in weight, the factor of safety should be minimum which is 2.

$$\text{Working stress} = \frac{\text{yield stress}}{\text{Factor of safety}} \rightarrow \sigma_w = \frac{\sigma_y}{n} = \frac{217\text{MPa}}{2} = 108.5\text{MPa}$$

Step 6: Detailed stress analysis: The cylinder cover is under shearing due to a pressure of 2.715 MPa distributed force. The magnitude of the force, which is applied on the cup, is equal to the product of pressure inside the cylinder and the net area of the cup in contact with the pressurized fluid (1826.312 N).

The shear stress due to the pressure force

$\sigma = \frac{F}{A}$, but $A = \pi D t$ and $A = \frac{F}{\sigma_w} = \frac{1826.312\text{N}}{108.5 \times 10^6\,\text{N/m}^2} = 16.832 \times 10^{-6}\text{m}^2 = 16.832\text{mm}^2$

$t = \frac{A}{\pi D} = \frac{16.832\text{mm}^2}{\pi \times 41.91\text{mm}} = 0.128\text{mm}$

Since the thickness becomes very small, it has to be maximized to a higher value. There is thread in its inside surface therefore its thickness is increased to the same as the thickness of the cylinder which is 3.175 mm, $t = 3\text{mm}$

Design of the Flange

Step 1: The flange is a circular shape used to join the cylinder with the cylinder support.

Step 2: Gathered information: The maximum force applied on the flange is 1826.312 N and the outer diameter of the cylinder is 48.26 mm.

Step 3: Problem statement: Designing of a flange, which is capable of resisting 1826.312 N forces

Step 4: Determining the shape of a flange that is compatible with the cylinder, cylinder support and the pump assembly. Among the alternative shapes shown in Appendix N 5.41, type A is selected because its shape can be manufactured easily. The cover is subjected to shearing stress. Therefore, the flange is designed based on the above induced stress.

Step 5: Material selection and working stress: The material should have resistance to corrosion and wear, has low coefficient of friction and relatively low cost and weight. The flange needs some machining, welding and it is subjected to the environment, so that the material should satisfy these requirements. Al-alloy is a good material to resist corrosion but it is the most expensive. Alloy-steel is also expensive. Hence, the galvanized carbon steel is selected due to its lowest cost and relatively good resistance to corrosion [Appendix D]. To make the system compact in size and light in weight, the factor of safety should be minimum which is 2.

$$\text{Working stress} = \frac{\text{yield stress}}{\text{Factor of safety}} \rightarrow \sigma_w = \frac{\sigma_y}{n} = \frac{217\text{MPa}}{2} = 108.5\text{MPa}$$

Step 6: Detailed stress analysis: The flange is under shearing due to a force of 1826.312 N.

The shear stress due to the force $\sigma = \frac{F}{A}$, but $A = \pi D t$

$$A = \frac{F}{\sigma_w} = \frac{1826.312\text{N}}{108.5 \times 10^6\,\text{N/m}^2} = 16.832 \times 10^{-6}\text{m}^2 = 16.832\text{mm}^2 \rightarrow t = \frac{A}{\pi D} = \frac{16.832\text{mm}^2}{\pi \times 48.26\text{mm}} = 0.111\text{mm}$$

Since the thickness becomes very small and connected with the cylinder by welding, we have to maximize it to a higher value. There is an attachment on the flange by welding hence its thickness is increased to 5 mm

The outer diameter of the flange is optimized using the distance across corner of nut. There are four nuts, which have distance across corner of 15 mm. The outer diameter of the flange becomes

$$\mathrm{D} = \text{outer diameter of cylinder} + \text{distance across corner} + \text{clearance between nut and cylinder}$$

$$= 48.26 + 2\times15 + 2 = 80.26\ \mathrm{mm}$$

Design of the pump 2

Step 1: The pump is positive displacement type of pump operated by hand. It has a uniquely designed shape manufactured by casting.

Step 2: Gathered information: The maximum pressure created inside the pump is 2.715 Mpa. The amount of fluid required to rotate the receptor within three months is found by using the following formula

$\mathrm{V} = \mathrm{AL}$, where A is net crossectional area of the cylinder and L is the stroke of the piston(434.812 mm.

$$\mathrm{V} = \frac{\pi}{4}(\mathrm{D}^2 - \mathrm{d}^2)\mathrm{L} \text{ to lower the panel support and } \mathrm{V} = \frac{\pi}{4}\mathrm{D}^2\mathrm{L} \text{ to lift the panel support}$$

where D is the internal diameter of the cylinder and d is the outer diameter of the piston rod

The amount of fluid required to lower the panel support is less than to lift it. The fluid during lowering is

$$\mathrm{V} = \frac{\pi}{4}(\mathrm{D}^2 - \mathrm{d}^2)\mathrm{L} = \frac{\pi}{4}(41.91^2 - 33.4^2)434.812 = 218863.636 mm^3 = 218.864\times10^{-6} m^3$$

A volume of $218.864\times10^{-6} m^3$ of fluid is required to lower the support within three months.

$$218.864\times10^{-6} m^3 = 90\ \text{days}$$

$$\mathrm{x} = 1\ \text{day} \qquad \rightarrow = 218.864\times10^{-6} m^3 \frac{1\text{day}}{90\ \text{days}} = 2.432\times10^{-6}\mathrm{m}^3 = 2431.822\frac{\mathrm{mm}^3}{day}$$

The receptor rotates 23.5^o within three months, i.e., 0.261^o per day. The 23.5^o rotation is covered by a vertical motion of a piston of stroke of 434.812 mm. The 0.261^o is attained by a displacement of 4.831 mm of the piston per day. Therefore, a volume of 2431.822 mm^3 is needed to rotate the receptor 0.261^o per day.

The volume of fluid delivered by the pump 2 per stroke should be less or equal to 2431.822 mm^3. This implies that the stroke of the piston is one or more. The diameter of the piston and the stroke length is unknown. These dimensions are optimized by iteration.

The required volume of fluid (2431.822 mm^3) is equal to the volume of fluid delivered by the pump times the number of stroke

$\mathrm{V} = 2431.822\mathrm{mm}^3 = \mathrm{nAL}$, where A is the area of the cylinder of the pump and L is the stroke length

The amount of fluid required by the cylinder during lifting the panel support is

$$\mathrm{V} = \frac{\pi}{4}\mathrm{D}^2\mathrm{L} = \frac{\pi}{4}\times41.91^2\times434.812\mathrm{mm}^3 = 499827.986\mathrm{mm}^3 \text{ per three month or } 6664.756\ \mathrm{mm}^3$$

per day. where D is the diameter of the piston

Therefore, 6664.756mm^3 volume of fluid should be pumped by the pump daily. This volume of fluid (6664.756 mm^3) is equal to the volume of fluid delivered by the pump times the number of stroke

$V = 6664.756\text{mm}^3 = \text{nAL}$, where A is the area of the cylinder of the pump and L is the stroke length

$$V = 6664.756\,\text{mm}^3 = \text{nAL} = \pi n\frac{d^2L}{4} \rightarrow n = \frac{4\times 6664.756}{\pi n d^2} = \frac{8485.830\,\text{mm}^3}{Ld^2} \quad \text{......................}\mathbf{5\text{-}16}$$

The number of stroke must be integer number for both lifting and lowering. Therefore, by referring to Appendix K, 4 strokes for lowering and 11 strokes for lifting is selected. The corresponding diameter and stroke length of the pump optimized to 9 mm and 9.6 mm respectively.

Step 3: Problem statement: Designing of a pump, which is capable of resisting 2.715 Mpa pressure force.

Step 4: Determining the shape of the pump, which is compatible with the covers, plunger, support and the fasteners, among the alternative shapes shown in Appendix N 5.42, type B is selected because its shape can be manufactured easily.

Step 5: Material selection and working stress: The material should have resistance to corrosion and wear, has low coefficient of friction and relatively low cost and weight. The pump needs some machining and it is subjected to the environment, so that the material should satisfy these requirements. Al-alloy is a good material to resist corrosion but it is the most expensive. Alloy-steel is also expensive. Hence, the galvanized carbon steel is selected due to its lowest cost and relatively good resistance to corrosion [Appendix D]. To make the system compact in size and light in weight, the factor of safety should be minimum which is 2.

$$\text{Working stress} = \frac{\text{Endurance limit stress}}{\text{Factor of safety}}$$

However, the cylinder is subjected to reverse axial loading. We know that for reversed axial load:

Correction factor $K_a = 0.8$ [2]

The endurance limit for reversed axial loading: $\sigma_{ea} = \sigma_e \times K_a \times K_{sur} \times K_{sz}$

Where k_{sur}= surface finish factor =0.89 for machined with ultimate strength of 435Mpa

k_{sz} = Size factor=0.85 since nominal diameter is between 7.65 mm and 50mm

σ_e =0.8σ_y for carbon steel=0.8×217=173.6Mpa

σ_{ea} =173.6×0.8×0.89×0.85=105.063Mpa

$$\text{Working stress} = \frac{\text{Endurance limit stress}}{\text{Factor of safety}} \quad \sigma_w = \frac{\sigma_{ea}}{n} = \frac{105.531}{2} = 52.531\,\text{MPa}$$

Step 6: Detailed stress analysis

1. Calculation of the minimal thickness of the cylinder:

The cylinder should be classified either thin or thick. If the ratio of the wall thickness and the internal diameter of the cylinder is less than 0.1 it is thin cylinder. On the other hand if it is greater than 0.1 the cylinder is thick [2]. Since the cylinder is manufactured by casting its thickness should be greater than 1 mm. So that the ratio becomes 1/9 (0.111), this implies that the cylinder is must be classified thick.

Clavarino's equation: This equation is based on the maximum-strain theory of failure, but it is applied to closed-end cylinders (or cylinders fitted with heads) made of ductile material. According to this equation, the thickness of a cylinder [2]:

$$t = r_i\left[\sqrt{\frac{\sigma + (1-2\mu)P}{\sigma - (1-2\mu)P}} - 1\right] = 4.5\text{mm}\left[\sqrt{\frac{52.531\text{MPa} + (1-2\times 0.3)2.715\text{MPa}}{52.531\text{MPa} - (1-2\times 0.1)2.715\text{MPa}}} - 1\right] = 4.5\text{mm}\times 0.0422 = 0.190\text{mm}$$

This is a small thickness so that the pump has a thickness of 2 mm. The dimension of the pump is shown in Appendix N 5.43.

Design of Lever

Step 1: The lever is operated by a human muscular force and it is applied using hand.

Step 2: Gathered information: The human muscular force applied on the lever is shown in table below.

Table 4.1 Human Muscular force [9]

Name of operation	Continuous	Intermittent	Instantaneous
Hand operation	70-100	200-250	350-400

Step 3: Problem statement: Designing of a lever, which is capable of resisting a maximum of 400 N forces.

Step 4: Determining the shape of a lever that is compatible with the cylinder, cylinder support and the pump assembly

Among the alternative shapes shown in Appendix N 5.44, type B is selected because its compact size.

The lever is subjected to bending stress. Therefore, the flange is designed based on this induced stress.

Step 5: Material selection and working stress: The material should have resistance to corrosion and wear, has low coefficient of friction and relatively low cost and weight. The lever needs some machining and it is subjected to the environment, so that the material should satisfy these requirements. Al-alloy is a good material to resist corrosion but it is the most expensive. Alloy-steel is also expensive. Hence, the galvanized carbon steel is selected due to its lowest cost and relatively good resistance to corrosion [Appendix D]. To make the system compact in size and light in weight, the factor of safety should be minimum which is 2.

$$\text{Working stress} = \frac{\text{yield stress}}{\text{Factor of safety}} \rightarrow \sigma_w = \frac{\sigma_y}{n}$$

However, the lever is under reversed bending stress. The endurance limit for reversed bending load;

$$\sigma_{eb} = \sigma_e \times k_b \times k_{sur} \times k_{sz}$$

$k_b = 1$ for reverse bending loading

k_{sur} = surface finish factor =0.89 for machined with ultimate strength of 435Mpa

k_{sz} = Size factor=0.85 since nominal diameter is between 7.65 mm and 50mm

$\sigma_e = 0.8\sigma_y$ for carbon steel=0.8×217=173.6Mpa

σ_{eb} =173.6×1×0.89×0.85=131.328Mpa

$$\text{Working stress} = \frac{\text{Endurance limit stress}}{\text{Factor of safety}} \quad \sigma_w = \frac{\sigma_{eb}}{n} = \frac{131.328\text{MPa}}{2} = 65.664\text{MPa}$$

Step 6: Detailed stress analysis: The lever is under bending stress and this bending stress, and the length of the lever is 500 mm

$$\sigma_b = \frac{M_b}{Z}, \text{ Where } Z = \frac{I}{Y} = \frac{\pi D^4}{64D} = \frac{\pi D^3}{32} \text{ and } M_b = \text{bending moment}$$

$$\sigma_b = \frac{M_b}{Z} = \frac{FL}{Z} = \frac{32FL}{\pi D^3} \rightarrow D^3 = \frac{32FL}{\pi\sigma_b} = \frac{32 \times 400N \times 0.5m}{\pi \times 65.664\text{MPa}} = 31.024 \times 10^{-6} m^3 \rightarrow D = 31.422mm$$

This diameter is for solid bar, it is possible to reduce the weight and cost by make it hollow. The standard size of the hollow lever becomes $D_o = 42.164$mm and $t = 2.972$ mm.

Design of the Panel support on the Pin End

The weight of the upper side components applied on this support is equal to the weight applied on the extending side. This weight is 1826.312 N. The designed dimension of the support in the extending side is 4.023 mm however; it is changed to a hollow bar of 33.4 mm outer diameter and 3 mm thickness. Therefore, the dimension of the support in the pin end is made the same with extending side support.

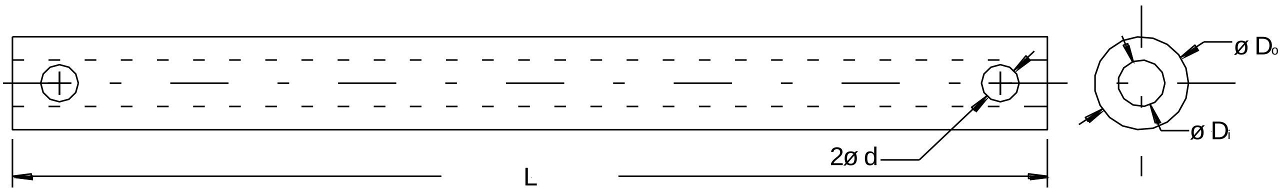

Figure 5.5-17 Panel support on the Fixed End

$D_o = 33.4$mm, $D_i = 27.4$ mm, $L = 1657.35$ mm and $d = 8$ mm

Chapter 6 Motor and Timer Selection

Motor Selection

The maximum and the minimum speed of the motor is depends on the season of the year and the place where the tracker is installed. Around equator, the length of the day throughout the year is almost constant but around the pole, the day length varies considerable seasonally. The speed of the motor should be set to track the sun accurately throughout the year.

A 0.25 hp pulse width modulation (PWM) motor is selected. The overall dimension of the motor is 143.51mmX91.44mmX79.248mm. PWM motor has accurate speed control system. In pulse width modulation (PWM) frequency converters, the consumption of reactive power is further reduced by the fact that the supply current drawn decrease as the speed is reduced. There is a thyristor bridge in regenerating PWM frequency converters and in those PWM converters, which also have intermediate circuit voltage control. However, the consumption of reactive power is relatively small, thanks to the small active power.

Timer Selection

The timer is used to start the motor in the morning so that it should be set for predetermined fixed duration of time. The type of timer, which fulfils this requirement, is the pulse timer. Pulse timers are used to produce a fixed duration output from some initiating input for a system that will give an output for a predetermined fixed length of time.

Chapter 7 Manufacturing Process

All the tubes are manufactured from the standard seamless tube that is the specified tubes are bought directly from the market and the required holes and threads are machined in the shop. All the covers and flanges are also manufactured from standard plate metals of 5 mm thickness and then the required shapes and holes are made in the shop. The plunger is taken from solid bar and machined as required. However, the pumps, the cylinder cup and valves are casted. On the other hand, the springs, bolts and nuts are taken from standard.

Manufacturing of pump 1

The plunger is prepared first, a bar is cut by power hacksaw, and then the threads on both ends are made by using lathe machine. It has a high surface finish by lathe machine. The valves are first casted and then machined by lathe to make fine surface finish. The cylinder cover is prepared from a plate metal of 5 mm thickness and the required dimension is cut by movable cutter. The holes are made by drilling machine.

Manufacturing of Powerhouse 1

The cylinder is manufactured from 217.934 mm and 210 mm outer and inner diameters respectively of seamless tube. The seamless tube is prepared and then cut as the required length. The piston rod is manufactured from 210 mm and 193.904 mm outer and inner diameter respectively of seamless tube. The seamless tube is prepared and then cut as the length. The piston head is prepared from a plate metal of thickness 5 mm and then cut by cutter. The cylinder cover 1, 2 & the flanges are prepared from a 5 mm thickness plate metal. The plate metal is prepared and then machined as the required dimension.

Manufacturing of Crank slider Mechanism

The upper panel support is manufactured from a seamless tube of 33.4 mm outer diameter and 3 mm thickness standard tube. After cutting the required length, the two holes are drilled. The upper panel support and piton rod hold is prepared from 39.4 mm outer diameter and 3 mm thickness standard tube. Then the holes are made by driller with 8 mm diameter.

Manufacturing of Powerhouse 2

The piston rod and panel support at the pined end are prepared from the same tube. The respective length is cut. The cylinder is manufactured from 48.26 mm outer diameter and 3.175 mm thickness standard seamless tube. The cylinder cup is first casted by sand casting then a thread is made by lathe internally. The flange is prepared from a 5 mm thickness plate metal. The plate metal is cut and the holes are drilled.

Manufacturing of Pump 2

The main housing is prepared by low-pressure die-casting. The lever handle is prepared from a standard tube of 39.4 mm outer diameter and 2.972 mm thickness. The lever handle hold is prepared from a 3 mm thickness plate metal by bending some its parts.

Chapter 8 Maintenance and Assembly

Assembly procedures

The different parts are assembled together to get the expected function. There are five main systems to be assembled together. These are the plunger pump 1, powerhouse 1, powerhouse 2, pump 2 and the motor speed controller and timer. After assembling these individual systems, they are again assembled together.

Assembly Procedures of Pump 1

In the suction side, the spring is inserted and then the valve, on contrary valve is first inserted and then spring in the discharge side. These valve-spring systems are hold by the cover using bolt and nut fasteners. After this, a nut is tightened on the plunger end. This nut plunger assembly is inserted into the pump housing. Insert the cover through the plunger and tighten by bolt and nut. After that insert the spring 3 above the cover then tighten by the cam follower.

Assembly Procedures of Powerhouse 1

The two flanges are welded at the two ends of the cylinder, then the cylinder cover with pin hold welded on it is tighten using bolt-nut system with the bottom flange. The piston is inserted from top into the cylinder through its piston head. A gasket with cylinder cover from top is inserted into the piston rod then tightens with bolt and nut.

Assembly Procedures of Powerhouse 2

The four lower supports are installed first. Then the cylinder-pump support is inserted into the lower supports. The cylinder is placed on the cylinder-pump support (base plate) from the top and tightened by nut. A piston is inserted into the cylinder. Finally A gasket with cylinder cover from the top is inserted into the piston rod and then tightened by bolt and nut.

Assembly Procedures of Pump 2

The valve and spring, and the spring and valve are inserted into the housing in the delivery and suction side of the pump respectively. Then the holes of the main housing is aligned with the holes of the cylinder-pump support (base plate) holes and tightened by the bolt and nut fasteners. The plunger is inserted into the housing, and then tighten the cover with bolt nut fasteners. The lever is attached with pin to the plunger and the fulcrum. Finally, these subassemblies are assembled in their respective places.

Maintenance

The total system is always subjected to atmospheric climate. Hence, it is likely subjected to corrosion. In order to protect the components from corrosion a sacrificial anode is applied.

The sacrificial anode is a special material that sacrifices itself to other components, i.e., the anode corroded first before the components are being corroded. The size of the sacrificial anode is very small so a considerable cost can be saved. When the anode sacrifices its body, it should be changed before the components are starting corrosion. The working fluid should be changed according to the designed working hours suggested by the manufacturer Appendix R.

Chapter 9 Cost analysis

The cost of the sun tracker is the sum of the raw material cost, manufacturing cost, overhead cost, cost of timer and motor and profit [Appendix Q].

$$\text{Total cost of the pump} = (\text{Total material cost} + \text{total manufacturing cost}) + \text{overheads} + \text{profit} + \text{motor cost} + \text{timer cost}$$

$$\text{Total cost of the pump} = (\text{Total material cost} + \text{total manufacturing cost}) + 15\%(\text{Total material cost} + \text{total manufacturing cost}) + 10\%(\text{Total material cost} + \text{total manufacturing cost}) + \text{motor cost} + \text{timer cost}$$

$$\text{Total cost of the pump} = 1880.11 + 15\% \times 1880.11 + 10\% \times 1880.11 + 376 + 281.624 = 3007.762 \text{ birr}$$

The single cost of the dual axis sun tracker is 3007.62 Birr by considering mass production. However, the cost becomes higher if it is required to manufacture only a single unit since the mechanism uses different dimensions of seamless tubes and bars. The standard length of the seamless tubes and the bars are 6 m but the required lengths are much less than 6 m. Therefore, the cost of a single unit is higher due to wastage.

Chapter 10 Conclusion and Recommendation

Conclusion

A chronological type of sun tracker is the most accurate way of tracking. However, it consumes more power. Hence, the designed tracker is accurate except some errors due to manufacturing of the parts, approximation of dimensions, measuring dimensions, setting the timer and installation of the systems.

It incorporates two powerhouse, two very small pumps, one motor, one timer and two-limit switch. The overall dimension of the tracker is 2000mmx1768mmx979mm and a weight of 40 kg and it costs 3007.76 birr. Since the sun tracker is dual axis, it can track the sun accurately. The azimuth rotation is operated automatically whereas the zenith rotation is operated manually.

The system rotates the panel 170^o from which it starts at 5^o and stops at 175^o in azimuth. This is due to the geometry limitation of the system. However, the panel rotates perfectly 47^o angle along zenith. The number of strokes to rotate in the azimuth angle is 88200 during extending and 8200 during retracting per day to cover 170^o. On the other hand, 360 strokes to lower and 990 strokes to lift the panel are required in the zenith direction to cover 23.5^o. A maximum of 0.017923 m^3 (17.923 Littre) fluid is required to extend both the azimuth and zenith rotation.

The receptor is at $\pm 23.5^o$ on June 21 and December 21 and 0^o on March 21 and September 21 in the zenith rotation.

The sun tracker increases the solar receptor from 0 to 91.33% in the azimuth direction and from 0 to 8.3 % in the zenith direction.

Recommendation

The viscosity of the fluid is depending on the atmospheric temperature value. It is absolutely recommended to use different viscous fluids for different places in order to have a good working fluid.

The timer is not working on the local standard time instead on the apparent local time. Therefore, we have to set the timer by calculating the apparent solar time for the intended places.

The components are protected from corrosion by the sacrificial anode. Therefore, it is advisable to check the life of the anode to change a new one. It is also recommended to make the sun tracker operational when the day length is more than 2 hours in the azimuth direction because the motor speed will be very high for day lengths less than 2 hours.

References

[1] ERIKOBERG, FRANKLIN D. JONES, HOLBROOK L. HORTON, ANDHENRY H. RYFFEL ,"Machinery's Handbook ," 27th Edition , INDUSTRIALPRESS INC, NEWYORK, 2004.

[2]. R.S. KHURMI and J.K. GUPTA, "A Text Book of Machine Design", EURASIA PUBLISHING HOUSE (PVT.) LTD. RAM NAGAR, NEW DELHI, 2005

[3] Joseph E. Shigley , "STANDARD HANDBOOK OF MACHINEDESIGN", Second Edition, McGraw-Hill, New York, 1996.

[4] Budynas−Nisbett , "Shigley's Mechanical Engineering Design", Eighth Edition, McGraw−Hill Primis.

[5] http://www.solars-panel.com/.

[6] Peter Keith Brian Hodges, "HYDRAULIC FLUIDS", F. I n st. Pet. Norway ARNOLD, First published in Great Britain in 1996.

[7] Dr. K. L. Narayana and Dr. P. Kannaiah , "Machine Drawing", 3rd edition, New Age International (P) Ltd., NewDelhi, 2006.

[8] Soteris Kalogirou , "Solar energy engineering: processes and systems ", 1st ed.p. cm., 2009

[9] Getaw Ayay, " Designing and Manufacturing of Manually Operated Plunger Pump", 2008

[10] Tiberiu Tudorache,Liviu Kreindler, "Design of a Solar Tracker System for PV Power Plants", 2010.

[11] Gustavo Ozuna, Carlos Anaya. Diana Figueroa. Nun Pitalua, "Solar Tracker of Two Degrees of freedom for Photovoltaic Solar Cell Using Fuzzy Logic", Proceedings of the World Congress on engineering 2011 Vol II WCE 2011, London, U.K, July 6 - 8, 2011.

[12] S. Lakeou, E. Ososanya, B.O. Latigo, W. Mahmoud, "Design of a Low-cost Solar Tracking Photo-Voltaic (PV) Module and Wind Turbine Combination System", University of the District of Columbia.

[13] Jeya Ganesh N, Maniprakash.S, Chandrasekaran L., Srinivasan, S.M., "Design and Development of a Sun Tracking mechanism using the Direct SMA actuation", USA.

[14] P. Roth, A. Georgiev, H. Boudinov, "Design and construction of a system for sun-tracking", Brazil, 2003.

[15] J. Rizk, and Y. Chaiko, "Solar Tracking System: More Efficient Use of Solar Panels", Sydney, 2008.

[16] N.Viswanatha, T.S Simil, N.Prasad, N.C.Bhat, and Y.S. Shankara Narayan, "A NOVEL SUN TRACKING MECHANISM", India.

[17] www.rockwellautomation.com.

[18] http://en.wikipedia.org/wiki/Solar_tracker

Appendixes

Appendix A Hours of Daylight by Latitude [Left: Northern hemisphere and Right: Southern hemisphere]

Length of Day at Various Latitudes (in Hours and Minutes on the 15th of Each Month)											
Month	Equator	10°	20°	30°	40°	50°	60°	70°	80°	Poles	Month
January	12:07	11:35	11:02	10:24	9:37	8:30	6:38	0:00	0:00	0:00	July
February	12:07	11:49	11:21	11:10	10:42	10:07	9:11	7:20	0:00	0:00	August
March	12:07	12:04	12:00	11:57	11:53	11:48	11:41	11:28	10:52	0:00	September
April	12:07	12:21	12:36	12:53	13:14	13:44	14:31	16:06	24:00	24:00	October
May	12:07	12:34	13:04	14:22	15:22	17:04	22:13	24:00	24:00	24:00	November
June	12:07	12:42	13:20	14:04	15:00	16:21	18:49	24:00	24:00	24:00	December
July	12:07	12:40	13:16	13:56	14:49	15:38	17:31	24:00	24:00	24:00	January
August	12:07	12:28	12:50	13:16	13:48	14:33	15:46	18:26	24:00	24:00	February
September	12:07	12:12	12:17	12:23	12:31	12:42	13:00	13:34	15:16	24:00	March
October	12:07	11:55	11:42	11:28	11:10	10:47	10:11	9:03	5:10	0:00	April
November	12:07	11:40	11:12	10:40	10:01	9:06	7:37	3:06	0:00	0:00	May
December	12:07	11:32	10:56	10:14	9:20	8:05	5:54	0:00	0:00	0:00	June

Appendix B Iteration of the length of the crank slider

L1(mm)	ΔL(mm)	Lmax(mm)	Lmin(mm)	L2(mm)	L1(mm)	ΔL(mm)	Lmax(mm)	Lmin(mm)	L2(mm)
100	200	600	400	500	560	1120	2440	1320	1880
110	220	640	420	530	570	1140	2480	1340	1910
120	240	680	440	560	580	1160	2520	1360	1940
130	260	720	460	590	590	1180	2560	1380	1970
140	280	760	480	620	600	1200	2600	1400	2000
150	300	800	500	650	610	1220	2640	1420	2030
160	320	840	520	680	620	1240	2680	1440	2060
170	340	880	540	710	630	1260	2720	1460	2090
180	360	920	560	740	640	1280	2760	1480	2120
190	380	960	580	770	650	1300	2800	1500	2150
200	400	1000	600	800	660	1320	2840	1520	2180
210	420	1040	620	830	670	1340	2880	1540	2210
220	440	1080	640	860	680	1360	2920	1560	2240
230	460	1120	660	890	690	1380	2960	1580	2270
240	480	1160	680	920	700	1400	3000	1600	2300
250	500	1200	700	950	710	1420	3040	1620	2330
260	520	1240	720	980	720	1440	3080	1640	2360
270	540	1280	740	1010	730	1460	3120	1660	2390
280	560	1320	760	1040	740	1480	3160	1680	2420
290	580	1360	780	1070	750	1500	3200	1700	2450
300	600	1400	800	1100	760	1520	3240	1720	2480
310	620	1440	820	1130	770	1540	3280	1740	2510
320	640	1480	840	1160	780	1560	3320	1760	2540
330	660	1520	860	1190	790	1580	3360	1780	2570
340	680	1560	880	1220	800	1600	3400	1800	2600

350	700	1600	900	1250	810	1620	3440	1820	2630
360	720	1640	920	1280	820	1640	3480	1840	2660
370	740	1680	940	1310	830	1660	3520	1860	2690
380	760	1720	960	1340	840	1680	3560	1880	2720
390	780	1760	980	1370	850	1700	3600	1900	2750
400	800	1800	1000	1400	860	1720	3640	1920	2780
410	820	1840	1020	1430	870	1740	3680	1940	2810
420	840	1880	1040	1460	880	1760	3720	1960	2840
430	860	1920	1060	1490	890	1780	3760	1980	2870
440	880	1960	1080	1520	900	1800	3800	2000	2900
450	900	2000	1100	1550	910	1820	3840	2020	2930
460	920	2040	1120	1580	920	1840	3880	2040	2960
470	940	2080	1140	1610	930	1860	3920	2060	2990
480	960	2120	1160	1640	940	1880	3960	2080	3020
490	980	2160	1180	1670	950	1900	4000	2100	3050
500	1000	2200	1200	1700	960	1920	4040	2120	3080
510	1020	2240	1220	1730	970	1940	4080	2140	3110
520	1040	2280	1240	1760	980	1960	4120	2160	3140
530	1060	2320	1260	1790	990	1980	4160	2180	3170
540	1080	2360	1280	1820	1000	2000	4200	2200	3200
550	1100	2400	1300	1850	1010	2020	4240	2220	3230
					1020	2040	4280	2240	3260

Appendix C Iteration of the dimension of internal diameter of the cylinders

r2(mm)	ΔL(mm)	V2(mm3/day)	Q2(mm3/s	r1(mm)	r1(mm)	L(mm)	V1(mm3/stroke	V1(mm3/stroke	A(plunger)	A(plunger)	v (mm/s)	t(s)	V(mm/s)	t(s)	n	n
50	500	3925000	45.428	2.5	5	10	196.25	785	19.625	78.5	2.31481	4.32	0.5787	17.3	20000	5000
55	500	4749250	54.968	2.5	5	10	196.25	785	19.625	78.5	2.80093	3.5702	0.70023	14.3	24200	6050
60	500	5652000	65.417	2.5	5	10	196.25	785	19.625	78.5	3.33333	3	0.83333	12	28800	7200
65	500	6633250	76.774	2.5	5	10	196.25	785	19.625	78.5	3.91204	2.5562	0.97801	10.2	33800	8450
70	500	7693000	89.039	2.5	5	10	196.25	785	19.625	78.5	4.53704	2.2041	1.13426	8.82	39200	9800
75	500	8831250	102.21	2.5	5	10	196.25	785	19.625	78.5	5.20833	1.92	1.30208	7.68	45000	11250
80	500	10048000	116.3	2.5	5	10	196.25	785	19.625	78.5	5.92593	1.6875	1.48148	6.75	51200	12800
85	500	11343250	131.29	2.5	5	10	196.25	785	19.625	78.5	6.68981	1.4948	1.67245	5.98	57800	14450
90	500	12717000	147.19	2.5	5	10	196.25	785	19.625	78.5	7.5	1.3333	1.875	5.33	64800	16200
95	500	14169250	164	2.5	5	10	196.25	785	19.625	78.5	8.35648	1.1967	2.08912	4.79	72200	18050
100	500	15700000	181.71	2.5	5	10	196.25	785	19.625	78.5	9.25926	1.08	2.31481	4.32	80000	20000
105	500	17309250	200.34	2.5	5	10	196.25	785	19.625	78.5	10.2083	0.9796	2.55208	3.92	88200	22050
110	500	18997000	219.87	2.5	5	10	196.25	785	19.625	78.5	11.2037	0.8926	2.80093	3.57	96800	24200
115	500	20763250	240.32	2.5	5	10	196.25	785	19.625	78.5	12.2454	0.8166	3.06134	3.27	105800	26450
120	500	22608000	261.67	2.5	5	10	196.25	785	19.625	78.5	13.3333	0.75	3.33333	3	115200	28800
125	500	24531250	283.93	2.5	5	10	196.25	785	19.625	78.5	14.4676	0.6912	3.6169	2.76	125000	31250
130	500	26533000	307.09	2.5	5	10	196.25	785	19.625	78.5	15.6481	0.6391	3.91204	2.56	135200	33800
135	500	28613250	331.17	2.5	5	10	196.25	785	19.625	78.5	16.875	0.5926	4.21875	2.37	145800	36450
140	500	30772000	356.16	2.5	5	10	196.25	785	19.625	78.5	18.1481	0.551	4.53704	2.2	156800	39200
145	500	33009250	382.05	2.5	5	10	196.25	785	19.625	78.5	19.4676	0.5137	4.8669	2.05	168200	42050
150	500	35325000	408.85	2.5	5	10	196.25	785	19.625	78.5	20.8333	0.48	5.20833	1.92	180000	45000
155	500	37719250	436.57	2.5	5	10	196.25	785	19.625	78.5	22.2454	0.4495	5.56134	1.8	192200	48050
160	500	40192000	465.19	2.5	5	10	196.25	785	19.625	78.5	23.7037	0.4219	5.92593	1.69	204800	51200
165	500	42743250	494.71	2.5	5	10	196.25	785	19.625	78.5	25.2083	0.3967	6.30208	1.59	217800	54450
170	500	45373000	525.15	2.5	5	10	196.25	785	19.625	78.5	26.7593	0.3737	6.68981	1.49	231200	57800
175	500	48081250	556.5	2.5	5	10	196.25	785	19.625	78.5	28.3565	0.3527	7.08912	1.41	245000	61250
180	500	50868000	588.75	2.5	5	10	196.25	785	19.625	78.5	30	0.3333	7.5	1.33	259200	64800
185	500	53733250	621.91	2.5	5	10	196.25	785	19.625	78.5	31.6898	0.3156	7.92245	1.26	273800	68450
190	500	56677000	655.98	2.5	5	10	196.25	785	19.625	78.5	33.4259	0.2992	8.35648	1.2	288800	72200
195	500	59699250	690.96	2.5	5	10	196.25	785	19.625	78.5	35.2083	0.284	8.80208	1.14	304200	76050

Appendix D Characteristic of materials [2]

Designation	Description	e%	Mn%	Si%	Mo%	Cu%	σy Mpa	Relative cost
40c - 8	Plian carbon steel	0.4	0.8	_	_	_	320	medium
35Mn 2 - Mo28	Alloy -steel	0.35	0.2	_	0.28	_	600	high
0.6Cu-0.3Mn-5Si	Al-alloy	_	0.3	-5	_	0.6	63	highest
Galvanized C-18	Carbon steel	0.18	-	-	-	-	217	lowest

Appendix E Characteristics of Spring Materials [3]

Common Name	Young's Modulus E (1) MPa 10^3	Young's Modulus E (1) psi 10^6	Modulus of Rigidity G (1) MPa 10^3	Modulus of Rigidity G (1) psi 10^6	Density (1) g/cm^3 (lb/in^3)	Electrical Conductivity (1) % IACS	Sizes Normally Available (2) Min. mm (in.)	Sizes Normally Available (2) Max. mm (in.)	Typical Surface Quality (3)	Maximum Service Temperature (4) °C	Maximum Service Temperature (4) °F
Carbon Steel Wires:											
Music (5)	207	(30)	79.3	(11.5)	7.86 (0.284)	7	0.10 (0.004)	6.35 (0.250)	a	120	250
Hard Drawn (5)	207	(30)	79.3	(11.5)	7.86 (0.284)	7	0.13 (0.005)	16 (0.625)	c	150	250
Oil Tempered	207	(30)	79.3	(11.5)	7.86 (0.284)	7	0.50 (0.020)	16 (0.625)	c	150	300
Valve Spring	207	(30)	79.3	(11.5)	7.86 (0.284)	7	1.3 (0.050)	6.35 (0.250)	a	150	300
Alloy Steel Wires:											
Chrome Vanadium	207	(30)	79.3	(11.5)	7.86 (0.284)	7	0.50 (0.020)	11 (0.435)	a,b	220	425
Chrome Silicon	207	(30)	79.3	(11.5)	7.86 (0.284)	5	0.50 (0.020)	9.5 (0.375)	a,b	245	475
Stainless Steel Wires:											
Austenitic Type 302	193	(28)	69.0	(10.)	7.92 (0.286)	2	0.13 (0.005)	9.5 (0.375)	b	260	500
Precipitation Hardening 17-7 PH	203	(29.5)	75.8	(11)	7.81 (0.282)	2	0.08 (0.002)	12.5 (0.500)	b	315	600
NiCr A286	200	(29)	71.7	(10.4)	8.03 (0.290)	2	0.40 (0.016)	5 (0.200)	b	510	950

Appendix E Characteristics of Spring Materials [2]

Material	Allowable shear stress (τ) MPa			Modulus of rigidity (G) kN/m^2	Modulus of elasticity (E) kN/mm^2
	Severe service	Average service	Light service		
1. Carbon steel					
(a) Upto to 2.125 mm dia.	420	525	651		
(b) 2.125 to 4.625 mm	385	483	595		
(c) 4.625 to 8.00 mm	336	420	525		
(d) 8.00 to 13.25 mm	294	364	455		
(e) 13.25 to 24.25 mm	252	315	392	80	210
(f) 24.25 to 38.00 mm	224	280	350		
2. Music wire	392	490	612		
3. Oil tempered wire	336	420	525		
4. Hard-drawn spring wire	280	350	437.5		
5. Stainless-steel wire	280	350	437.5	70	196
6. Monel metal	196	245	306	44	105
7. Phosphor bronze	196	245	306	44	105
8. Brass	140	175	219	35	100

Appendix F Iteration of spring 1 wire and mean diameter

d(m)	0.00130	0.00140	0.00150	0.00160	0.00170	0.00180	0.00190	0.00200	0.00210	0.00220	0.00230	0.00240	0.00250	0.00260	0.00270	0.00280	0.00290
D(m)	0.00598	0.00758	0.00944	0.01157	0.01398	0.01671	0.01976	0.02315	0.02691	0.03104	0.03558	0.04053	0.04592	0.05176	0.05807	0.06487	0.07218

d(m)	0.00300	0.00310	0.00320	0.00330	0.00340	0.00350	0.00360	0.00370	0.00380	0.00390	0.00400	0.00410	0.00420	0.00430	0.00440	0.00450	0.00460	0.00470
D(m)	0.08001	0.08838	0.09732	0.10684	0.11695	0.12768	0.13905	0.15106	0.16375	0.17712	0.19120	0.20601	0.22156	0.23787	0.25495	0.27284	0.29154	0.31107

d(m)	0.00480	0.00490	0.00500	0.00510	0.00520	0.00530	0.00540	0.00550	0.00560	0.00570	0.00580	0.00590	0.00600	0.00610	0.00620	0.00630	0.00635
D(m)	0.33146	0.35271	0.37485	0.39790	0.42187	0.44678	0.47265	0.49950	0.52735	0.55621	0.58611	0.61705	0.64906	0.68216	0.71637	0.75169	0.76979

Appendix H Iteration of numbers of active coils and pitch of spring 2

N	38.000	37.000	36.000	35.000	34.000	33.000	32.000	31.000	30.000	29.000	28.000	27.000	26.000	25.000	24.000	23.000	22.000	21.000
P(mm)	0.579	0.595	0.611	0.629	0.647	0.667	0.688	0.710	0.733	0.759	0.786	0.815	0.846	0.880	0.917	0.957	1.000	1.048

N	20.000	19.000	18.000	17.000	16.000	15.000	14.000	13.000	12.000	11.000	10.000	9.000	8.000	7.000	6.000	5.000	4.000	3.000	2.000	1.000
P(mm)	1.100	1.158	1.222	1.294	1.375	1.467	1.571	1.692	1.833	2.000	2.200	2.444	2.750	3.143	3.667	4.400	5.500	7.333	11.000	22.000

Appendix I standard representation of ground closed end spring [4]

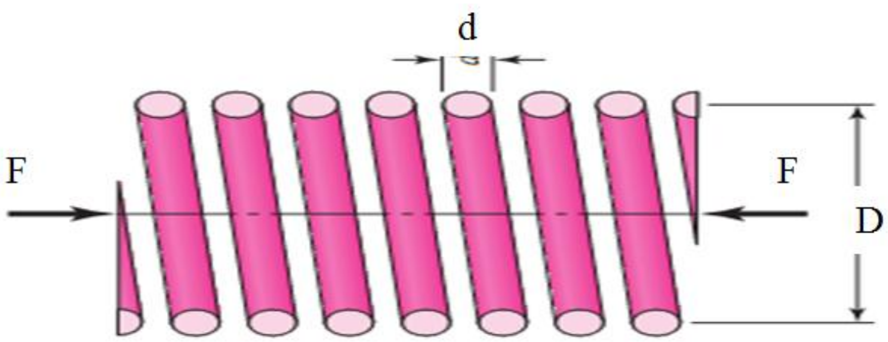

Appendix K iteration of the diameter of the pump 2 and numbers of strokes during lifting and lowering of panel support

D(mm)	Lowering	Lifting	Lowering	Lifting	Lowering	Lifting	Lowering	Lifting	Lowering	Lifting	Lowering	Lifting	Lowering	Lifting
	n=1	n	n=2	n	n=3	n	n=4	n	n=5	n	n=6	n	n=7	n
	L (mm)		L (mm)		L (mm)		L (mm)		L (mm)		L (mm)		L (mm)	
1.0	3096.3	2.7	1548.1	5.5	1032.1	8.2	774.1	11.0	617.3	13.7	516.0	16.4	442.3	19.2
2.0	774.1	2.7	387.0	5.5	258.0	8.2	193.5	11.0	154.3	13.7	129.0	16.4	110.6	19.2
3.0	344.0	2.7	172.0	5.5	114.7	8.2	86.0	11.0	68.6	13.7	57.3	16.4	49.1	19.2
4.0	193.5	2.7	96.8	5.5	64.5	8.2	48.4	11.0	38.6	13.7	32.3	16.4	27.6	19.2
5.0	123.9	2.7	61.9	5.5	41.3	8.2	31.0	11.0	24.7	13.7	20.6	16.4	17.7	19.2
6.0	86.0	2.7	43.0	5.5	28.7	8.2	21.5	11.0	17.1	13.7	14.3	16.4	12.3	19.2
7.0	63.2	2.7	31.6	5.5	21.1	8.2	15.8	11.0	12.6	13.7	10.5	16.4	9.0	19.2
8.0	48.4	2.7	24.2	5.5	16.1	8.2	12.1	11.0	9.6	13.7	8.1	16.4	6.9	19.2
9.0	38.2	2.7	19.1	5.5	12.7	8.2	9.6	11.0	7.6	13.7	6.4	16.4	5.5	19.2
10.0	31.0	2.7	15.5	5.5	10.3	8.2	7.7	11.0	6.2	13.7	5.2	16.4	4.4	19.2
11.0	25.6	2.7	12.8	5.5	8.5	8.2	6.4	11.0	5.1	13.7	4.3	16.4	3.7	19.2
12.0	21.5	2.7	10.8	5.5	7.2	8.2	5.4	11.0	4.3	13.7	3.6	16.4	3.1	19.2
13.0	18.3	2.7	9.2	5.5	6.1	8.2	4.6	11.0	3.7	13.7	3.1	16.4	2.6	19.2
14.0	15.8	2.7	7.9	5.5	5.3	8.2	3.9	11.0	3.1	13.7	2.6	16.4	2.3	19.2
15.0	13.8	2.7	6.9	5.5	4.6	8.2	3.4	11.0	2.7	13.7	2.3	16.4	2.0	19.2
16.0	12.1	2.7	6.0	5.5	4.0	8.2	3.0	11.0	2.4	13.7	2.0	16.4	1.7	19.2
17.0	10.7	2.7	5.4	5.5	3.6	8.2	2.7	11.0	2.1	13.7	1.8	16.4	1.5	19.2
18.0	9.6	2.7	4.8	5.5	3.2	8.2	2.4	11.0	1.9	13.7	1.6	16.4	1.4	19.2
19.0	8.6	2.7	4.3	5.5	2.9	8.2	2.1	11.0	1.7	13.7	1.4	16.4	1.2	19.2
20.0	7.7	2.7	3.9	5.5	2.6	8.2	1.9	11.0	1.5	13.7	1.3	16.4	1.1	19.2

The number of stroke both for lifting and lowering of the panel support is shown below.

Lowering (n)	1	2	3	4	5	6	7	8	9	10
Lifting (n)	2.7	5.5	8.2	11.0	13.7	16.4	19.2	21.9	24.7	27.4
Lowering (n)	11	12	13	14	15	16	17	18	19	20
Lifting (n)	30.2	32.9	35.6	38.4	41.1	43.9	46.6	49.3	52.1	54.8

Appendix L Day length and speed of motor

day length (hr)	speed (rpm)	day length (hr)	speed (rpm)	day length (hr)	speed (rpm)	day length (hr)	speed (rpm)	day length (hr)	speed (rpm)	day length (hr)	speed (rpm)	day length (hr)	speed (rpm)	day length (hr)	speed (rpm)
24.0	61.3	21.0	70.0	18.0	81.7	15.0	98.0	12.0	122.5	9.0	163.3	6.0	245.0	3.0	490.0
23.9	61.5	20.9	70.3	17.9	82.1	14.9	98.7	11.9	123.5	8.9	165.2	5.9	249.2	2.9	506.9
23.8	61.8	20.8	70.7	17.8	82.6	14.8	99.3	11.8	124.6	8.8	167.0	5.8	253.4	2.8	525.0
23.7	62.0	20.7	71.0	17.7	83.1	14.7	100.0	11.7	125.6	8.7	169.0	5.7	257.9	2.7	544.4
23.6	62.3	20.6	71.4	17.6	83.5	14.6	100.7	11.6	126.7	8.6	170.9	5.6	262.5	2.6	565.4
23.5	62.6	20.5	71.7	17.5	84.0	14.5	101.4	11.5	127.8	8.5	172.9	5.5	267.3	2.5	588.0
23.4	62.8	20.4	72.1	17.4	84.5	14.4	102.1	11.4	128.9	8.4	175.0	5.4	272.2	2.4	612.5
23.3	63.1	20.3	72.4	17.3	85.0	14.3	102.8	11.3	130.1	8.3	177.1	5.3	277.4	2.3	639.1
23.2	63.4	20.2	72.8	17.2	85.5	14.2	103.5	11.2	131.3	8.2	179.3	5.2	282.7	2.2	668.2
23.1	63.6	20.1	73.1	17.1	86.0	14.1	104.3	11.1	132.4	8.1	181.5	5.1	288.2	2.1	700.0
23.0	63.9	20.0	73.5	17.0	86.5	14.0	105.0	11.0	133.6	8.0	183.8	5.0	294.0	2.0	735.0
22.9	64.2	19.9	73.9	16.9	87.0	13.9	105.8	10.9	134.9	7.9	186.1	4.9	300.0	1.9	773.7
22.8	64.5	19.8	74.2	16.8	87.5	13.8	106.5	10.8	136.1	7.8	188.5	4.8	306.3	1.8	816.7
22.7	64.8	19.7	74.6	16.7	88.0	13.7	107.3	10.7	137.4	7.7	190.9	4.7	312.8	1.7	864.7
22.6	65.0	19.6	75.0	16.6	88.6	13.6	108.1	10.6	138.7	7.6	193.4	4.6	319.6	1.6	918.8
22.5	65.3	19.5	75.4	16.5	89.1	13.5	108.9	10.5	140.0	7.5	196.0	4.5	326.7	1.5	980.0
22.4	65.6	19.4	75.8	16.4	89.6	13.4	109.7	10.4	141.3	7.4	198.6	4.4	334.1	1.4	1050.0
22.3	65.9	19.3	76.2	16.3	90.2	13.3	110.5	10.3	142.7	7.3	201.4	4.3	341.9	1.3	1130.8
22.2	66.2	19.2	76.6	16.2	90.7	13.2	111.4	10.2	144.1	7.2	204.2	4.2	350.0	1.2	1225.0
22.1	66.5	19.1	77.0	16.1	91.3	13.1	112.2	10.1	145.5	7.1	207.0	4.1	358.5	1.1	1336.4
22.0	66.8	19.0	77.4	16.0	91.9	13.0	113.1	10.0	147.0	7.0	210.0	4.0	367.5	1.0	1470.0
21.9	67.1	18.9	77.8	15.9	92.5	12.9	114.0	9.9	148.5	6.9	213.0	3.9	376.9	0.9	1633.3
21.8	67.4	18.8	78.2	15.8	93.0	12.8	114.8	9.8	150.0	6.8	216.2	3.8	386.8	0.8	1837.5
21.7	67.7	18.7	78.6	15.7	93.6	12.7	115.7	9.7	151.5	6.7	219.4	3.7	397.3	0.7	2100.0
21.6	68.1	18.6	79.0	15.6	94.2	12.6	116.7	9.6	153.1	6.6	222.7	3.6	408.3	0.6	2450.0
21.5	68.4	18.5	79.5	15.5	94.8	12.5	117.6	9.5	154.7	6.5	226.2	3.5	420.0	0.5	2940.0
21.4	68.7	18.4	79.9	15.4	95.5	12.4	118.5	9.4	156.4	6.4	229.7	3.4	432.4	0.4	3675.0
21.3	69.0	18.3	80.3	15.3	96.1	12.3	119.5	9.3	158.1	6.3	233.3	3.3	445.5	0.3	4900.0
21.2	69.3	18.2	80.8	15.2	96.7	12.2	120.5	9.2	159.8	6.2	237.1	3.2	459.4	0.2	7350.0
21.1	69.7	18.1	81.2	15.1	97.4	12.1	121.5	9.1	161.5	6.1	241.0	3.1	474.2	0.1	14700.0

Appendix M iteration for change in angle and length

β (deg)	β (rad)	cos(β)	L1 (mm)	L2 (mm)	L3 (mm)		β (deg)	β (rad)	cos(β)	L1 (mm)	L2 (mm)	L3 (mm)

0	0.00	1.00	250	950	700.0		46	0.80	0.69	250	950	796.8
1	0.02	1.00	250	950	700.1		47	0.82	0.68	250	950	800.6
2	0.03	1.00	250	950	700.2		48	0.84	0.67	250	950	804.4
3	0.05	1.00	250	950	700.5		49	0.85	0.66	250	950	808.2
4	0.07	1.00	250	950	700.8		50	0.87	0.64	250	950	812.1
5	0.09	1.00	250	950	701.3		51	0.89	0.63	250	950	816.0
6	0.10	0.99	250	950	701.9		52	0.91	0.62	250	950	820.0
7	0.12	0.99	250	950	702.5		53	0.92	0.60	250	950	824.0
8	0.14	0.99	250	950	703.3		54	0.94	0.59	250	950	828.0
9	0.16	0.99	250	950	704.2		55	0.96	0.57	250	950	832.1
10	0.17	0.98	250	950	705.1		56	0.98	0.56	250	950	836.2
11	0.19	0.98	250	950	706.2		57	0.99	0.55	250	950	840.3
12	0.21	0.98	250	950	707.4		58	1.01	0.53	250	950	844.4
13	0.23	0.97	250	950	708.6		59	1.03	0.52	250	950	848.6
14	0.24	0.97	250	950	710.0		60	1.05	0.50	250	950	852.8
15	0.26	0.97	250	950	711.5		61	1.06	0.49	250	950	857.0
16	0.28	0.96	250	950	713.0		62	1.08	0.47	250	950	861.3
17	0.30	0.96	250	950	714.7		63	1.10	0.45	250	950	865.5
18	0.31	0.95	250	950	716.4		64	1.12	0.44	250	950	869.8
19	0.33	0.95	250	950	718.2		65	1.13	0.42	250	950	874.1
20	0.35	0.94	250	950	720.2		66	1.15	0.41	250	950	878.4
21	0.37	0.93	250	950	722.2		67	1.17	0.39	250	950	882.7
22	0.38	0.93	250	950	724.3		68	1.19	0.38	250	950	887.0
23	0.40	0.92	250	950	726.4		69	1.20	0.36	250	950	891.3
24	0.42	0.91	250	950	728.7		70	1.22	0.34	250	950	895.7
25	0.44	0.91	250	950	731.1		71	1.24	0.33	250	950	900.0
26	0.45	0.90	250	950	733.5		72	1.26	0.31	250	950	904.4
27	0.47	0.89	250	950	736.0		73	1.27	0.29	250	950	908.8
28	0.49	0.88	250	950	738.6		74	1.29	0.28	250	950	913.1
29	0.51	0.87	250	950	741.3		75	1.31	0.26	250	950	917.5
30	0.52	0.87	250	950	744.0		76	1.33	0.24	250	950	921.8
31	0.54	0.86	250	950	746.8		77	1.34	0.23	250	950	926.2
32	0.56	0.85	250	950	749.7		78	1.36	0.21	250	950	930.5
33	0.58	0.84	250	950	752.7		79	1.38	0.19	250	950	934.9
34	0.59	0.83	250	950	755.7		80	1.40	0.17	250	950	939.2
35	0.61	0.82	250	950	758.8		81	1.41	0.16	250	950	943.6
36	0.63	0.81	250	950	762.0		82	1.43	0.14	250	950	947.9
37	0.65	0.80	250	950	765.2		83	1.45	0.12	250	950	952.2
38	0.66	0.79	250	950	768.5		84	1.47	0.11	250	950	956.6
39	0.68	0.78	250	950	771.9		85	1.48	0.09	250	950	960.9
40	0.70	0.77	250	950	775.3		86	1.50	0.07	250	950	965.1
41	0.72	0.75	250	950	778.7		87	1.52	0.05	250	950	969.4
42	0.73	0.74	250	950	782.2		88	1.54	0.04	250	950	973.7
43	0.75	0.73	250	950	785.8		89	1.55	0.02	250	950	977.9
44	0.77	0.72	250	950	789.4		90	1.57	0.00	250	950	982.2
45	0.79	0.71	250	950	793.1		91	1.59	-0.02	250	950	986.4

β (deg)	β (rad)	cos(β)	L1 (mm)	L2 (mm)	L3 (mm)		β (deg)	β (rad)	cos(β)	L1 (mm)	L2 (mm)	L3 (mm)
92	1.60	-0.03	250	950	990.6		138	2.41	-0.74	250	950	1147.9
93	1.62	-0.05	250	950	994.7		139	2.42	-0.75	250	950	1150.3
94	1.64	-0.07	250	950	998.9		140	2.44	-0.77	250	950	1152.6
95	1.66	-0.09	250	950	1003.0		141	2.46	-0.78	250	950	1154.9
96	1.67	-0.10	250	950	1007.1		142	2.48	-0.79	250	950	1157.1
97	1.69	-0.12	250	950	1011.2		143	2.49	-0.80	250	950	1159.3
98	1.71	-0.14	250	950	1015.2		144	2.51	-0.81	250	950	1161.4
99	1.73	-0.16	250	950	1019.3		145	2.53	-0.82	250	950	1163.5
100	1.74	-0.17	250	950	1023.3		146	2.55	-0.83	250	950	1165.5
101	1.76	-0.19	250	950	1027.2		147	2.56	-0.84	250	950	1167.5
102	1.78	-0.21	250	950	1031.2		148	2.58	-0.85	250	950	1169.4
103	1.80	-0.22	250	950	1035.1		149	2.60	-0.86	250	950	1171.3
104	1.81	-0.24	250	950	1039.0		150	2.62	-0.87	250	950	1173.1
105	1.83	-0.26	250	950	1042.8		151	2.63	-0.87	250	950	1174.8
106	1.85	-0.27	250	950	1046.7		152	2.65	-0.88	250	950	1176.5
107	1.87	-0.29	250	950	1050.5		153	2.67	-0.89	250	950	1178.1
108	1.88	-0.31	250	950	1054.2		154	2.69	-0.90	250	950	1179.7
109	1.90	-0.32	250	950	1057.9		155	2.70	-0.91	250	950	1181.2
110	1.92	-0.34	250	950	1061.6		156	2.72	-0.91	250	950	1182.7
111	1.94	-0.36	250	950	1065.3		157	2.74	-0.92	250	950	1184.1
112	1.95	-0.37	250	950	1068.9		158	2.76	-0.93	250	950	1185.4
113	1.97	-0.39	250	950	1072.5		159	2.77	-0.93	250	950	1186.7
114	1.99	-0.41	250	950	1076.0		160	2.79	-0.94	250	950	1187.9
115	2.01	-0.42	250	950	1079.5		161	2.81	-0.95	250	950	1189.1
116	2.02	-0.44	250	950	1083.0		162	2.83	-0.95	250	950	1190.2
117	2.04	-0.45	250	950	1086.4		163	2.84	-0.96	250	950	1191.2
118	2.06	-0.47	250	950	1089.8		164	2.86	-0.96	250	950	1192.2
119	2.08	-0.48	250	950	1093.1		165	2.88	-0.97	250	950	1193.2
120	2.09	-0.50	250	950	1096.4		166	2.90	-0.97	250	950	1194.0
121	2.11	-0.51	250	950	1099.6		167	2.91	-0.97	250	950	1194.9
122	2.13	-0.53	250	950	1102.8		168	2.93	-0.98	250	950	1195.6
123	2.15	-0.54	250	950	1106.0		169	2.95	-0.98	250	950	1196.3
124	2.16	-0.56	250	950	1109.1		170	2.97	-0.98	250	950	1196.9
125	2.18	-0.57	250	950	1112.2		171	2.98	-0.99	250	950	1197.5
126	2.20	-0.59	250	950	1115.2		172	3.00	-0.99	250	950	1198.0
127	2.22	-0.60	250	950	1118.2		173	3.02	-0.99	250	950	1198.5
128	2.23	-0.61	250	950	1121.2		174	3.04	-0.99	250	950	1198.9
129	2.25	-0.63	250	950	1124.1		175	3.05	-1.00	250	950	1199.2
130	2.27	-0.64	250	950	1126.9		176	3.07	-1.00	250	950	1199.5
131	2.29	-0.66	250	950	1129.7		177	3.09	-1.00	250	950	1199.7
132	2.30	-0.67	250	950	1132.4		178	3.11	-1.00	250	950	1199.9
133	2.32	-0.68	250	950	1135.1		179	3.12	-1.00	250	950	1200.0
134	2.34	-0.69	250	950	1137.8		180	3.14	-1.00	250	950	1200.0
135	2.36	-0.71	250	950	1140.4							

136	2.37	-0.72	250	950	1142.9							
137	2.39	-0.73	250	950	1145.4							

Appendix N Alternative Forms (shapes)

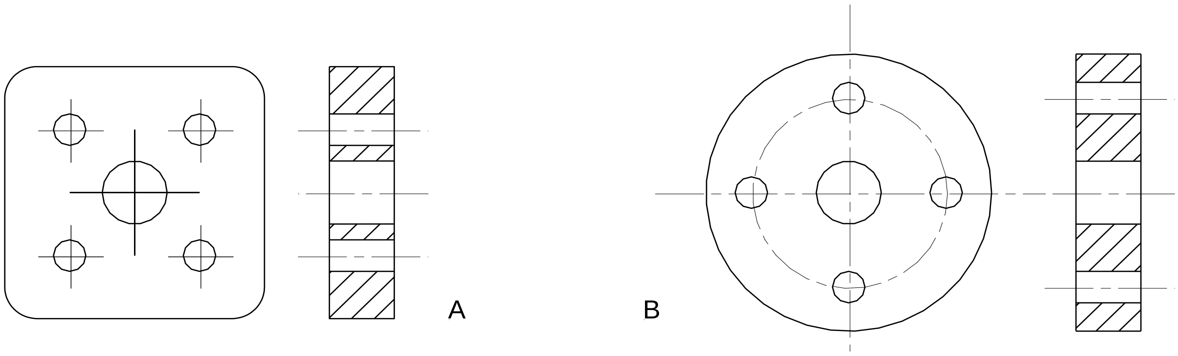

Figure 5.10-1 Forms of Cylinder Cover

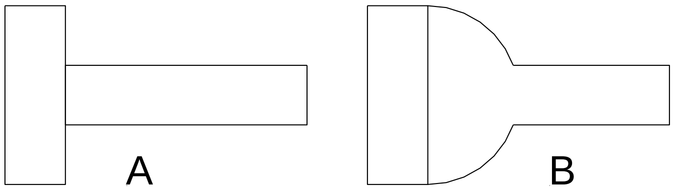

Figure 5.10-2 Valve Forms

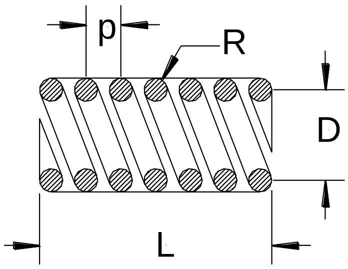

Figure 5.10-3 Spring 2

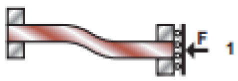

Figure 5.10-4 Buckling type

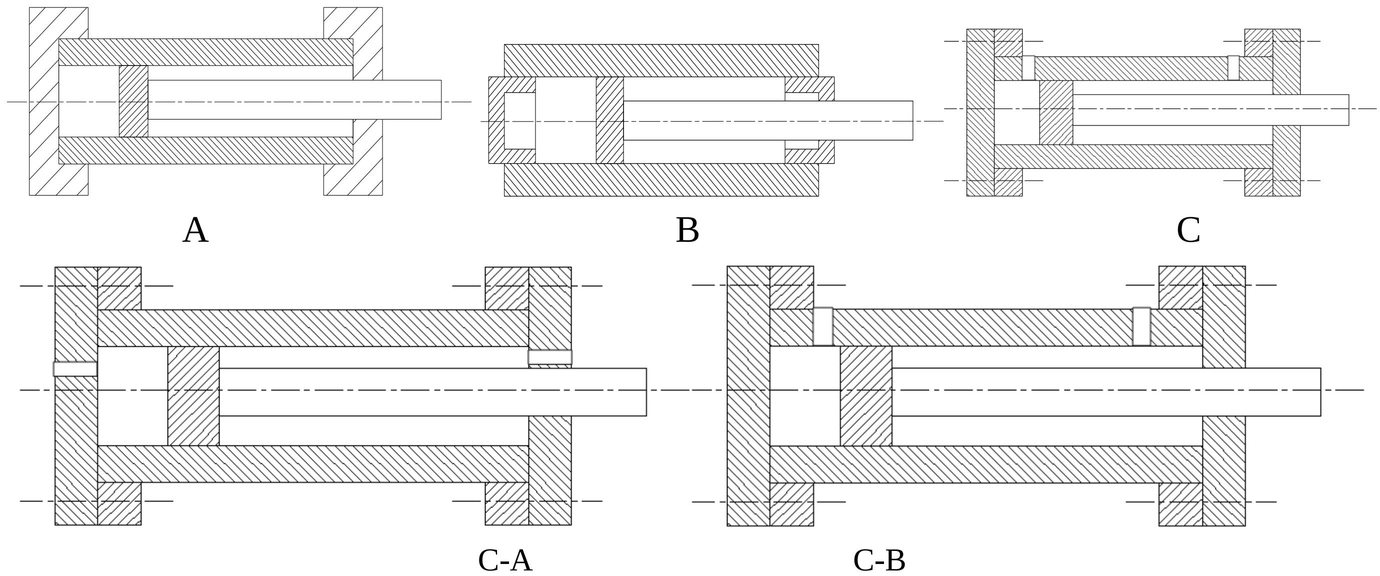

Figure 5.10-5 Forms of cylinder

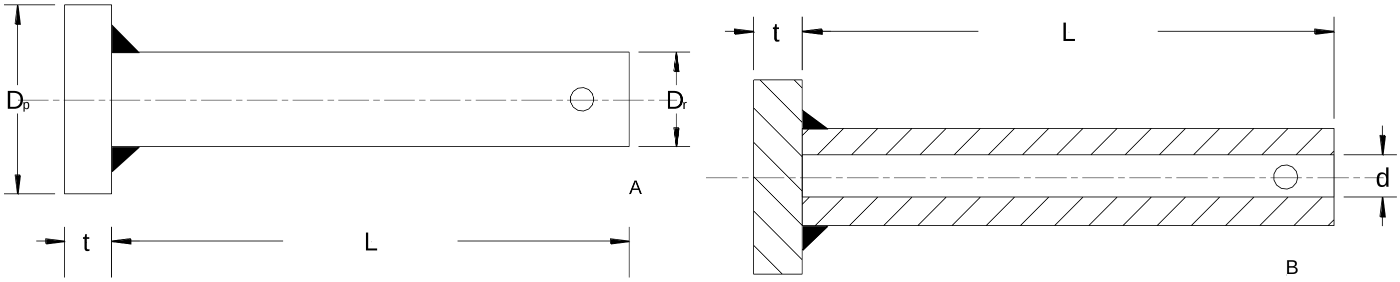

Figure 5.10-6 Forms of piston

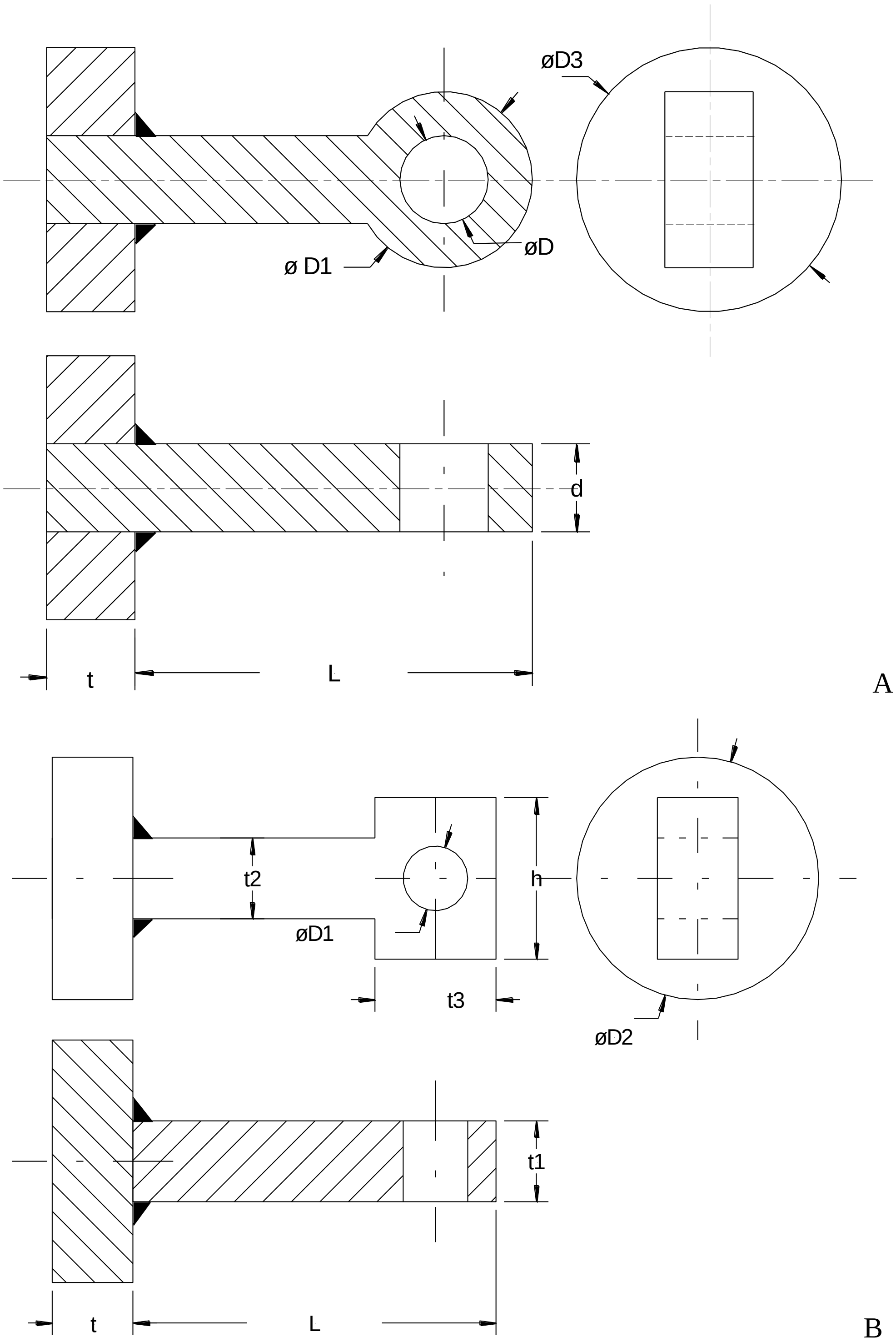

Figure 5.10-7 Hook and plunger end cover

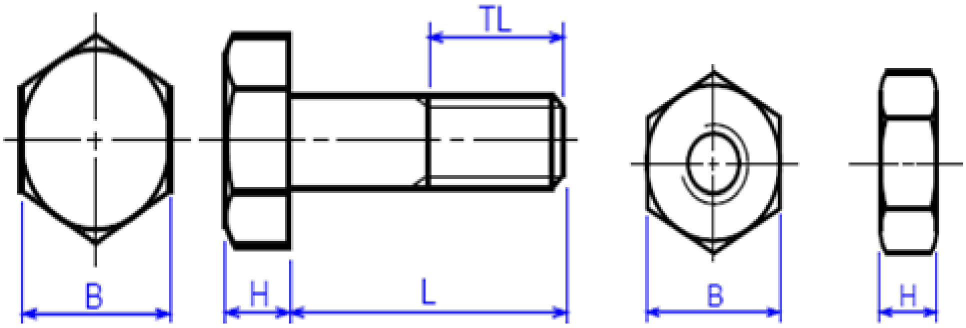

Figure 5.10-8 Standard Representation of Bolt and Nut

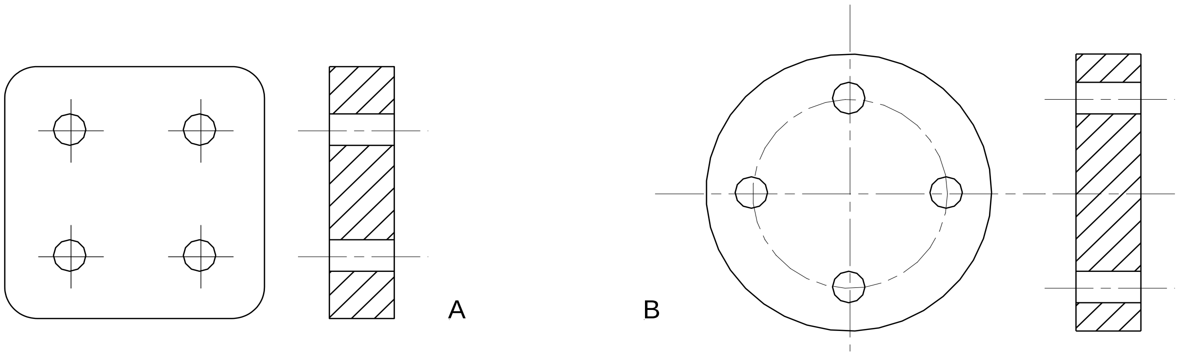

Figure 5.10-9 Cylinder Cover

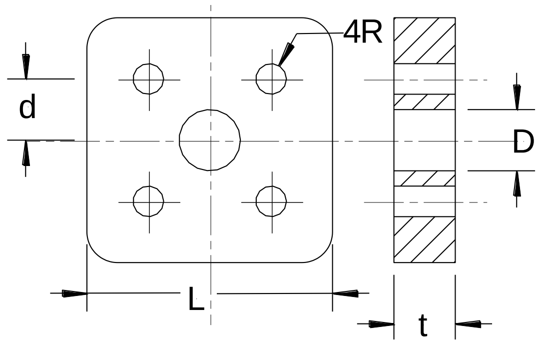

Figure 5.10-10 Cylinder cover 2

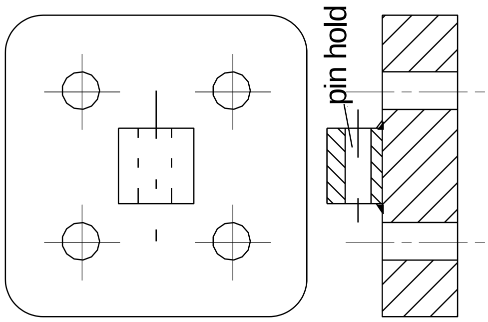

Figure 5.10-11 Cylinder Cover Pin Hold

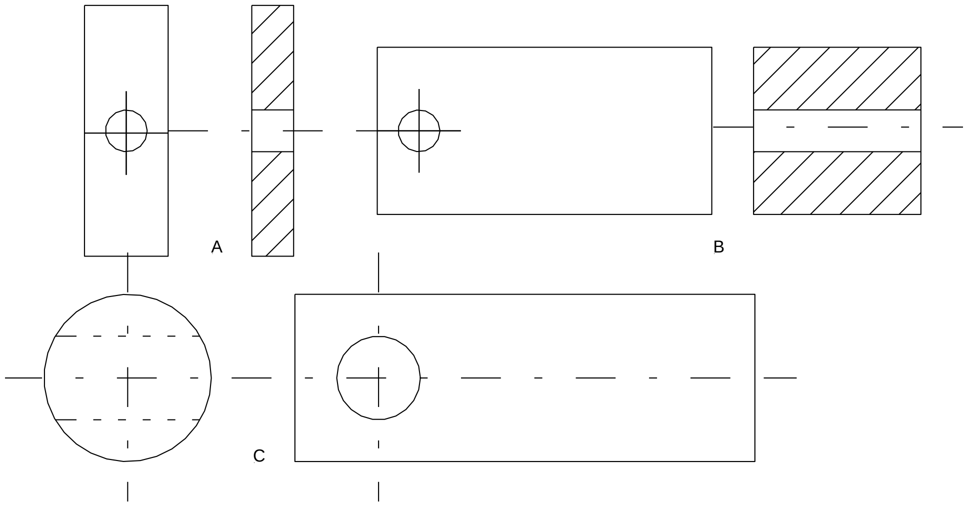

Figure 5.10-12 Forms Pin hold

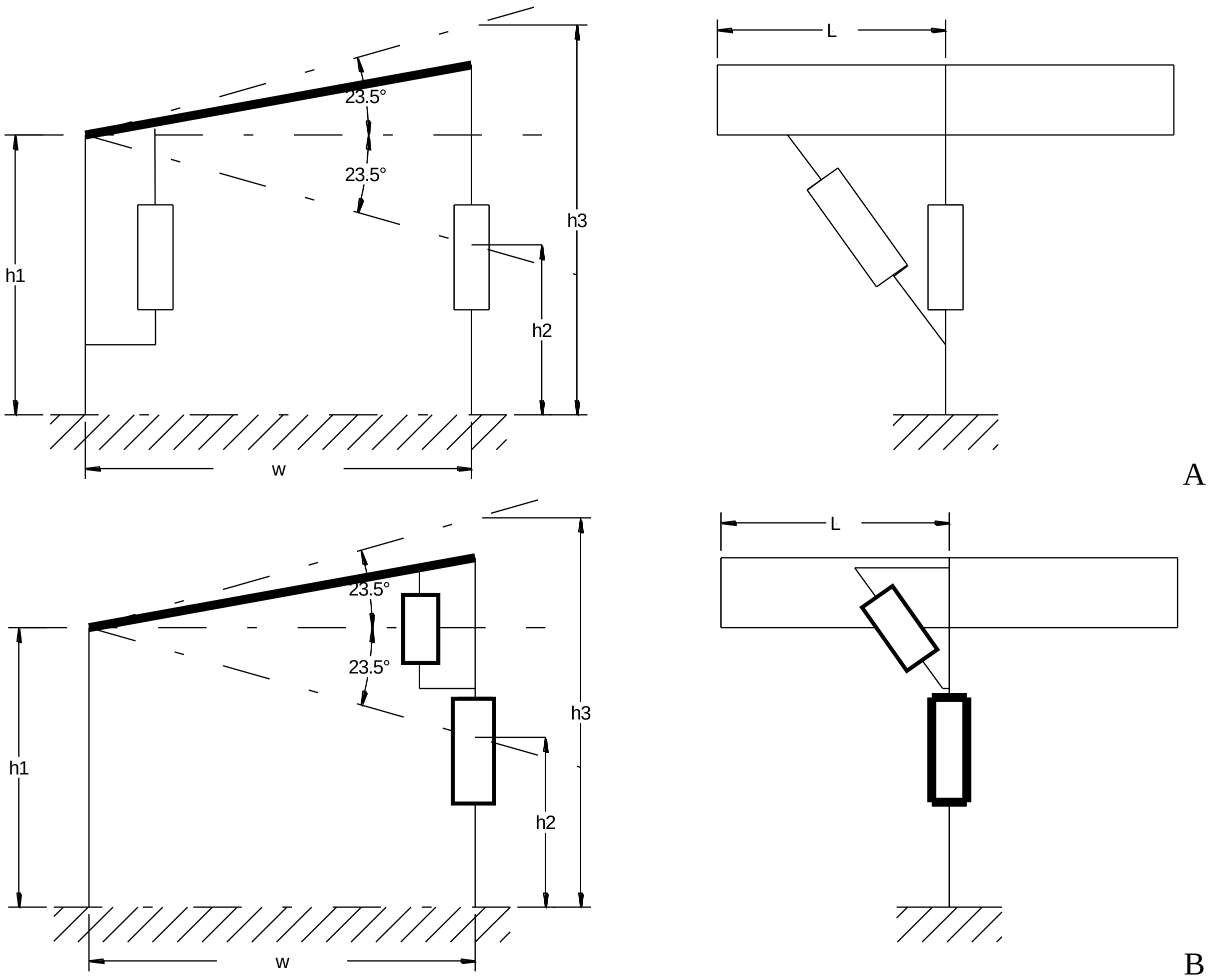

Figure 5.10-13 Forms of Crank Slider

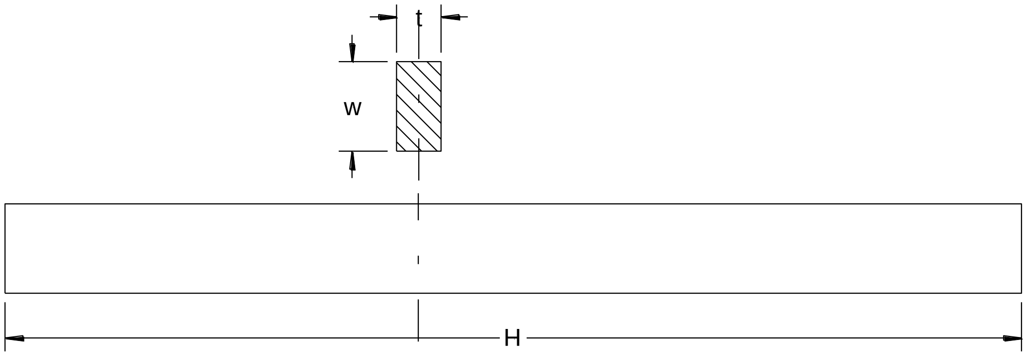

Figure 5.10-14 Solar panel support

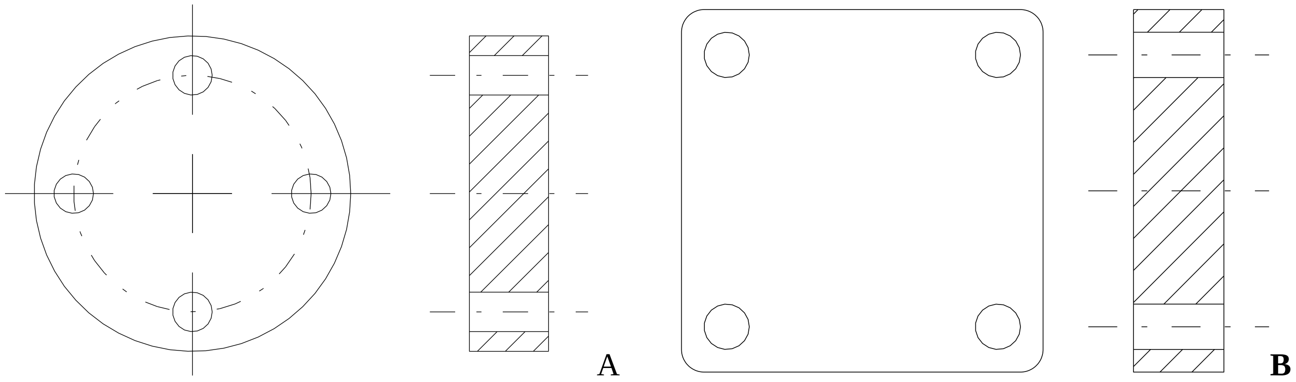

Figure 5.10-15 Alternative shape of flange

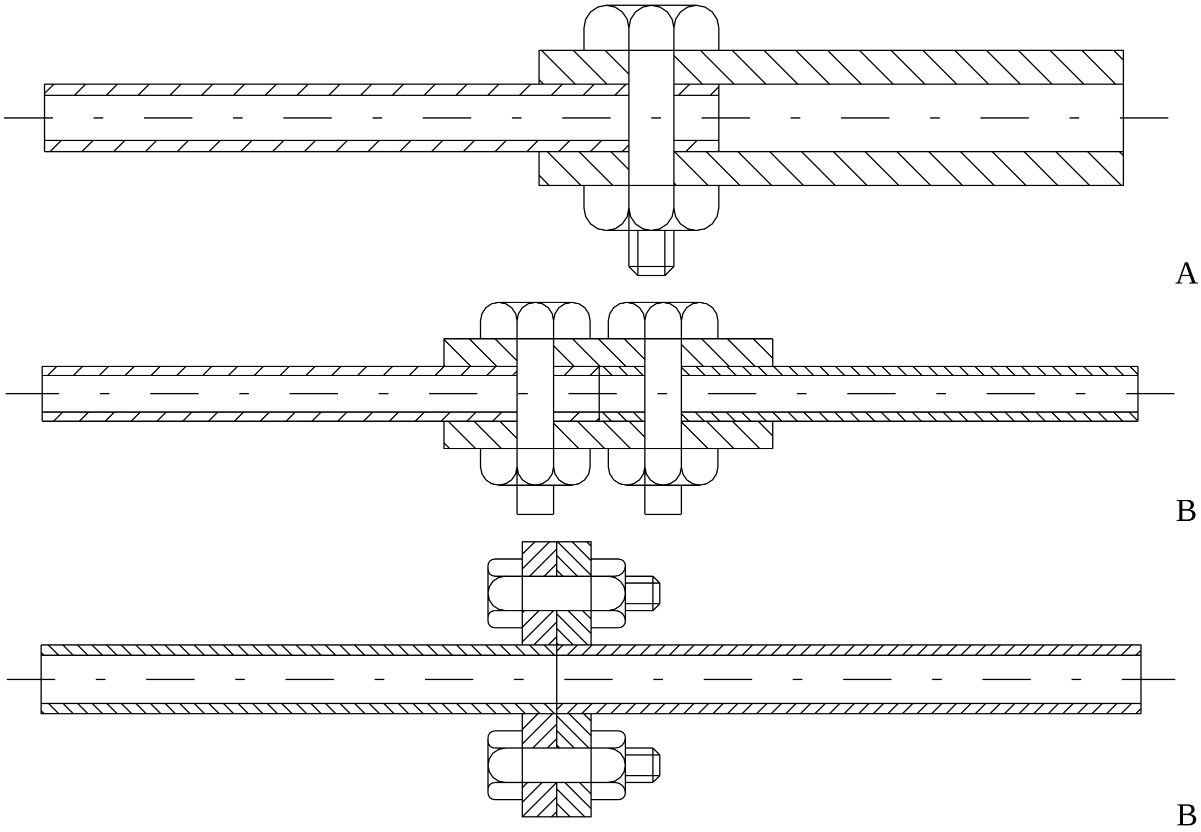

Figure 5.10-16 Alternatives form of connection of support and piston rod

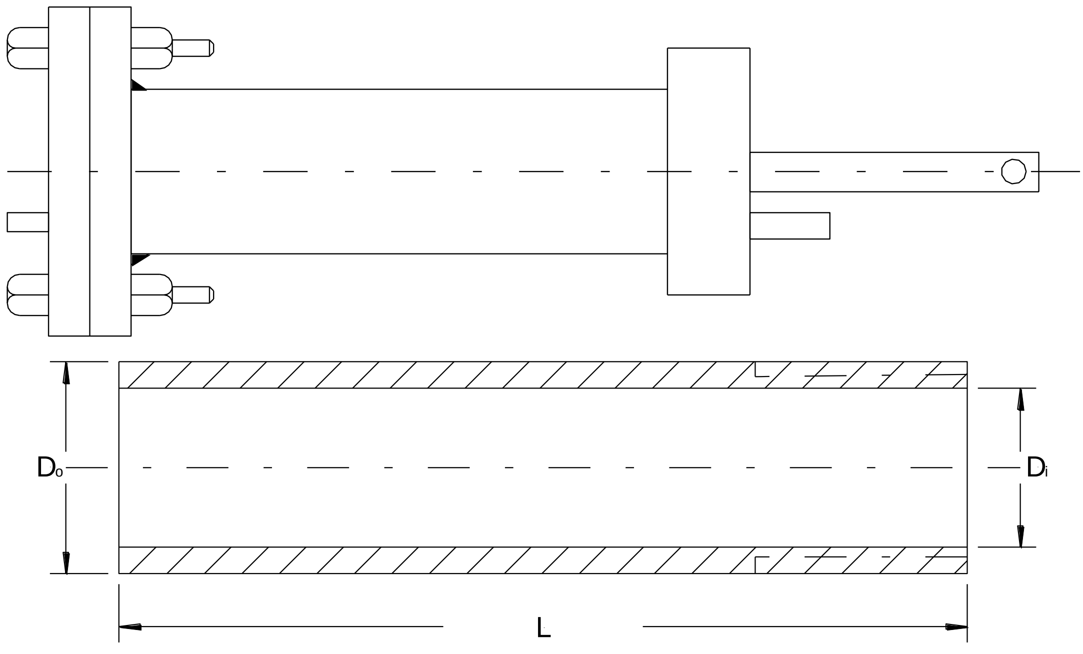

Figure 5.10-17 cylinder 2

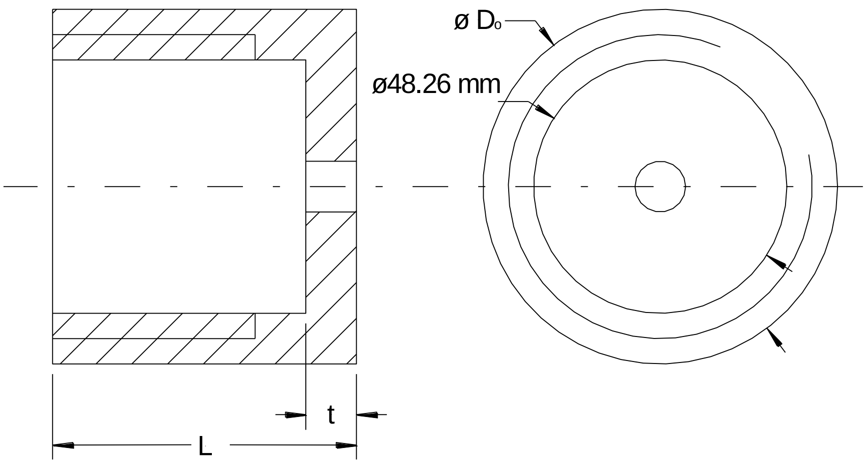

Figure 5.10-18 Cylinder cup

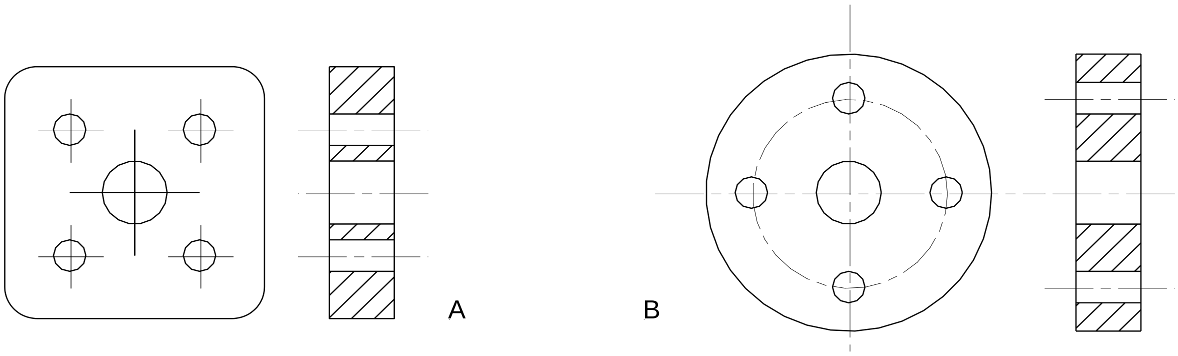

Figure 5.10-19 Flange

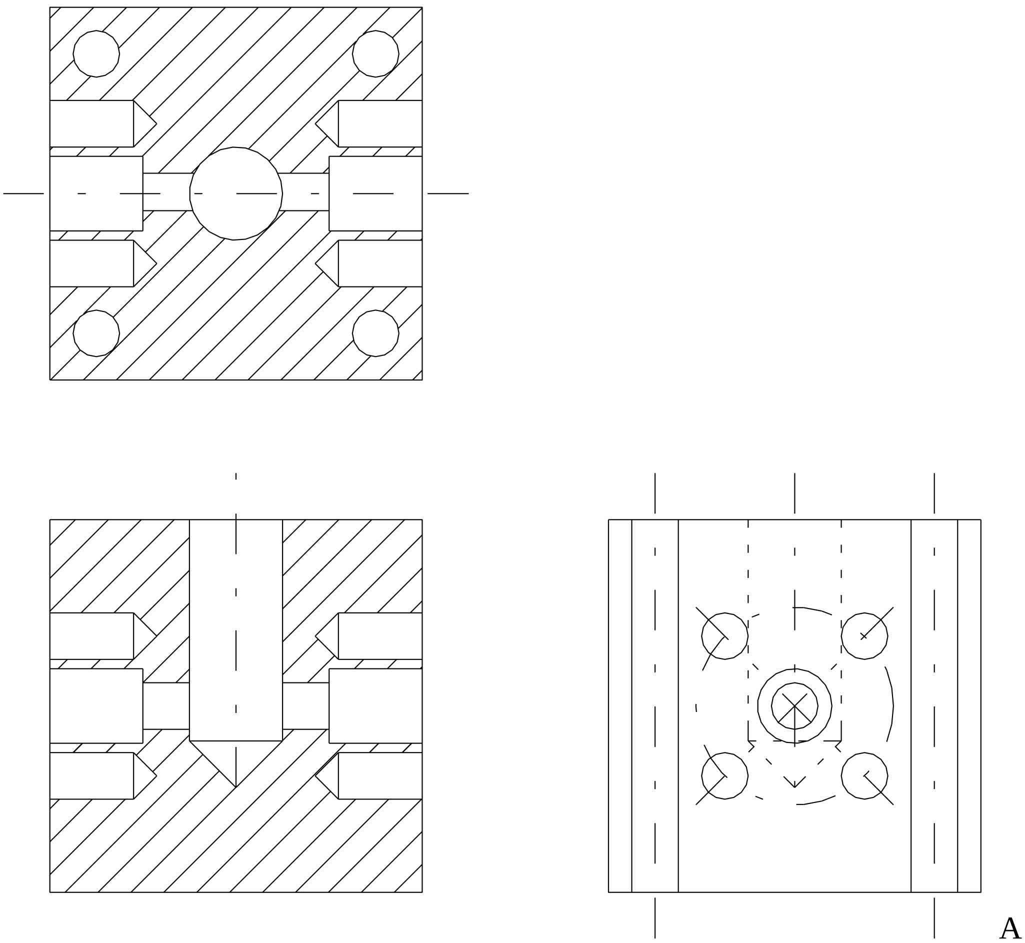

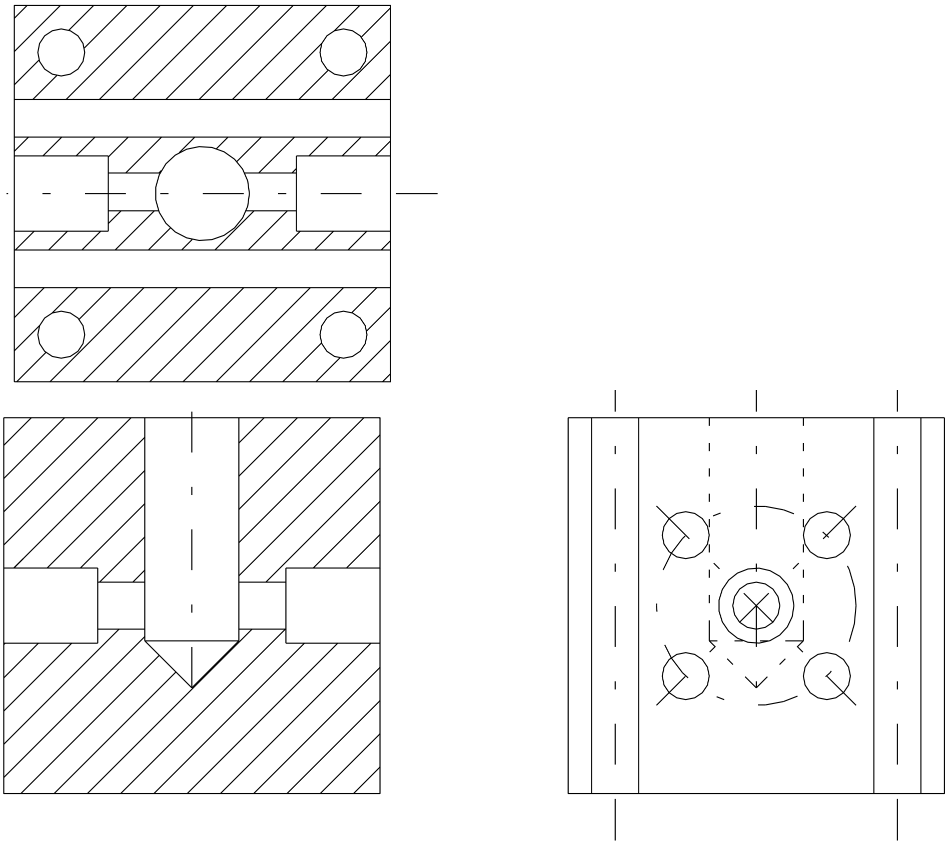

Figure 5.10-20 Pump 2

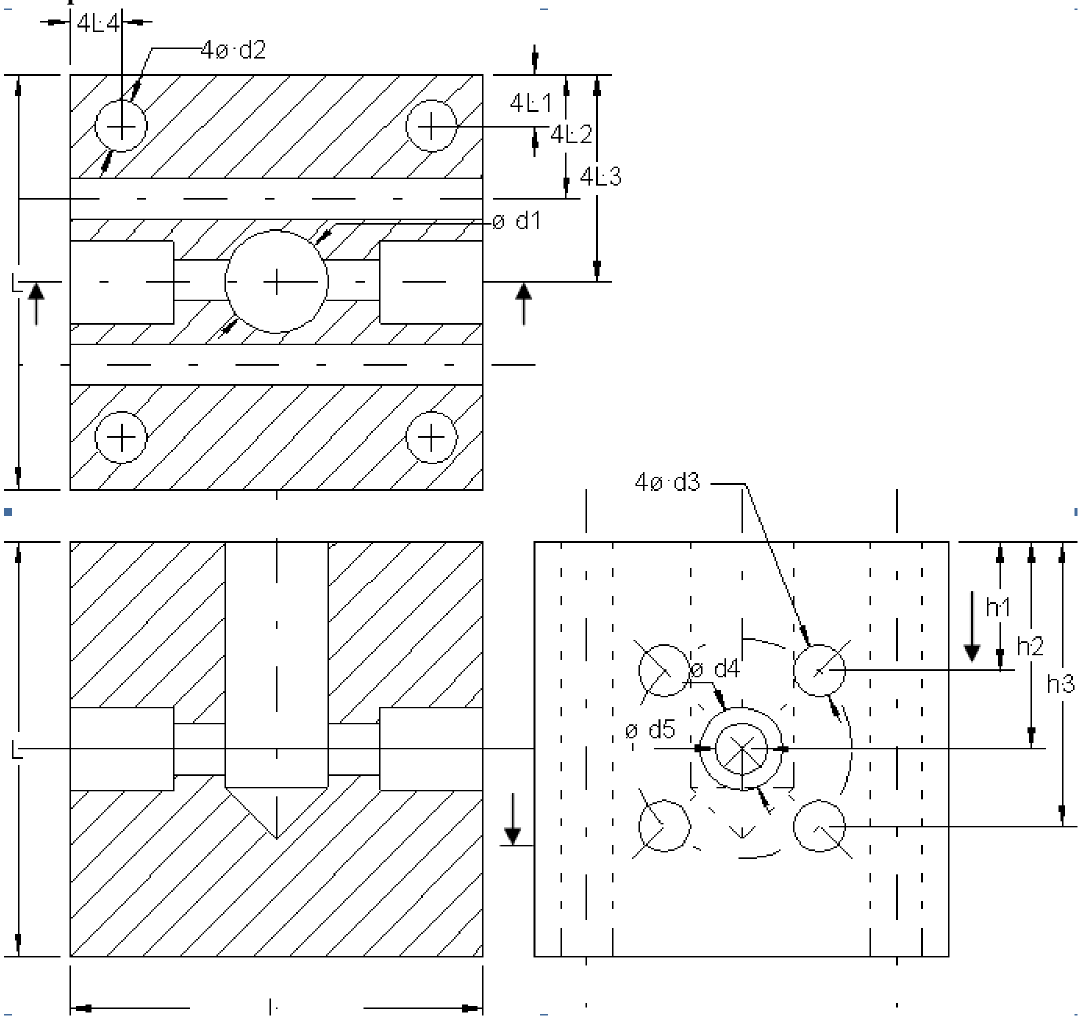

Figure 10-21 Detail of Pump

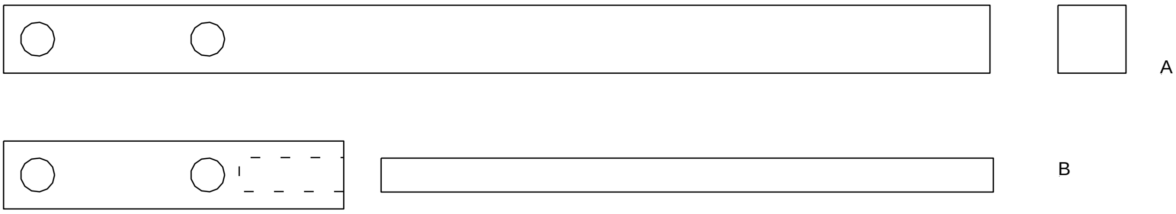

Figure 5.10-22 Forms of lever

Appendix O Upper side weight of flange

S. No.	part	Qnty	Volume formula	Volume $10^{-3}m^3$	Unit weight KN/m^3	Weight N
1	Cylinder	1	$\frac{\pi}{4}(D_o^2 - D_i^2)\Delta L$	1.333	76.5	101.975
2	Piston rod	1	$\frac{\pi}{4}(D_o^2 - D_i^2)\Delta L$	0.928	76.5	70.992
3	Cylinder tail cover	1	$L \times L \times t$	0.3125	76.5	23.906
4	Cylinder head cover	1	$L^2 t - \frac{\pi}{4} D_o^2 t$	0.155	76.5	11.8575
5	Flange	2	$L^2 t - \frac{\pi}{4} D_o^2 t$	0.252	76.5	19.278
6	Piston head	1	$\frac{\pi}{4} D_o^2 t$	0.173	76.5	13.235
7	Bolt and nut	8	$\pi B^2 \times H + \pi(B^2 - d^2) \times H + \frac{\pi}{4} d^2 \times L$	0.046	76.5	3.519
8	Piston rod cover	1	$\frac{\pi}{4} D_o^2 t$	0.148	76.5	11.322
Total						256.085

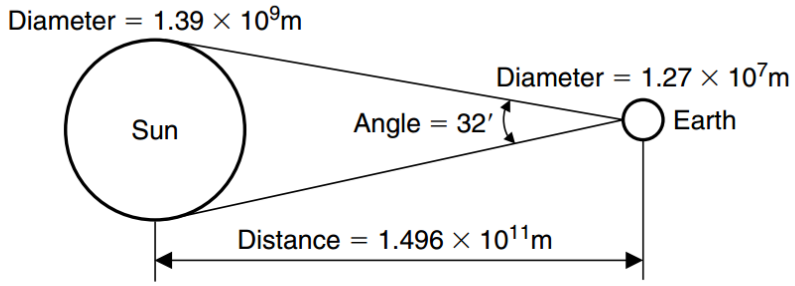

Figure 2.10-23 Sun-earth relationship

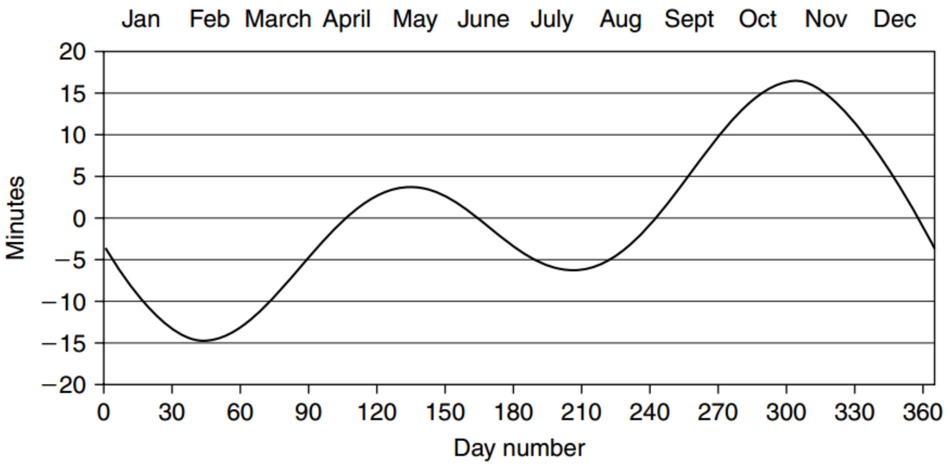

Figure 2.10-24 Equation of time

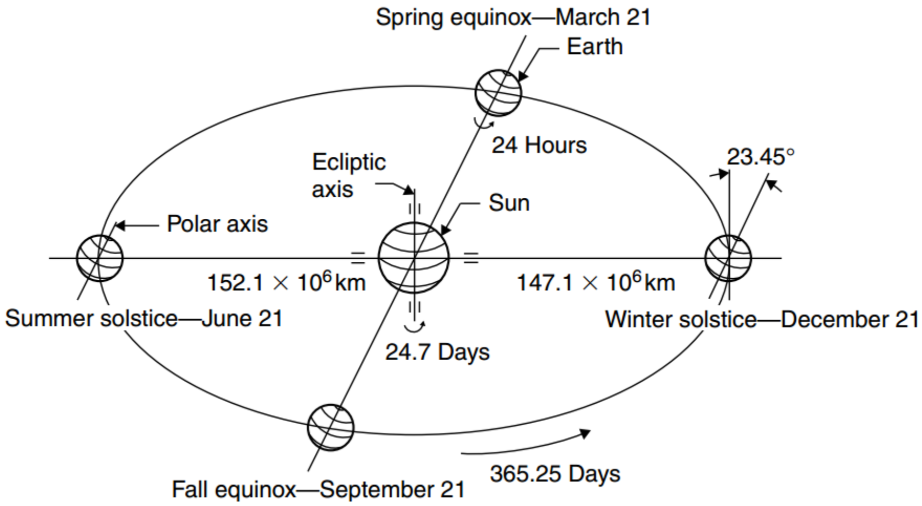

Figure 2.10-25 Annual motion of the earth about the sun

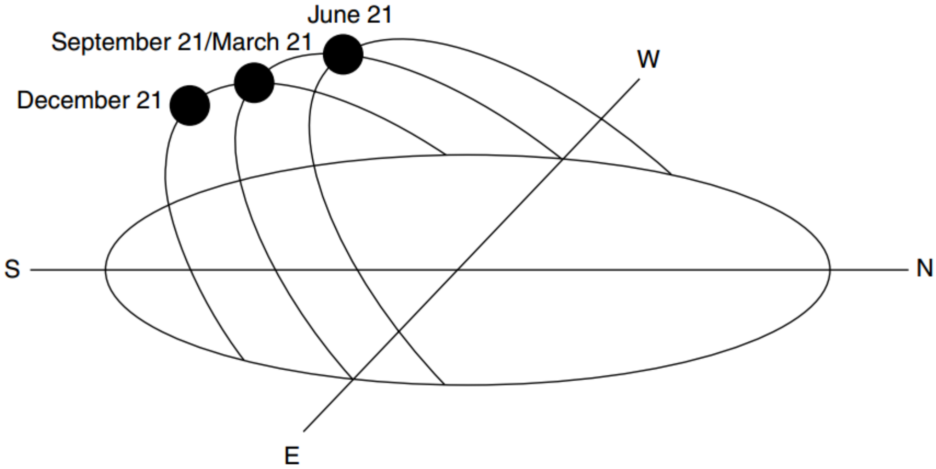

Figure 2.10-26 Annual changes in the sun's position in the (Northern Hemisphere)

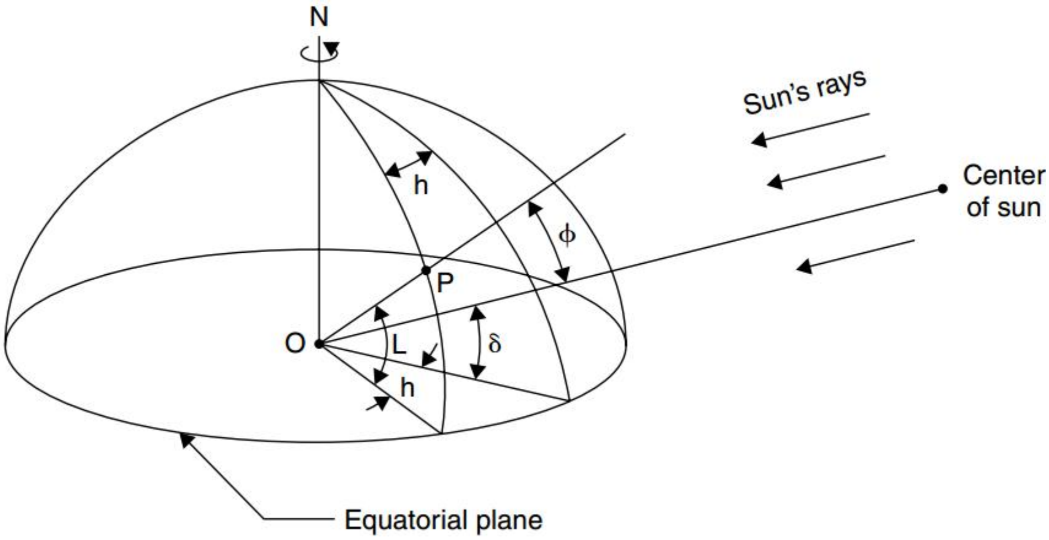

Figure 2.10-27 Definition of latitude, hour angle, and solar declination

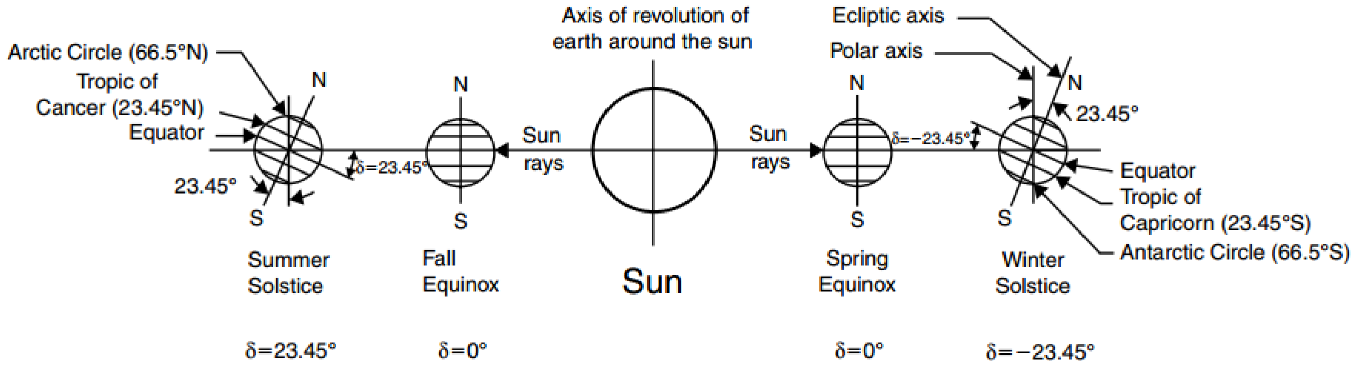

Figure 2.10-28 Yearly variation of solar declination

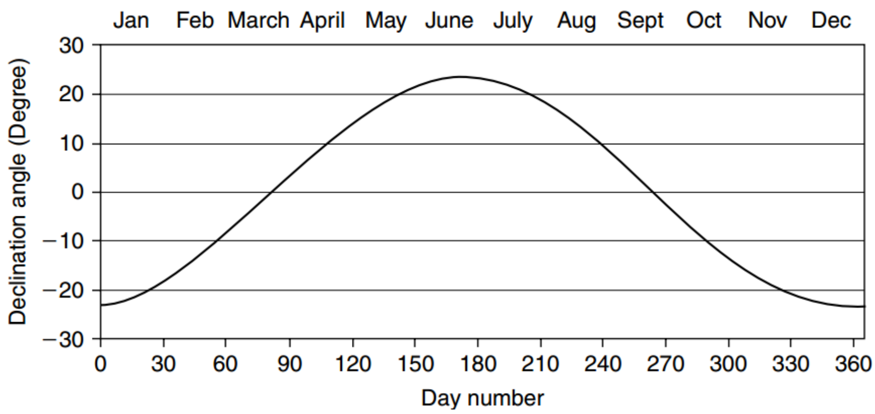

Figure 2.10-29 Declination of the sun

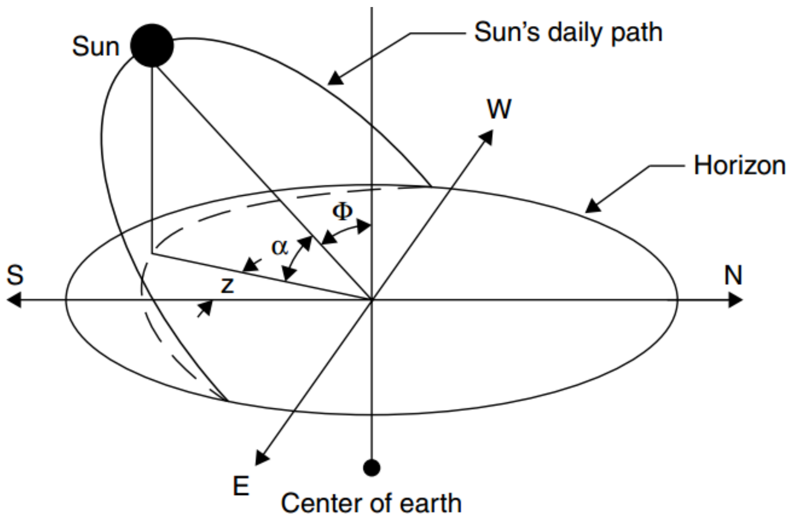

Figure 2.10-30 Apparent daily path of the sun across the sky from sunrise to sunset

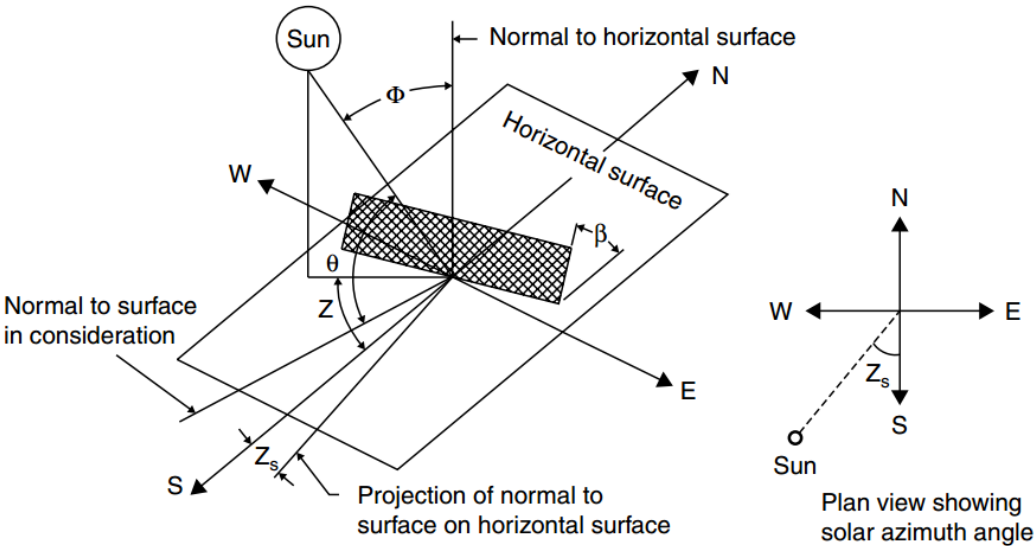

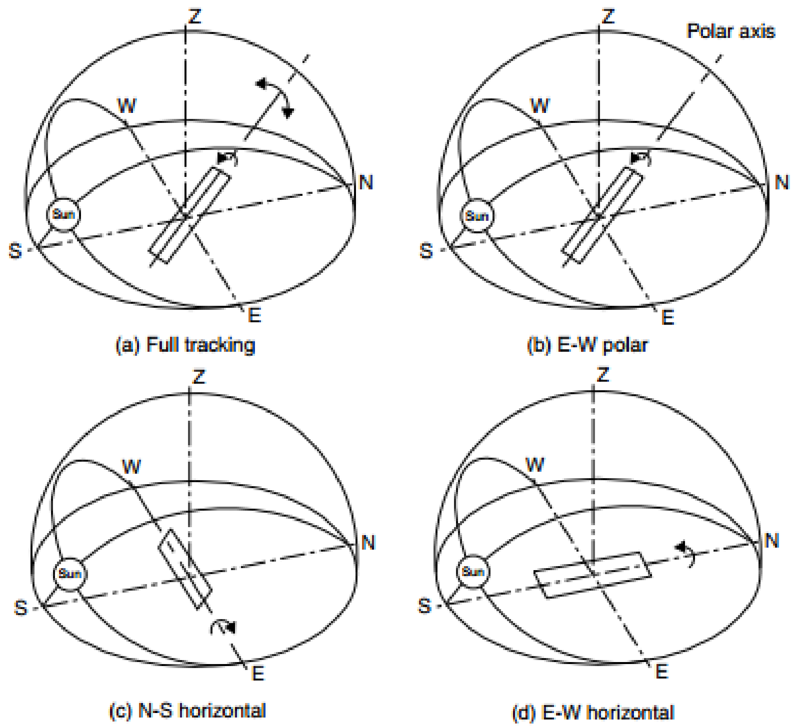

Figure 2.10-31 collector geometry for various modes of tracking

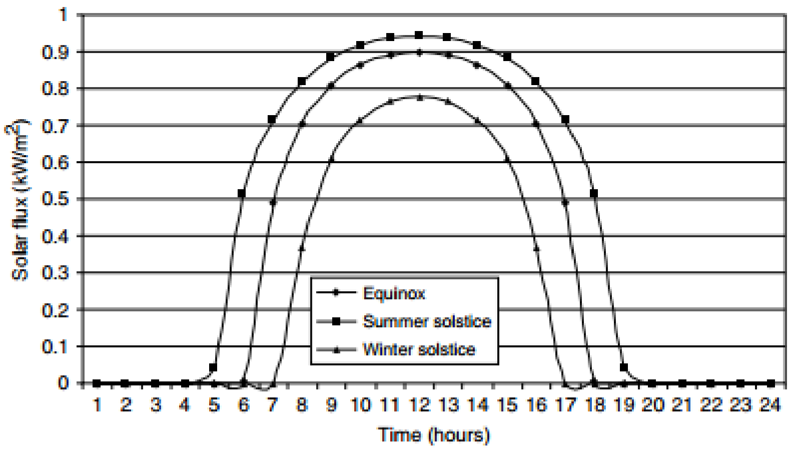

Figure 2.10-32 Daily variation of solar flux, full tracking

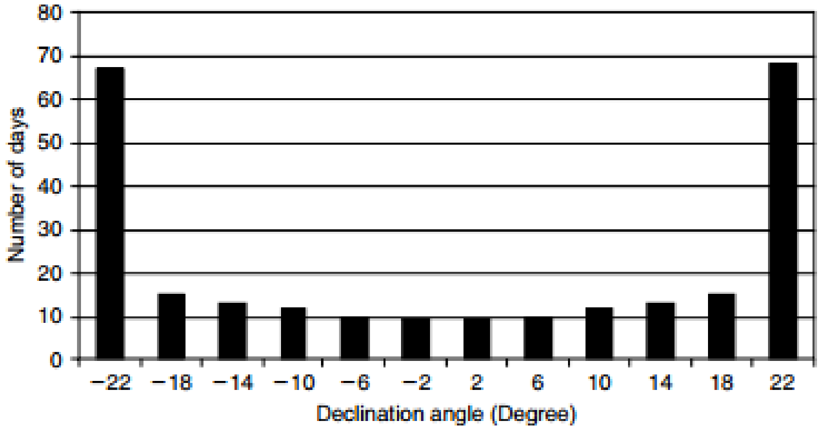

Figure 2.10-33 Number of consecutive days the sun remains within 4° declination

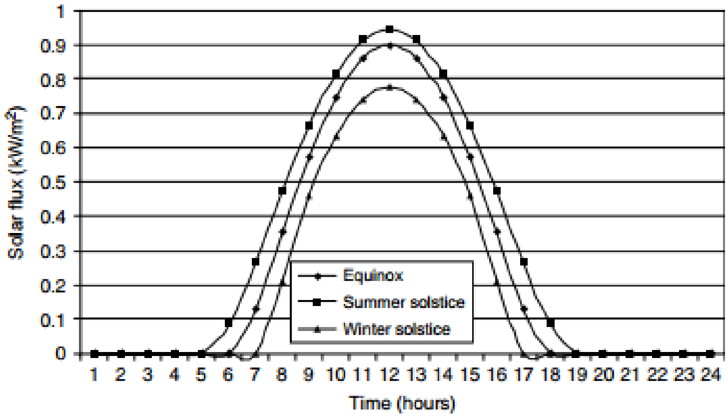

Figure 2.10-34 Daily variation of solar flux; tilted N-S axis with tilt adjusted daily

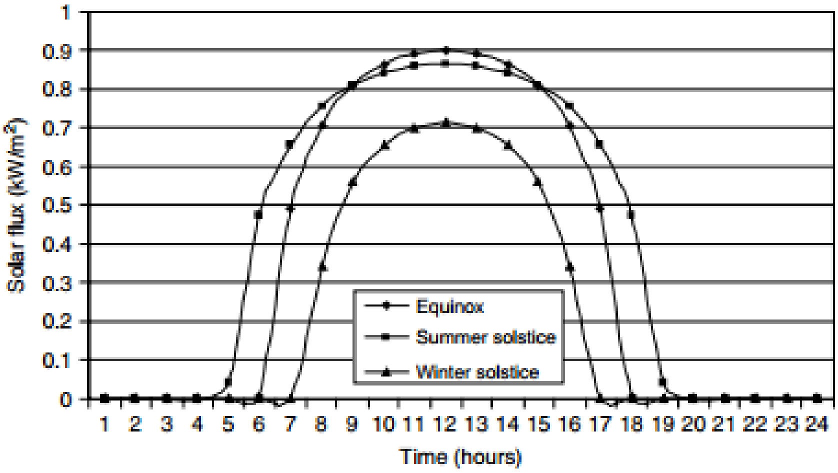

Figure 2.10-35 Daily variation of solar flux: polar N-S axis with E-W tracking

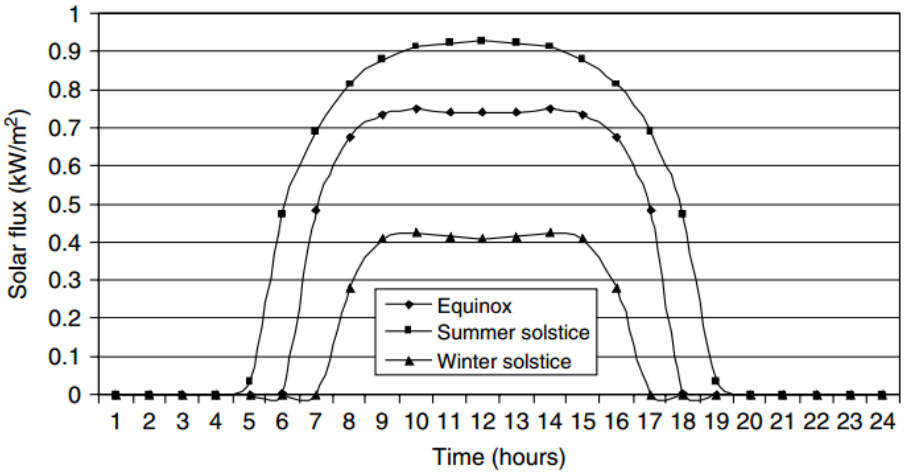

Figure 2.10-36 Daily variation of flux: horizontal E-W axit N-S tracking

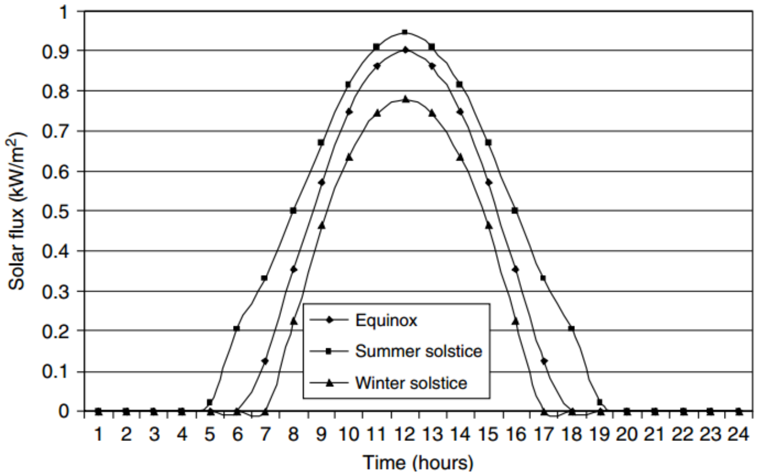

Figure 2.10-37 Daily variation of solar flux: horizontal N-S axis and E-W tracking

Table 2.5 Comparison of energy received for various modes of tracking

Tracking mode	Solar energy received (kWh/m^2)			Percentage to full tracking		
	E	SS	WS	E	SS	WS
Full tracking	8.43	10.60	5.70	100	100	100
E-W polar	8.43	9.73	5.23	100	91.7	91.7
N-S horizontal	7.51	10.36	4.47	89.1	97.7	60.9
E-W horizontal	6.22	7.85	4.91	73.8	74.0	86.2

Notes: E = equinoxes, SS = summer solstice, WS = winter solstice.

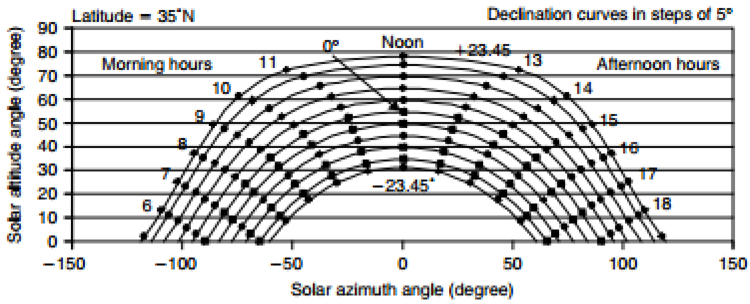

Figure 2.10-38 Sun path diagram for 35^{o}N latitude

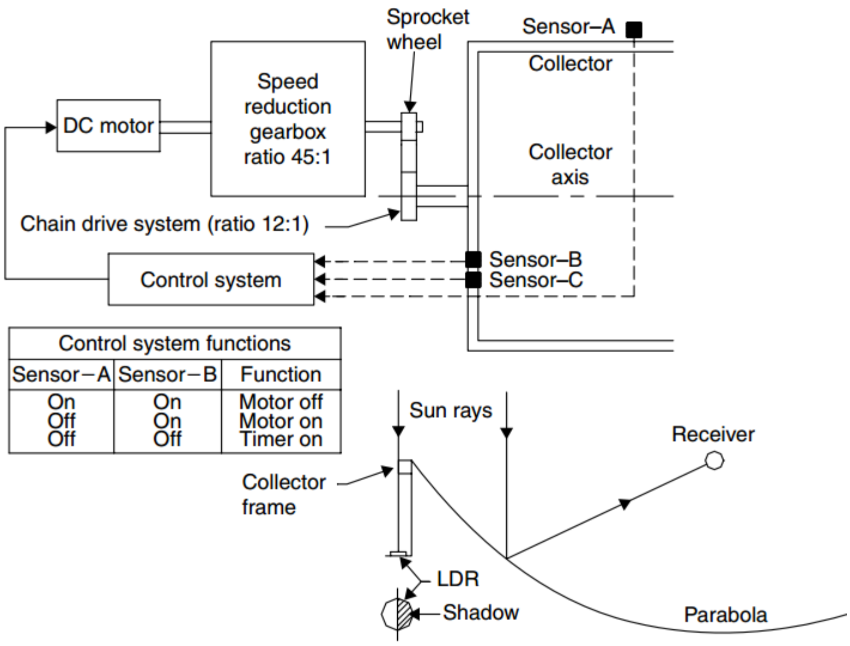

Figure 2.10-39 Tracking mechanism system diagram

Appendix Q Cost analysis

Table 6 cost of pump 1

Part name	Qty	Mass (kg)	Material	Cost per kg	Raw material cost (Birr)	Machine	Process	Time (min.)	Cost (Birr/hr)	Total Manu. Cost (Birr)	Total cost (Birr)
Pump hosing 1	1	0.8936	C.S	16	14.298	Casting machines	Casting	20	90	30	49.298
						Lathe	Drilling	5	60	5	
Pump cover	3	0.1272	C.S	16	6.106	Cutter	Cutting	3	20	1	9.106
						driller	Drilling	4	30	2	
Spring	5	0.0024	steel	pc	pc	pc	pc	pc	pc	20	25
valves	2	0.0031	C.S	16	0.099	Casting machines	Casting	15	90	22.5	22.599
Plunger	1	0.0111	C.S	16	0.178	Lathe	Facing & turning	10	60	10	10.178

Table 7 cost of powerhouse 1

Part name	Qty	Mass (kg)	Material	Cost per kg	Raw material cost (birr)	Machine	Process	Time (min.)	Cost (Birr)	Total Manu. Cost (Birr)	Total cost (Birr)
Cylinder	1	10.7804	C.S	16	172.486	Lathe	Turning	4	60	4	176.486
piston	1	9.0578	C.S	16	144.925	Lathe	Turning	3	60	3	152.925
						Welding machine	Welding	5	60	5	
Pin hold	2	0.0785	C.S	16	2.512	Cutter	Cutting	10	20	3.33	22.512
Cylinder cover	4	2.4531	C.S	16	156.998	Cutter	Cutting	25	20	8.33	171.998
						Driller	Drilling	20	20	6.67	

Table 8 cost of crank slider

Part name	Qty	Mass (kg)	Material	Cost per kg	Raw material cost (birr)	Machine	Process	Time (min.)	Cost (Birr)	Total Manu. Cost (Birr)	Total cost (Birr)
Panel upper support	1	2.7552	C.S	16	44.083	Lathe	Turning	5	60	5	50.413
						Grinder	Grinding	4	20	1.33	
Joint	1	0.1225	C.S	16	1.960	Lathe	Turning	4	60	4	9.29
						Driller	Drilling	10	20	3.33	

Table 9 cost of powerhouse 2

Part name	Qty	Mass (kg)	Material	Cost per kg	Raw material cost (birr)	Machine	Process	Time (min.)	Cost (Birr)	Total Manu. Cost (Birr)	Total cost (Birr)
piston	1	1.1289	C.S	16	18.062	Lathe	facing	4	60	4	27.062
						Welding machine	Welding	5	60	5	
Cylinder	1	1.5886	C.S	16	25.418	Lathe	Turning	6	60	6	31.418
Cylinder cup	1	0.0924	C.S	16	1.478	Casting machine	Casting	15	90	22.5	23.978
Flange	1	0.2528	C.S	16	4.045	Cutter	Cutting	5	20	1.67	7.385
						Driller	Drilling	5	20	1.67	

Table 10 cost of Pump 2

Part name	Qty	Mass (kg)	Material	Cost per kg	Raw material cost (birr)	Machine	Process	Time (min.)	Cost (Birr)	Total Manu. Cost (Birr)	Total cost (Birr)
Housing	1	0.8936	C.S	16	14.298	Casting machine	Casting	20	90	30	49.298
						Lathe	Drilling	5	60	5	
lever	1	2.8725	C.S	16	45.96	Hack saw	Cutting	4	30	2	48.63
						Driller	Drilling	2	20	0.67	

Table 11 cost of others

Part name	Qty	Mass (kg)	Material	Cost per kg	Raw material cost (birr)	Machine	Process	Time (min.)	Cost (Birr)	Total Manu. Cost (Birr)	Total cost (Birr)
Support at pin end	1	5.4302	C.S	16	86.883	Lathe	Facing	4	60	4	94.213
						Driller	Drilling	10	20	3.33	
Pump support	1	0.4481	C.S	16	7.17	Cutter	Cutting	15	20	5	18.84
						Driller	Drilling	20	20	6.67	
Lower support bar	4	0.2752	C.S	16	17.613	Lathe	Threading	60	60	60	77.613
Cam	1	0.6126	CS	16	9.802	Casting machine	Casting	15	90	22.5	32.302
Cam follower	1	0.2972	CS	16	4.595	Casting machine	Casting	15	90	22.5	27.095
Bolt	31		C.S	0.019	18.067	pc	pc	pc	pc	pc	18.067
Nut	35		C.S	0.752	26.32	pc	pc	pc	pc	pc	26.32
Gasket	10		C.S	pc	209.284	pc	pc	pc	pc	pc	209.284

Timer	1		pc	pc	pc	pc	pc	pc	pc	pc	281.624
Limit switch	1		pc	pc	pc	pc	pc	pc	pc	pc	488.8
Motor	1		pc	pc	pc	pc	pc	pc	pc	pc	376

Appendix R Metallic series for sacrificial anode protection

1. Magnesium 2.Zinc 3.Aluminium (2S) 4.Cadmium 5.Aluminium (175T) 6.Steel or iron	7.Cast iron 8.Lead-Tin Solder 9.Lead 10.Nickel 11.Brasses 12.Copper	13.Bronzes 14.Stainless Steel (304) 15.Monel 16.Silver 17.Graphite 18.Gold

Appendix S Part Drawing

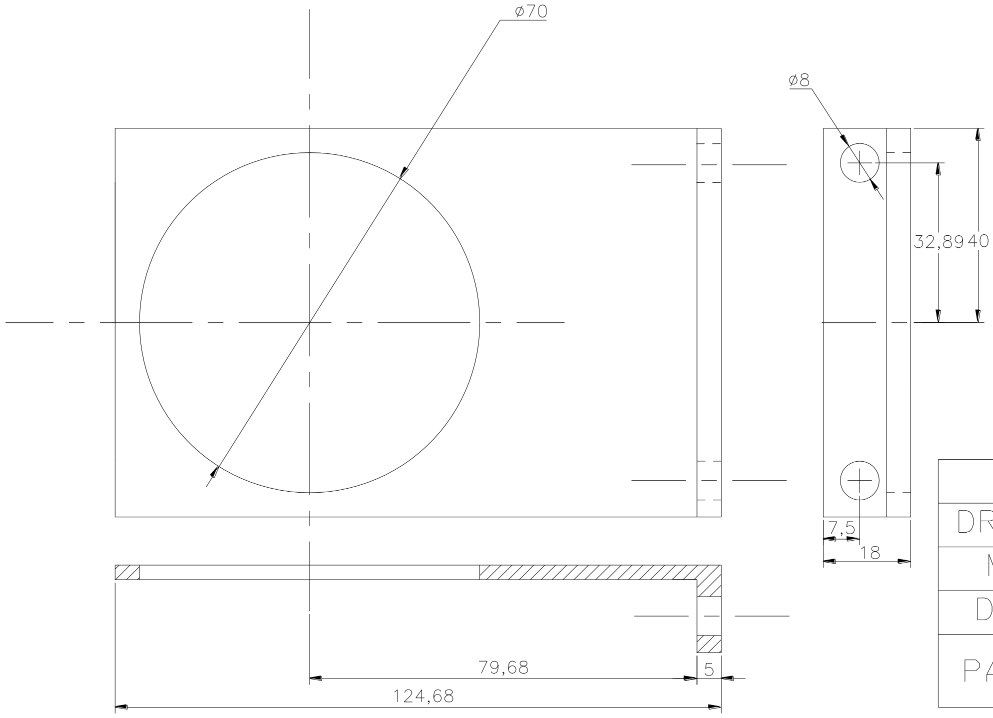

QTY	1
DRAWING NO.	1
MATERIAL	CS
DIMENSION	125X18X80
PART NAME	PUMP-MOTOR CONNECTOR

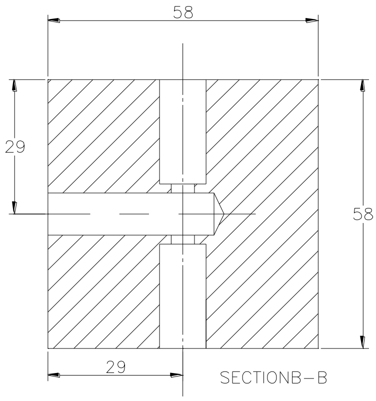

QTY	2
DRAWING NO.	2
MATERIAL	CS
DIMENSION	58X58X58
PART NAME	PUMP CASING

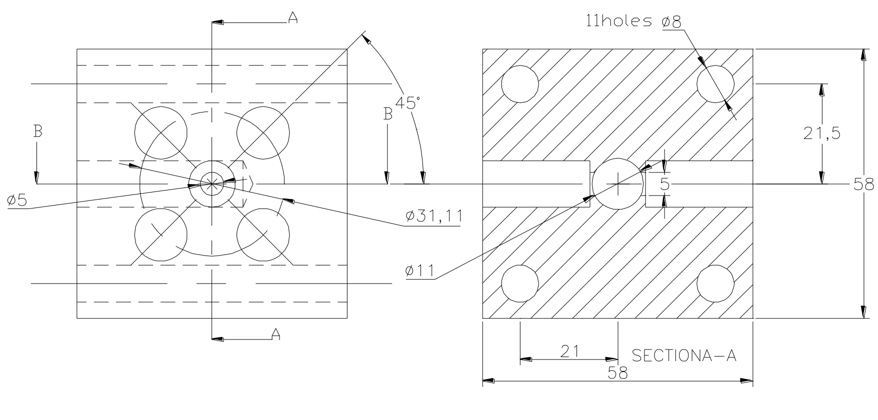

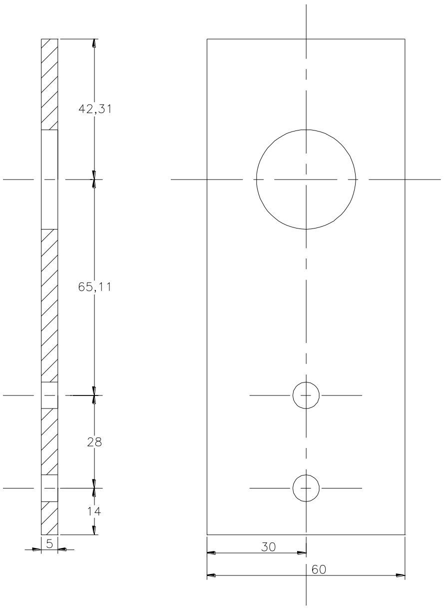

QTY	2
DRAWING NO.	4
MATERIAL	CS
DIMENSION	58X58X58
PART NAME	PUMP CASING

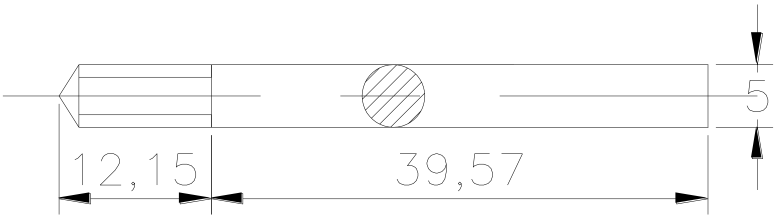

QTY	1
DRAWING NO.	5
MATERIAL	CS
DIMENSION	52XØ5X1.25
PART NAME	PLUNGER 1

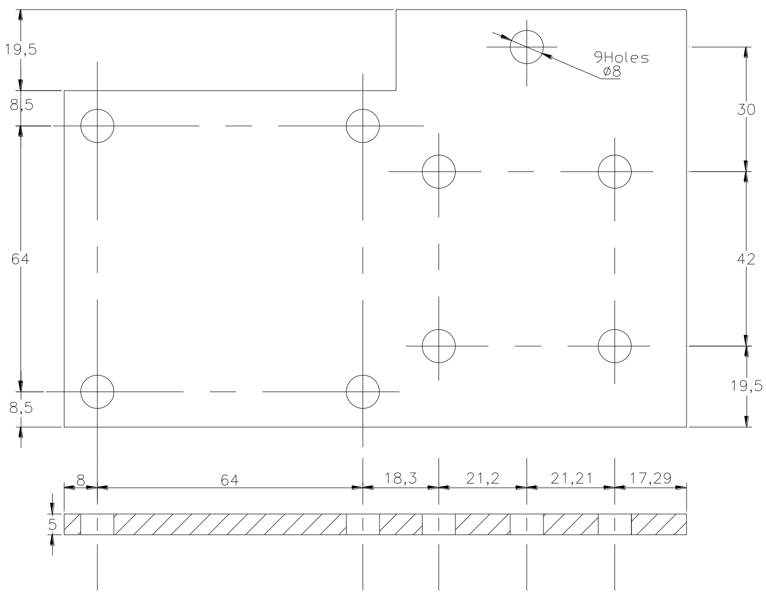

QTY	1
DRAWING NO.	6
MATERIAL	CS
DIMENSION	150X100X5
PART NAME	BASE PLATE

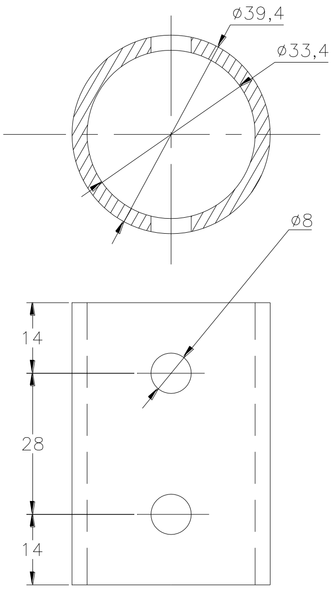

QTY	1
DRAWING NO.	7
MATERIAL	CS
DIMENSION	56Xø39.4X3
PART NAME	JOINT SHAFT

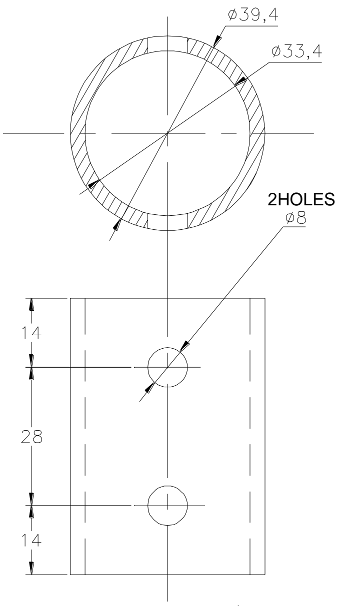

QTY	1
DRAWING NO.	7
MATERIAL	CS
DIMENSION	56Xø39.4X3
PART NAME	JOINT SHAFT

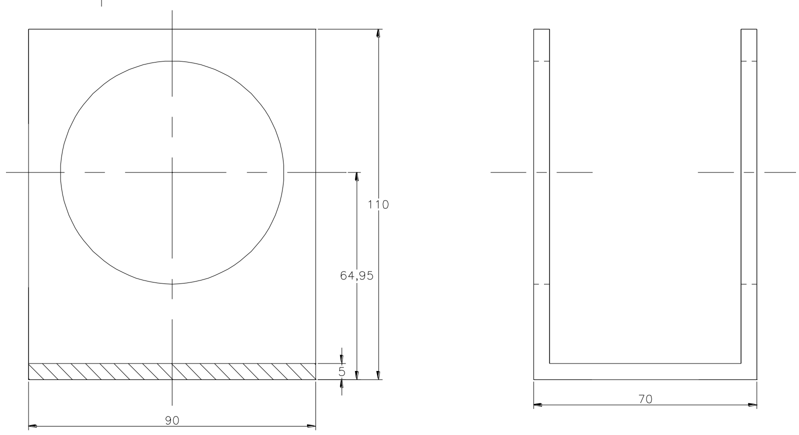

QTY	1
DRAWING NO.	8
MATERIAL	CS
DIMENSION	80X70X110
PART NAME	EYE JOINT

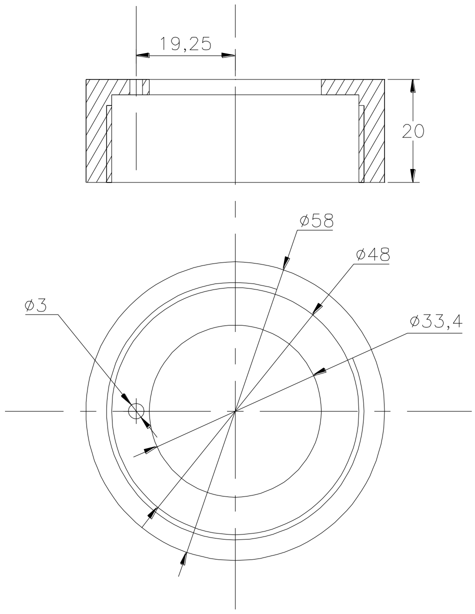

QTY	1
DRAWING NO.	9
MATERIAL	CS
DIMENSION	ø58X20
PART NAME	CYLINDER CUP

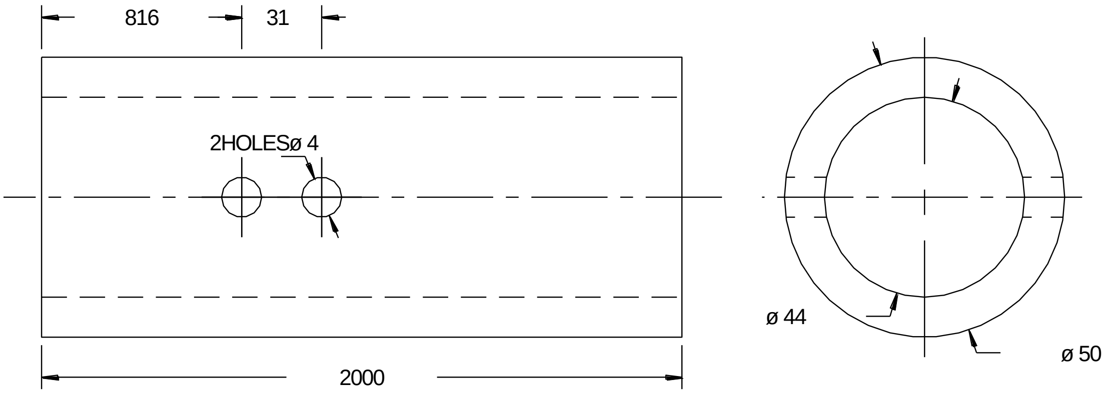

QTY	1
DRAWING NO.	10
MATERIAL	CS
DIMENSION	2000Xø50X3
PART NAME	MAIN SHAFT

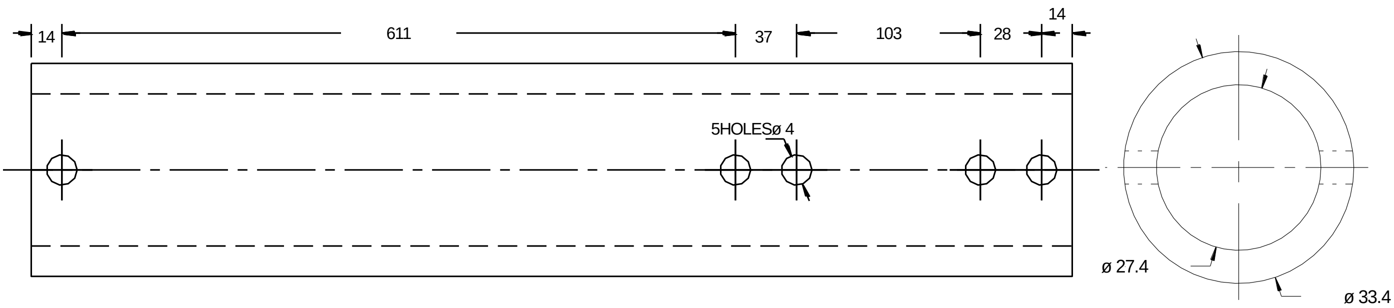

QTY	1
DRAWING NO.	11
MATERIAL	CS
DIMENSION	807XXø33.4X3
PART NAME	PANEL UPPER SUPPORT

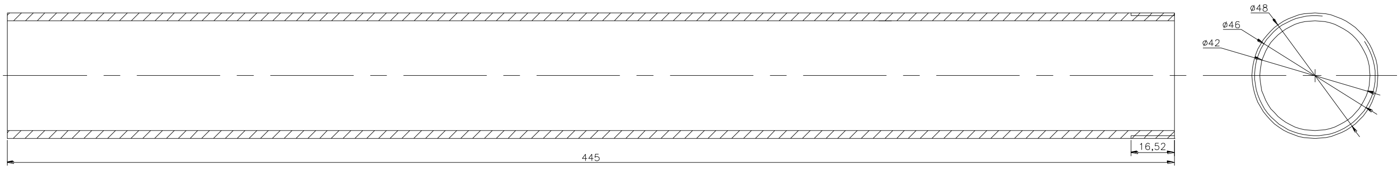

QTY	1
DRAWING NO.	12
MATERIAL	CS
DIMENSION	45Xø48X3
PART NAME	CYLINDER 2

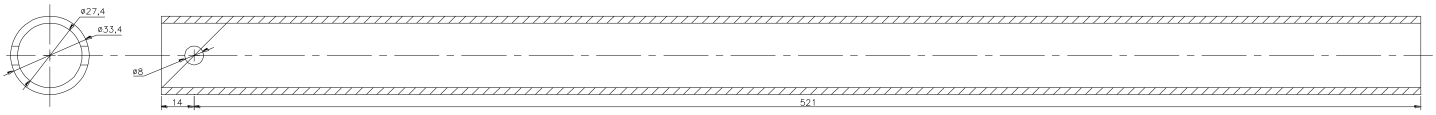

QTY	1
DRAWING NO.	13
MATERIAL	CS
DIMENSION	535Xø33.4X3
PART NAME	PISTON2

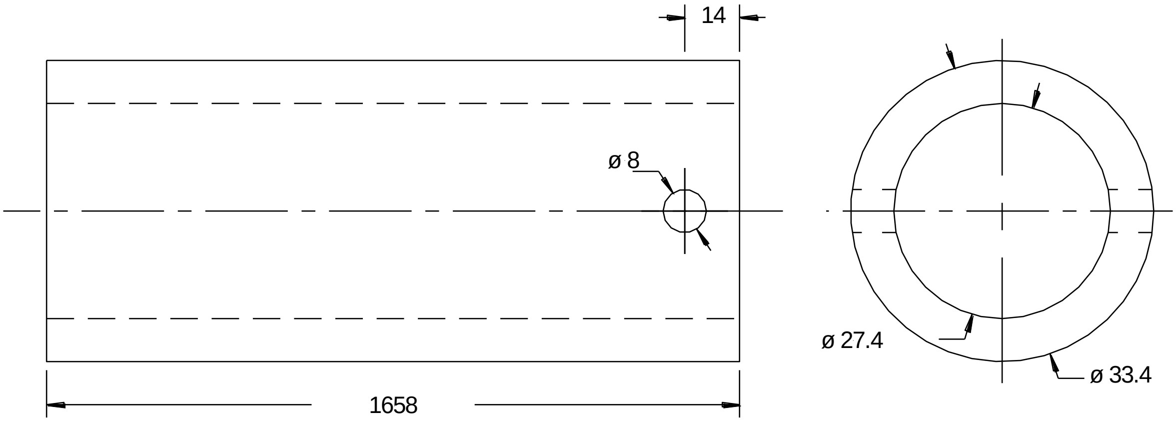

QTY	1
DRAWING NO.	14
MATERIAL	CS
DIMENSION	1658Xø33.4X3
PART NAME	PIN END SUPPORT

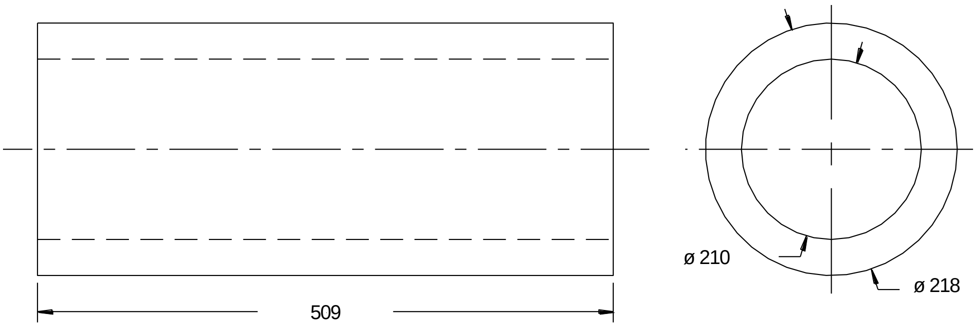

QTY	1
DRAWING NO.	15
MATERIAL	CS
DIMENSION	509Xø218X4
PART NAME	CYLINDER 1

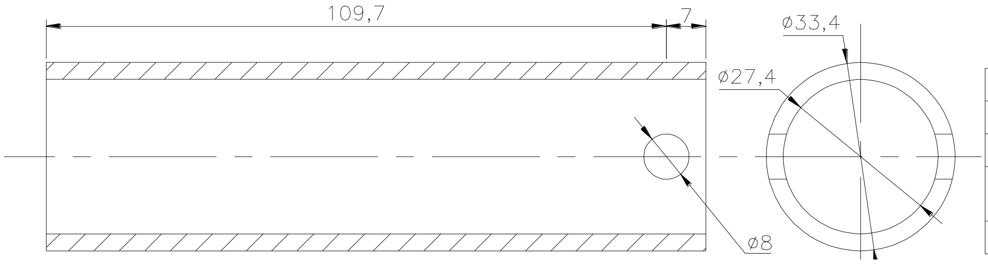

QTY	2
DRAWING NO.	16
MATERIAL	CS
DIMENSION	116.7Xø33.4X3
PART NAME	HOOK

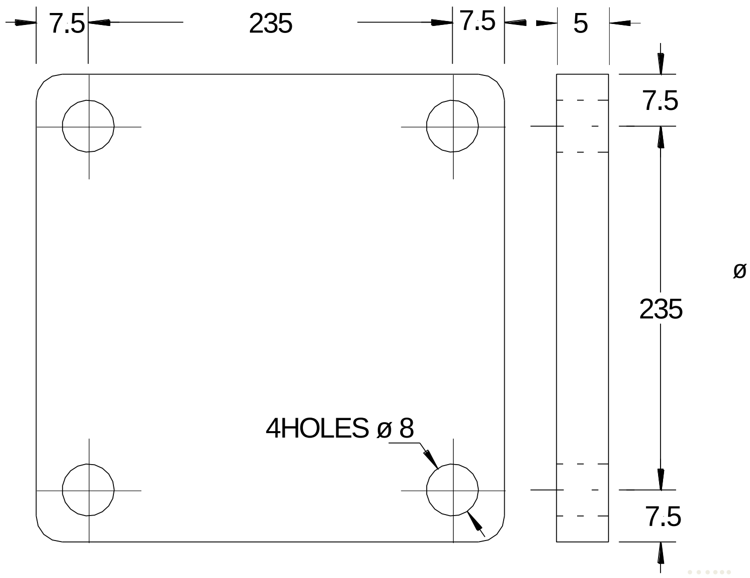

QTY	2
DRAWING NO.	17
MATERIAL	CS
DIMENSION	250X250X5
PART NAME	CYLINDER 1 COVER

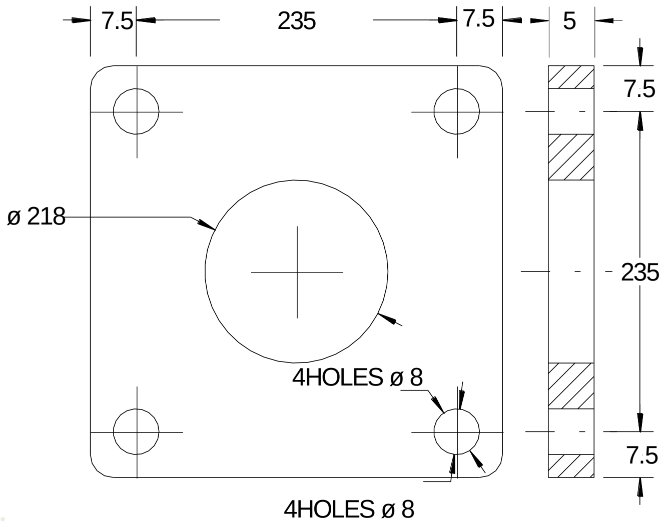

QTY	2
DRAWING NO.	18
MATERIAL	CS
DIMENSION	250X250X5
PART NAME	CYLINDER 1 FLANGE

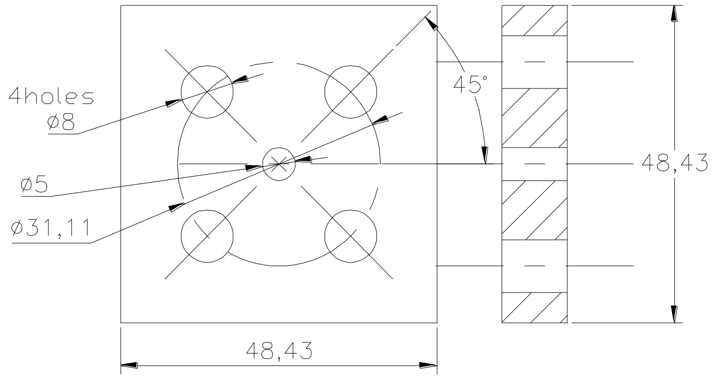

QTY	4
DRAWING NO.	19
MATERIAL	CS
DIMENSION	48.5X48.5X5
PART NAME	PUMP COVER 1

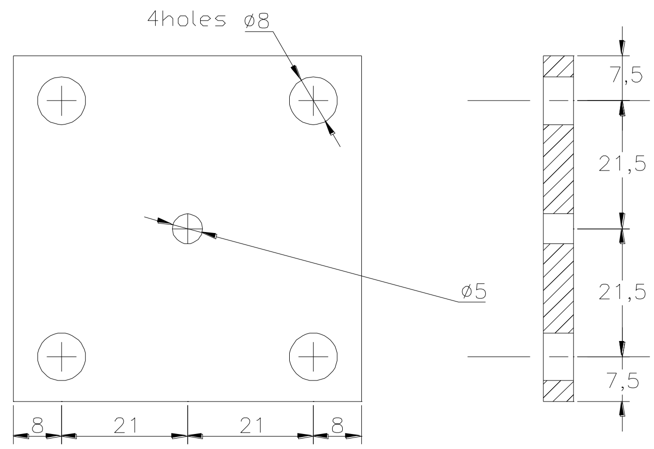

QTY	4
DRAWING NO.	20
MATERIAL	CS
DIMENSION	58X58X5
PART NAME	PUMP COVER 2

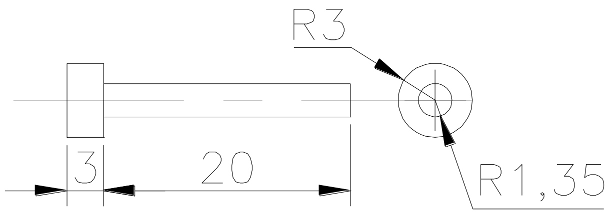

QTY	1
DRAWING NO.	21
MATERIAL	CS
DIMENSION	23XØ6
PART NAME	VALVE

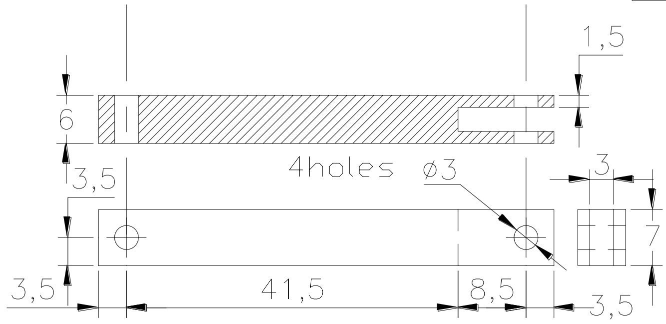

QTY	1
DRAWING NO.	22
MATERIAL	CS
DIMENSION	57X7X6
PART NAME	CRANK

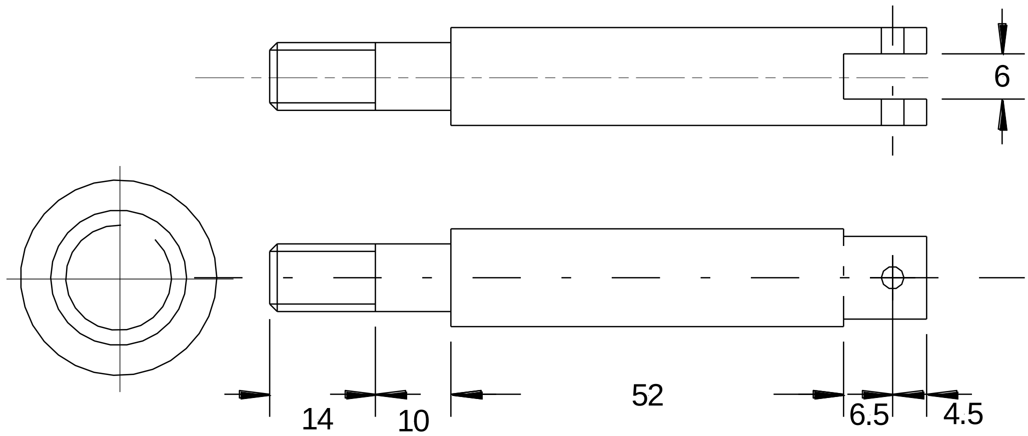

QTY	1
DRAWING NO.	23
MATERIAL	CS
DIMENSION	87XØ13
PART NAME	pLUNGER

Note: All dimensions are in mm.